



**Role of Hypoxia-Inducible Factor (HIF) 1 α in Dendritic Cells in
Immune Regulation of Atherosclerosis**

*Rolle von Hypoxie induziertem Faktor (HIF) 1 α in dendritischen Zellen in der
Immunregulation der Atherosklerose*

Doctoral thesis for a doctoral degree
at the Graduate School of Life Sciences
Julius-Maximilians-Universität Würzburg
Section Biomedicine

Submitted by

Sweena M. Chaudhari

from

Mumbai, India

Würzburg, 2013

Submitted on:

Members of the *Promotionskomitee*:

Chairperson: Prof. Dr. Utz Fischer

Primary supervisor: Prof. Dr. Alma Zerneck

Supervisor (second): Prof. Dr. Thomas Hünig

Supervisor (third): Prof. Dr. Christian Weber

Date of Public Defense:

Date of Receipt of Certificate:

“Strive not to be a success, but rather to be of value”

- Albert Einstein

TABLE OF CONTENTS

SUMMARY.....	10
ZUSAMMENFASSUNG	12
ABBREVIATIONS	14
1. INTRODUCTION.....	20
1.1 Dendritic cells.....	20
1.1.1 Origin of dendritic cells.....	20
1.1.2 DC markers and subtypes	21
1.1.3 Relation of DCs to monocytes and macrophages.....	22
1.1.4 CD11c marker and the CD11c-cre mouse model	22
1.1.5 Functions of DCs	23
1.1.6 DCs regulate helper T-cell balance.....	24
1.1.7 DC migration.....	26
1.2 Atherosclerosis.....	27
1.2.1 Atherosclerosis – a global burden.....	27
1.2.2 Pathogenesis of Atherosclerosis.....	27
1.2.3 Monocytes and macrophages in atherosclerosis	28
1.2.4 Dendritic cells in atherosclerosis.....	29
1.2.5 T cells in atherosclerosis.....	30
1.2.6 Mouse models to study atherogenesis	32
1.3 Hypoxia-inducible factor 1 α	33
1.3.1 Hypoxia and oxygen homeostasis in cells	33
1.3.2 Biology of the Hypoxia-inducible factors	34
1.3.3 Non-hypoxic regulation of HIF1 α	36
1.3.4 HIF1 α in immunity – lymphoid cells	36
1.3.5 HIF1 α in immunity – myeloid cells	37
1.3.6 HIF1 α in immunity – dendritic cells	38
1.3.7 HIF1 α in innate immunity.....	39
1.3.8 HIF1 α in physiology and disease	40
1.3.9 Hypoxia in atherosclerosis.....	41
1.3.10 Role of HIF1 α in myeloid cells in atherosclerosis.....	42
1.3.11 Role of HIF1 α in T cells in atherosclerosis.....	42

1.3.12 Non-hypoxic triggers of HIF1 α leading to atherosclerosis.....	43
1.4 Aim of this project.....	43
2. MATERIALS.....	45
2.1 Chemicals	45
2.2 Kits and reagents	46
2.2.1 Kits.....	46
2.2.2 Molecular Biology reagents.....	46
2.2.3 Cell culture reagents.....	47
2.3 Cytokines	47
2.4 Antibodies	48
2.4.1 Fluorescent antibodies.....	48
2.4.2 Primary antibodies	48
2.4.3 Secondary antibodies and detection reagents.....	49
2.5 Primers.....	49
2.5.1 qPCR primers	49
2.5.2 Genotyping primers	50
2.5.3 ChIP primers.....	51
2.6 Plasmids	51
2.7 Animals	51
2.8 Cell lines	51
2.9 Plasticware, glassware and other consumables.....	52
2.10 Instruments	53
2.11 Softwares	54
2.12 Buffers, solutions and media.....	54
2.12.1 Buffers	54
2.12.2 Solutions.....	56
2.12.3 Media.....	57
3. METHODS	59
3.1 Animal work.....	59
3.1.1 Mice experiments.....	59
3.1.2 Generation of <i>Cd11c-cre⁺ Hif1a^{flox/flox} Ldlr^{-/-}</i> transgenic mice.....	59
3.1.3 Generation of <i>LysM-cre⁺ Hif1a^{flox/flox} Ldlr^{-/-}</i> transgenic mice.....	59
3.1.4 Generation of transgenic mice with STAT3 overexpression in DCs	60
3.1.5 Sacrificing mice and harvesting organs	60

3.1.6 Processing of organs	60
3.2 Histology	61
3.2.1 Oil-Red O staining of aortas for plaque analysis	61
3.2.2 Analysis of aortic plaque area	62
3.2.3 Preparation of aortic roots for paraffin sectioning	62
3.2.4 De-paraffinization of aortic roots	62
3.2.5 Collagen-elastin staining of aortic roots for plaque analysis	63
3.2.6 Analysis of aortic root plaque area	63
3.2.7 Antigen retrieval of aortic roots	64
3.2.8 Macrophage-Smooth muscle cell staining of aortic roots	64
3.2.9 T-cell staining of aortic roots	64
3.2.10 Preparation of aortic roots for frozen sectioning	65
3.2.11 CD11c ⁺ cell staining of aortic roots	65
3.2.12 Analysis of aortic root plaque cell content	66
3.2.13 CD11c ⁺ cell and HIF1 α staining of aortic roots	67
3.2.14 Detection of hypoxia	68
3.3 Cell culture techniques	69
3.3.1 Bone marrow derived dendritic cell (BMDC) culture	69
3.3.2 Bone marrow derived macrophage (BMM) culture	69
3.3.3 Stimulation of cultured cells	70
3.3.4 Isolation of splenic DCs	70
3.3.5 Isolation of splenic CD4 ⁺ T cells	70
3.3.6 Isolation of naive CD4 ⁺ T cells	71
3.3.7 Isolation of lineage depleted BM cells	71
3.3.8 Antigen specific T-cell proliferation	71
3.3.9 Antigen specific T-cell polarization	72
3.3.10 BMDC transmigration assay	72
3.3.11 Transfection of DCs with inhibition and overexpression plasmids	72
3.3.12 Maintenance of HEK293F cells	72
3.4 Nucleic acid detection techniques	73
3.4.1 Genomic DNA isolation	73
3.4.2 Total RNA isolation	73
3.4.3 cDNA synthesis	73
3.4.4 Conventional PCR for genotyping	74

3.4.5 Quantitative real time PCR	75
3.5 Protein detection techniques.....	76
3.5.1 Flow cytometry.....	76
3.5.2 ELISA.....	77
3.6 Lipid detection techniques.....	77
3.6.1 Cholesterol assay	77
3.6.2 Triglyceride assay	78
3.7 Bacterial techniques.....	78
3.7.1 Eluting plasmids from filter paper spots	78
3.7.2 Preparation of LB plates	78
3.7.3 Transformation of bacterial cells	78
3.7.4 Growth of transformed cells for plasmid DNA isolation	78
3.7.5 Plasmid DNA isolation	79
3.7.6 Lentiviral vector – Cre vector co-transfection.....	79
3.8 Lentivirus techniques	79
3.8.1 Transfection of HEK293F cells for lentivirus production	79
3.8.2 Harvesting of lentivirus.....	79
3.8.3 Virus titration.....	80
3.8.4 Viral transduction of BM cells for <i>in vitro</i> analysis	80
3.8.5 Viral transduction of Lin- BM cells for <i>in vivo</i> transplantation	81
3.9 Transcription factor binding site analysis	81
3.9.1 Transcription factor binding site prediction.....	81
3.9.2 Chromatin immunoprecipitation assay.....	81
3.10 Statistics.....	83
4. RESULTS	84
4.1 Presence of hypoxia and HIF1 α in atherosclerotic mice	84
4.2 Generation of mice deficient for HIF1 α in CD11c ⁺ cells	86
4.3 Analysis of atherosclerosis progression in mice with DCs deficient for HIF1 α and fed a high fat diet.....	88
4.4 Analysis of immune cell phenotype in mice with DCs deficient for HIF1 α and fed a high fat diet	92
4.5 Analysis of immune cell phenotype in mice with DCs deficient for HIF1 α at the baseline level	97
4.6 Characterization of mature BMDCs deficient for HIF1 α	99

4.7 Characterization of splenic DCs isolated from atherosclerotic WT <i>Ldlr</i> ^{-/-} and CKO <i>Ldlr</i> ^{-/-} mice.....	104
4.8 Expression of STAT proteins in DCs deficient in HIF1 α	108
4.9 A HIF1 α -STAT3-IL-12-IFN γ pathway in atherosclerosis	110
4.10 Determination of HIF1 α binding sites on gene promoters and evidence of direct transcription factor activity by CHIP	113
5. DISCUSSION.....	116
6. REFERENCES.....	131
ACKNOWLEDGEMENTS	156
CURRICULUM VITAE.....	158
LIST OF PUBLICATIONS	159
LIST OF ORAL AND POSTER PRESENTATIONS	160
AFFIDAVIT.....	161

SUMMARY

Atherosclerosis is the underlying cause of cardiovascular diseases and a major threat to human health worldwide. It involves not only accumulation of lipids in the vessel wall but a chronic inflammatory response mediated by highly specific cellular and molecular responses. Macrophages and dendritic cells (DCs) play an essential role in taking up modified lipids and presenting them to T and B lymphocytes, which promote the immune response. Enhanced activation, migration and accumulation of inflammatory cells at the local site leads to formation of atherosclerotic plaques.

Atherosclerotic plaques become hypoxic due to reduced oxygen diffusion and high metabolic demand of accumulated cells. The various immune cells experience hypoxic conditions locally and inflammatory stimuli systemically, thus up-regulating Hypoxia-inducible factor 1 α . Though the role of HIF1 α in macrophages and lymphocytes has been elucidated, its role in DCs still remains controversial, especially with respect to atherosclerosis. In this project work, the role of HIF1 α in DCs was investigated by using a cell specific knockout mouse model where HIF1 α was deleted in CD11c⁺ cells.

Aortic root sections from atherosclerotic mice showed presence of hypoxia and up-regulation of HIF1 α which co-localized with CD11c⁺ cells. Atherosclerotic splenic DCs also displayed enhanced expression of HIF1 α , proving non-hypoxic stimulation of HIF1 α due to systemic inflammation. Conditional knockout (CKO) mice lacking HIF1 α in CD11c⁺ cells, under baseline conditions did not show changes in immune responses suggesting effects of HIF1 α only under inflammatory conditions. When these mice were crossed to the *Ldlr*^{-/-} line and placed on 8 weeks of high fat diet, they developed enhanced plaques with higher T-cell infiltration as compared to the wild-type (WT) controls. The plaques were of a complex phenotype, defined by increased percent of smooth muscle cells (SMCs) and necrotic core area and reduced percent of macrophages and DCs. The mice also displayed enhanced T-cell activation and a T_h1 bias in the periphery.

The CKO DCs themselves exhibited increased expression of IL-12 and a higher capacity to proliferate and polarize naive T cells to the T_h1 phenotype

in vitro. The DCs also showed decreased expression of STAT3, in line with the inhibitory effects of STAT3 on DC activation seen in previous studies. When STAT3 was overexpressed in DCs *in vitro*, IL-12 was down-regulated, but its expression increased significantly on STAT3 inhibition using a mutant vector. In addition, when STAT3 was overexpressed in DCs *in vivo* using a Cre-regulated lentiviral system, the mice showed decreased plaque formation compared to controls. Interestingly, the effects of STAT3 modulation were similar in WT and CKO mice, intending that STAT3 lies downstream of HIF1 α . Finally, using a chromatin immunoprecipitation assay (ChIP), it was confirmed that HIF1 α binds to hypoxia responsive elements (HREs) in the *Stat3* gene promoter thus regulating its expression. When DCs lack HIF1 α , STAT3 expression is not stimulated and hence IL-12 production by DCs is uninhibited. This excessive IL-12 can activate naive T cells and polarize them to the T_h1 phenotype, thereby enhancing atherosclerotic plaque progression.

This project thus concludes that HIF1 α restrains DC activation via STAT3 generation and prevents excessive production of IL-12 that helps to keep inflammation and atherosclerosis under check.

ZUSAMMENFASSUNG

Atherosklerose ist die zugrundeliegende Ursache kardiovaskulärer Erkrankungen und stellt weltweit eine bedeutende Gesundheitsgefahr dar. An der Erkrankung ist nicht nur eine Anreicherung von Lipiden in der Gefäßwand beteiligt, sondern auch eine chronische Entzündungsantwort, welche durch hochspezifische zelluläre sowie molekulare Reaktionen vermittelt wird. Makrophagen und dendritische Zellen (DCs) sind essentiell an der Aufnahme von modifizierten Lipiden sowie deren Präsentation gegenüber T und B Lymphozyten beteiligt, die ihrerseits wiederum Immunantworten fördern. Eine lokal gesteigerte Aktivierung, Migration und Akkumulation inflammatorischer Zellen trägt letztlich zur Bildung atherosklerotischer Plaques bei.

Atherosklerotische Plaques werden aufgrund reduzierter Sauerstoff-Diffusion und hoher metabolischer Aktivität der akkumulierten Zellen hypoxisch. Die verschiedenen Immunzellen sind lokal hypoxischen Bedingungen sowie systemisch inflammatorischen Stimuli ausgesetzt, wodurch sie Hypoxie-induzierten Faktor 1a (HIF1 α) hochregulieren. Obwohl die Bedeutung von HIF1 α in Makrophagen und Lymphozyten weitgehend aufgeklärt ist, ist dessen Rolle in DCs immer noch umstritten, insbesondere in Bezug auf Atherosklerose. In diesem Projekt wurde die Rolle von HIF1 α in DCs mittels eines zellspezifischen Knockout Mausmodells untersucht, in welchem HIF1 α in CD11c⁺ DCs deletiert wurde.

Schnitte der Aortenwurzel aus atherosklerotischen Mäusen zeigten das Bestehen von Hypoxie und die Hochregulation von HIF1 α , welches mit CD11c⁺ Zellen kolokalisierte. DCs aus der Milz atherosklerotischer Tiere wiesen ebenfalls eine erhöhte Expression von HIF1 α auf, was eine nicht-hypoxische Stimulation von HIF1 α aufgrund systemischer Inflammation beweist. Konditionelle Knockout (CKO) Mäuse zeigten im Ausgangszustand keine Veränderung der Immunantwort was einen Einfluss von HIF1 α unter ausschließlich inflammatorischen Bedingungen nahelegt. Eine achtwöchige atherogene Diät dieser Mäuse im *Ldlr*^{-/-} Hintergrund resultierte in der Entwicklung größerer Plaques mit gesteigerter T Zell Infiltration im Vergleich zu wildtypischen (WT) Kontrollen. Die Plaques wiesen einen komplexen Phänotyp auf, der sich durch einen erhöhten prozentualen Anteil glatter

Muskelzellen, nekrotischer Fläche sowie einen verminderten prozentualen Anteil an Makrophagen auszeichnete. Die Mäuse zeigten ferner eine erhöhte T Zell Aktivierung und eine Tendenz zur Th1 Antwort in der Peripherie.

In vitro zeigten die konditionellen knockout DCs eine gesteigerte IL-12 Expression und eine gesteigerte Fähigkeit die Proliferation naiver T Zellen zu induzieren beziehungsweise in Richtung Th1 zu polarisieren. Die DCs wiesen ferner eine verminderte STAT3 Expression auf. Dies stimmt mit den in früheren Studien beobachteten inhibitorischen Effekten von STAT3 auf die Aktivierung von DCs überein. Eine Überexpression von STAT3 in DCs *in vitro* führte zu einer Herunterregulation von IL-12. Bei Inhibition von STAT3 mittels eines mutierten Vektors steigerte sich die Expression jedoch signifikant. Ferner führte eine STAT3 Überexpression in DCs mittels eines Cre-regulierten lentiviralen Systems *in vivo* zu einer verminderten Plaqueformation in den Mäusen im Vergleich zu Kontrollen. Interessanterweise waren die Auswirkungen der STAT3 Modulation in WT und CKO Mäusen ähnlich, was vermuten lässt, dass STAT3 HIF1 α nachgeschaltet ist. Mittels eines Chromatin Immunpräzipitations-Assays wurde letztlich bestätigt, dass HIF1 α an Hypoxie-responsive Elemente im *Stat3* Genpromotor bindet und dadurch seine Expression reguliert.

Wenn DCs HIF1 α fehlt wird keine STAT3 Expression gefördert, was eine ungebremste IL-12 Produktion durch DCs zur Folge hat. Dieses überschüssige IL-12 Sekretion kann naive T Zellen aktivieren und in Richtung eines Th1 Phänotyps polarisieren, wodurch das Voranschreiten atherosklerotischer Plaques gefördert wird.

Dieses Projekt kommt folglich zu dem Schluss, dass HIF1 α die Aktivierung von DCs über STAT3-Bildung beschränkt und eine übermäßige Produktion von IL-12 verhindert, wodurch Inflammation und Atherosklerose im kontrolliert werden.

ABBREVIATIONS

Ab	Antibody
ABTS	2,2'-azino-bis(3-ethylbenzothiazoline-6-sulphonic acid)
AhR	Aryl hydrocarbon receptor
APC	Antigen presenting cell
APC	Allophycocyanin
ApoE	Apolipoprotein E
ATP	Adenosine triphosphate
BM	Bone marrow
BMDC	Bone marrow derived dendritic cell
β -ME	Beta mercaptoethanol
BMM	Bone marrow derived macrophage
BMT	Bone marrow transplantation
BSA	Bovine serum albumin
CAD	Coronary artery diseases
CCR	Chemokine receptor
CD	Cluster of differentiation
cDC	Conventional dendritic cell
cDNA	Complementary DNA
CFSE	Carboxyfluorescein succinimidyl ester
ChIP	Chromatin immunoprecipitation assay
CKO	Conditional knockout
CLP	Common lymphoid precursor
CMP	Common myeloid precursor
CMV	Cytomegalovirus
CO ₂	Carbon dioxide
Cre	Cre recombinase
Ctrl	Control

CVD	Cardiovascular diseases
CXCR	Chemokine receptor
Da	Dalton
DAB	3,3'-Diaminobenzidine
DAPI	4',6-Diamidino-2-phenylindole
DC	Dendritic cell
DDW	Double distilled water
DEAE	Diethylaminoethanol
D-MEM	Dulbecco's modified Eagle's medium
DNA	Deoxyribonucleic acid
dNTP	Deoxyribonucleotide triphosphate
D-PBS	Dulbecco's phosphate buffered saline
<i>E.coli</i>	<i>Escherichia coli</i>
EDTA	Ethylenediaminetetraacetic acid
ELISA	Enzyme linked immunosorbent assay
FACS	Fluorescence activated cell sorting
FBS	Fetal bovine serum
Fig	Figure
FITC	Fluorescein isothiocyanate
flox	Flanked by loxP sites
Flt3	FMS like tyrosine kinase 3
Flt3L	Flt3 ligand
FoxP3	Forkhead box P3
FSC	Forward scatter
Fwd primer	Forward primer
g	Relative centrifugal force
gDNA	Genomic DNA
GFP	Green fluorescent protein
GM-CSF	Granulocyte macrophage colony stimulating factor
GMP	Granulocyte and macrophage precursor

Gy	Gray
HAS	HIF1 α ancillary sequence
HBS	HIF1 α binding sequence
HBSS	Hank's balanced salt solution
HCl	Hydrochloric acid
H&E	Haematoxylin and Eosin
HEK	Human embryonic kidney
HEPES	4-(2-hydroxyethyl)-1-piperazineethanesulfonic acid
HIF	Hypoxia-inducible factor
HLA	Human leukocyte antigen
HPRT	Hypoxanthine-guanine phosphoribosyltransferase
HRE	Hypoxic response element
HRP	Horse radish peroxidase
HSC	Hematopoietic stem cell
IFN	Interferon
Ig	Immunoglobulin
IGF1	Insulin like growth factor 1
IgG	Immunoglobulin isotype G
I κ B α	Inhibitors of κ B alpha
IKK α	I κ B kinase alpha
IL	Interleukin
iNOS	Inducible nitric oxide synthase
i.p.	Intraperitoneal
i.v.	Intravenous
k	kilo
LB	Lysogeny broth
LDL	Low-density lipoprotein
LDLR	LDL receptor
lin	Lineage
LN	Lymph node

LN ₂	Liquid nitrogen
loxP	Locus of X over P1
LPS	Lipopolysaccharide
LysM	Lysozyme M
mAb	Monoclonal antibody
MACS	Magnetic activated cell sorting
M-CSF	Macrophage colony stimulating factor
M-DC	Macrophage and DC precursor
MEP	Megakaryocyte and erythrocyte precursor
MFI	Mean fluorescence intensity
MHC	Major histocompatibility complex
MOI	Multiplicity of infection
MPP	Multipotent progenitors
MRC1	C-type mannose receptor 1
mRNA	Messenger RNA
N ₂	Nitrogen
NFκB	Nuclear factor kappa light chain enhancer of activated B cells
NK	Natural killer
NO	Nitric oxide
NOS2	Nitric oxide synthase 2
O ₂	Oxygen
OCT	Optimal cutting temperature
O/N	Overnight
OVA	Ovalbumin
oxLDL	Oxidized low-density lipoprotein
PBS	Phosphate buffered saline
PCR	Polymerase chain reaction
pDC	Plasmacytoid dendritic cell
PE	Phycoerythrin

PerCP	Peridinin chlorophyll
PFA	Paraformaldehyde
PHD	Prolyl hydroxylase
PMA	Phorbol 12-myristate 13-acetate
PMSF	Phenylmethylsulfonyl fluoride
P/S	Penicillin and Streptomycin
PVDF	Polyvinylidene fluoride
qPCR	Quantitative real time PCR
RAR	Retinoic acid receptor
RBC	Red blood cell
Rev primer	Reverse primer
RIPA	Radioimmunoprecipitation assay
RNA	Ribonucleic acid
ROR γ t	RAR related orphan receptor γ t
ROS	Reactive oxygen species
rpm	Rotations per minute
RPMI	Roswell park memorial institute
RT	Room temperature
SAV	Streptavidin
SD	Standard deviation
SDS	Sodium dodecyl sulphate
SEM	Standard error of mean
siRNA	Small interfering RNA
SMC	Smooth muscle cell
SOCS	Suppressors of cytokine signaling
SSC	Sideward scatter
STAT	Signal transducers and activators of transcription
TAE	Tris acetate EDTA
TBS	Tris buffered saline
TGF β	Transforming growth factor beta

Th	Helper T cell
TLR	Toll like receptor
TMB	3,3',5,5'-Tetramethylbenzidine
TNF α	Tumor necrosis factor alpha
T _{reg}	Regulatory T cell
Tris	Tris(hydroxymethyl)aminomethane
UTR	Untranslated region
VEGF	Vascular endothelial growth factor
WT	Wildtype

1. INTRODUCTION

1.1 Dendritic cells

1.1.1 Origin of dendritic cells

Dendritic cells (DCs) were first described in the skin by Paul Langerhans in 1868, when he believed them to be nerve cells. Steinman and Cohn later identified DCs as antigen presenting cells (APCs) and noted that they originated in the bone marrow (BM) and were mainly present in the spleen where they made up 1 – 1.6% of total nucleated cells^{1,2}. Steinman also provided a description of their morphology, distribution and functions and listed histological stains to distinguish them from other cell types, mainly macrophages.

DCs have been shown to have a myeloid origin. The common myeloid precursors (CMPs) give rise to DCs, monocytes and macrophages as well as granulocytes and erythrocytes³⁻⁵. The MHCII negative myeloid progenitors from the BM develop into DCs in the presence of granulocyte macrophage colony stimulating factor (GM-CSF), these DCs being distinct from other cells in that they have high levels of MHCII and are capable of stimulating a T-cell immune response⁴. Murine DCs are commonly obtained from BM hematopoietic stem cells *in vitro* by culturing them with GM-CSF for 7-12 days to obtain high numbers of pure and functionally viable DCs^{6,7}. Human and murine DCs are also capable of differentiating from blood or BM monocytes in the presence of GM-CSF and IL-4 both *in vitro* and *in vivo*⁸⁻¹¹. This further demonstrates the common myeloid origin of DCs and phagocytic monocytes (**Figure 1.1**).

The presence of lymphoid specific markers like CD8 α , CD4, CD2, BP1 and CD25 on DCs from mouse spleens and LNs suggests that some DCs have a lymphoid origin. The common lymphoid precursors (CLPs) that generally give rise to T cells, B cells and natural killer (NK) cells are capable of differentiating into DCs both *in vitro* and *in vivo*^{3,12,13}. Though CLPs show a bias towards producing the CD8⁺ DC population, they are capable of generating all types of splenic and thymic DC subsets^{12,14}.

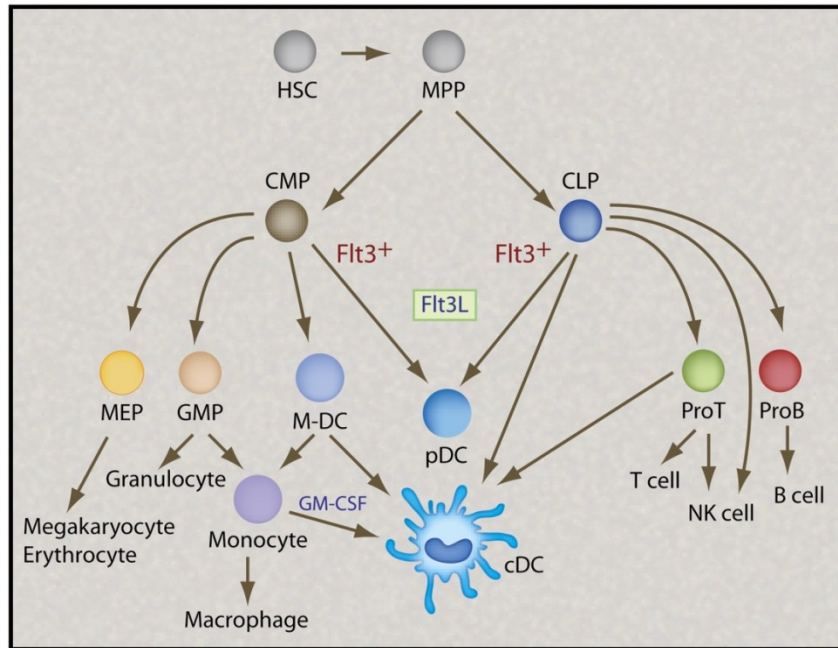


Figure 1.1 DC development from BM; hematopoietic stem cells can occur via both the CMPs or the CLPs. Source: Wu and Liu 2007³.

1.1.2 DC markers and subtypes

DCs are commonly known to express the integrins CD11c and CD11b, the multi-lectin receptor CD205 and the antigen presenting complex MHCII along with co-stimulatory molecules CD40, CD80 and CD86^{15,16}. Depending on expression levels of CD8, CD4, CD205 and CD11b on the surface of DCs, origin, surrounding tissues and location; DCs are divided into various subtypes. Broadly speaking, DCs can be sub-divided into conventional DCs (cDCs) and plasmacytoid DCs (pDCs). cDCs are classical DCs with high expression of CD11c and CD11b and could be lymphoid (CD8^{hi}CD205^{hi}CD11b⁻) or myeloid (CD8⁻CD205^{-/+}CD11b⁺) DCs. Though originally the lymphoid and myeloid subtypes were thought to derive from their particular origin lineages, it is now known that this is not entirely true and the expression of CD4 and CD8 on DCs vary irrespective of their origins^{16,17}. On the basis of location, cDCs are differentiated as resident (MHCII^{lo}, high phagocytic capacity) or migratory (MHCII^{hi}, low phagocytic capacity) and clearly show varied functions^{18,19}. cDCs are the prime APCs and are distinguished by their secretion of the cytokine IL-12, ability to activate and polarize T cells and by the presence of toll like receptors (TLRs) 2 and 4 on

their surface. On the other hand, pDCs are circulating cells, express TLRs 7 and 9, lack CD11b and distinctly produce IFN α in response to viruses. Human pDCs are characterized by the presence of CD303 or CD123 whereas murine pDCs typically express CD45RA and BST2²⁰⁻²². The DCs mentioned in this thesis refer to cDCs specifically.

1.1.3 Relation of DCs to monocytes and macrophages

Under certain inflammatory conditions, monocytes express and up-regulate the DC marker CD11c along with MHCII and co-stimulatory molecules, acquiring a DC phenotype but retaining functional characteristics of monocytes²³. In mice, 40% of the monocytes and alveolar macrophages express CD11c¹⁷. Also, under inflammatory conditions of hypercholesterolemia monocytes up-regulate CD11c that plays an important role in monocyte recruitment and atherosclerosis development²⁴. This makes it difficult to phenotypically analyze DCs and separately distinguish the DC subset from the monocyte-macrophage population.

Since the surface marker expression of DCs, monocytes and macrophages have been critically analyzed and studied; it is becoming clear that the mononuclear phagocyte cell family is highly heterogeneous. The various cells can differentiate into each other and show high adaptability and plasticity depending on immune conditions. These cells also share various markers that change expression considerably during their life cycle or with origin, location and immune challenge making it difficult to characterize them specifically into subtypes and define them phenotypically and functionally^{17,25}.

1.1.4 CD11c marker and the CD11c-cre mouse model

Despite the limited specificity of the CD11c molecule, it is the most commonly used marker for identifying DCs and generating DC conditional knockout (CKO) mice. The B6.Cg-Tg(I $tgax$ -cre)1-1Reiz/J mouse model (commonly called *CD11c-cre*) was first developed in the lab of Boris Reizis to study Notch signaling in DCs. Cre-mediated recombination was detected in more than 95% cDCs and very low levels of recombination were seen in lymphocytes (<10%), NK cells (12%) and myeloid cells (<1%)²⁶. This mouse

model is a universally accepted model for deleting the required gene from the DC lineage by the Cre-flox system or to deplete DCs using a diphtheria toxin model²⁷⁻²⁹. Considering the efficiency and universal acceptability of this mouse model, it was used in this project to delete the gene of interest from DCs and any monocyte-macrophage contributions to the effects seen have been clarified by other experimental methods.

1.1.5 Functions of DCs

DCs are a part of both the innate and adaptive arms of the immune system and hence form a bridge between the two, leading to a potent defense in an immune response. Innate immunity represents the first barrier against an immune attack and is an essential first line defense. DCs, like macrophages, have phagocytic capacity, though only to a limited extent. Phagocytosis for the purpose of clearance and killing is not as pronounced in DCs as for antigen processing and presentation³⁰.

DCs induce tolerance of T cells both centrally and in the periphery. Central tolerance is induced in the thymus by specialized intrathymic non-migratory DCs that lead to apoptotic death of potentially self-reactive T cells^{16,31,32}. Peripheral tolerance is maintained by DCs outside of the thymus. Various theories exist to explain how DCs balance between tolerance and immunity. One line of thought suggests the presence of a specialized type of regulatory DC in the periphery, solely responsible for tolerance³³, whereas a second concept is based on the fact that tolerance is induced by immature DCs or mature but quiescent DCs while immunity is induced by mature and fully activated DCs³⁴⁻³⁶.

Immature DCs are adept at endocytosis and express very low levels of MHC molecules on their surface. Though MHC molecules are constantly produced, they are sequestered in the endocytic compartment^{37,38}. DCs patrol body surfaces and mature or are activated on encountering inflammatory cytokines or on recognition of special microbial products – CpG motifs in bacterial DNA, double stranded RNA from viruses, LPS from bacterial walls, or heat shock proteins from necrotic cells using pattern recognition receptors or TLRs on their surface¹⁶. DCs take up these antigens, migrate to lymphocyte

rich areas in the lymph nodes and spleen and can then effectively process and present the peptide fragments of protein antigens on MHC molecules to lymphocytes rather than simply digesting them. Exogenous antigens are presented on MHC class II molecules whereas endogenous or self-antigens are presented on MHC class I. Mature DCs have enhanced expression of MHC on their surface and hence a distinct capacity to activate lymphocytes but low antigen uptake compared to their immature counterparts. Mature DCs also begin to release large amounts of cytokines to further the inflammatory response^{30,37,38}.

1.1.6 DCs regulate helper T-cell balance

One of the most important roles of DCs is directing a helper T-cell response. Apart from presenting antigens to naive T-cell receptors via MHC molecules, the co-stimulatory molecules on DCs send activating signals to T cells through CD28 and additionally release cytokines to direct T-cell responses. These triggers cause not only T-cell proliferation but also polarize them to one of the many T helper cell subsets³⁹⁻⁴² (**Figure 1.2**).

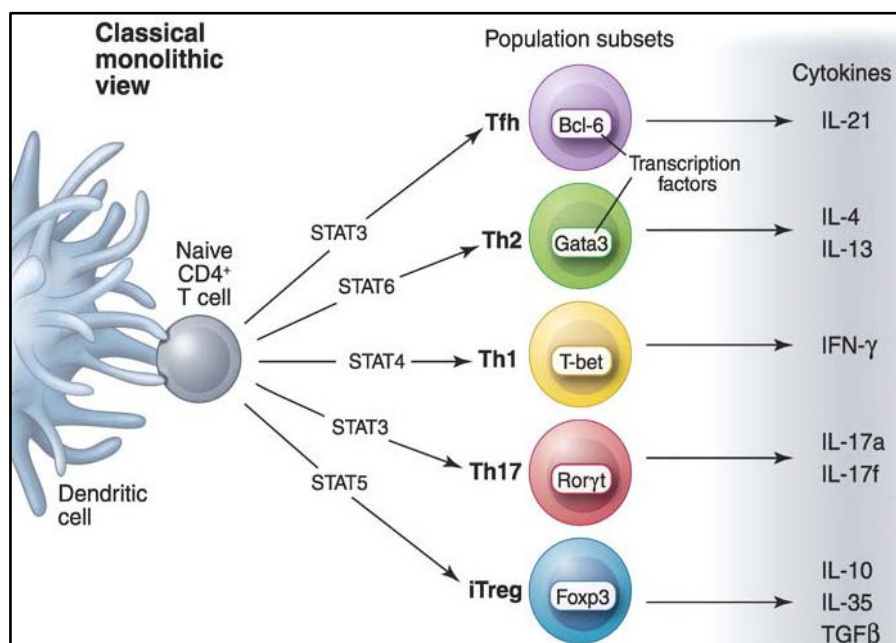


Figure 1.2 DCs polarize naive CD4 T cells to one of the many helper T-cell subsets which are defined by up-regulation of a certain transcription factor and release of signature cytokines. Source: O'Shea and Paul 2010⁴³.

The most important of these are the pro-inflammatory T_h1 and the essentially anti-inflammatory T_h2 responses that are balanced and well regulated by DCs^{44,45}. DCs, along with macrophages, induce a T_h1 response by secretion of IL-12^{46,47}. Via the JAK-STAT pathway, T_h1 cells up-regulate the transcription factor T-bet which leads to enhanced production of effector cytokine IFN γ ^{48,49}. IFN γ directs a pro-inflammatory response by polarizing other naive T cells to T_h1 and inhibiting T_h2 responses. It orchestrates the activation and migration of other immune cells like macrophages and NK cells among a variety of other functions to counter the immune threat. It also acts in a positive-feedback loop to induce DCs to produce more IL-12^{49,50}. The importance of the IL-12-IFN γ axis in immune responses is confirmed by studies which show that IL-12 or IFN γ deletion, deficiency or unresponsiveness leads to higher incidence of tumor formation and infections but reduced autoimmune disorders like diabetes, systemic lupus erythematosus or experimental neuritis in both mice and humans⁵¹. CD11b⁻CD8 α ⁺ DCs are considered to be major T_h1 inducers, whereas CD11b⁺CD8 α ⁻ DCs are shown to induce polarization of CD4 T cells to the T_h2 phenotype⁵². The factors responsible for induction of a T_h2 response by DCs are not clearly understood and no specific cytokine released by DCs is known to noticeably induce T_h2 responses. Though earlier studies implicated DC derived IL-4 or IL-6 in this process, it is now known that these cytokines are not firm T_h2 inducers and play a variety of roles in both T_h1 and T_h2 responses⁵³⁻⁵⁵. Some studies point to the fact that T_h2 is a default pathway that exists in the absence of a T_h1 pathway and hence absence of IL-12 leads to T_h2 induction. DCs have also been shown to produce IL-4 or TGF β in order to inhibit IL-12 production and indirectly influence a T_h2 response⁵⁵. Also the co-stimulatory protein B7-H2 is known to induce T_h2 responses⁵⁶. T cells stimulated towards a T_h2 response up-regulate the transcription factor GATA3 and release cytokines IL-4 and IL-10 mainly but also IL-13 and IL-5 which are all anti-inflammatory cytokines. T_h2 responses affect B cells and eosinophils and are mainly implicated in hypersensitivity reactions and graft-versus-host disease (GVHD)^{55,57}.

Apart from the classical T_h1/T_h2 balance, other T helper cell subsets essentially controlled by DCs and holding great importance in progression of

immune responses are the T_{h17} and T_{reg} cell types. $TGF\beta$ is responsible for differentiation of both the T_{h17} and T_{reg} pathways. $TGF\beta$ alone causes a T_{reg} induction whereas the presence of IL-6 along with $TGF\beta$ abrogates T_{reg} differentiation and instead polarizes naive T cells to the T_{h17} phenotype⁵⁸. Absence of IL-6 in mice causes enhanced generation of T_{regs} but reduced T_{h17} population⁵⁹. Naive T cells up-regulate the transcription factor ROR γ t and release cytokines IL-17a/f, IL-22 and IL-23 to become T_{h17} cells⁶⁰, whereas they up-regulate the transcription factor FOXP3, express high levels of CD25 and release $TGF\beta$, IL-10 and IL-35 to become T_{regs} . Originally T_{h17} cells have been identified as strong inducers of tissue inflammation and implicated in numerous autoimmune diseases with a pathogenic phenotype. This may hold true for classical IL-17 secreting T_{h17} cells, though newer variations in the transcription factors and cytokines in T_{h17} cells lead to alternative T_{h17} cells with varied functions. These T_{h17} cells are shown to produce IFN γ , IL-10 and GM-CSF in addition to classical cytokines⁶¹. The role of T_{h17} in various autoimmune and pathogenic diseases varies greatly and different studies provide contradicting data about its functions^{62,63}. T_{regs} , on the other hand, suppress immune activation and prevent self-reactivity, thus playing a protective role in autoimmune dysfunction and transplantation⁶⁴. T_{reg} functioning depends on affecting other effector T cells via cytokines but also by down-regulating co-stimulatory molecules and IL-12 on APCs⁶⁵⁻⁶⁷.

1.1.7 DC migration

DCs are highly efficient at migration to T cell rich areas, a unique characteristic that distinguishes them from macrophages⁶⁸. DCs patrol tissue surfaces and are abundantly present in the spleen. Once they encounter an antigen, they are activated and up-regulate various chemokine receptors, the most crucial of which is CCR7, which helps them to migrate towards ligands CCL21 and CCL19 in T cell rich areas of secondary lymphoid organs⁶⁹. They traffic to lymph nodes through the afferent lymph and encounter naive T cells where they present antigen and activate lymphocytes⁷⁰. DCs fail to migrate to lymph nodes and activate lymphocytes in mice deficient in CCR7, corroborating the importance of CCR7 in DC migration and function⁷¹.

1.2 Atherosclerosis

1.2.1 Atherosclerosis – a global burden

Atherosclerosis - an underlying cause of cardiovascular diseases (CVD) like ischemia, aortic aneurysm, myocardial infarction, heart diseases and stroke - is a chronic inflammatory disease increasingly threatening human health globally^{72,73}. CVD are the leading cause of death worldwide, accounting for around 16.7 million deaths each year, and predicted to increase to approximately 25 million deaths by 2020⁷⁴. The process of atherogenesis was initially thought to simply consist of accumulation of lipids within the arterial wall, however it is now clear that it is a chronic inflammatory disease involving highly specific cellular and molecular responses⁷⁵.

1.2.2 Pathogenesis of Atherosclerosis

Various risk factors for CVD – obesity, hypertension, smoking, diabetes, stress, increased lipid levels, lack of sleep and exercise, wrong diet, elevated and modified LDL, genetic alterations, infectious organisms, among others – have been identified and continue to increase worldwide^{74,75}. These risk factors cause injury and endothelial dysfunction in the arteries, which increases endothelial permeability and adhesiveness, leads to enhanced migration and proliferation of smooth muscle cells (SMCs) and thickening of the arterial wall⁷⁵. Inflammatory cells are attracted to the arterial wall in response to adhesion molecules and chemo-attractants and an additional activation of these cells leads to release of cytokines, chemokines and growth factors causing further damage and focal necrosis. The cycle of cellular migration, activation and damage continues leading to further enlargement and restructuring of the arterial wall forming arterial lesions. These lesions acquire a fibrous cap that covers a complex necrotic core consisting of cellular debris, lipids, foam cells and activated immune cells responsible for a full-blown inflammatory response. Platelets adhere to the dysfunctional endothelium and contribute to migration and proliferation of SMCs and immune cells. They release vasoconstricting and platelet aggregating substances that can recruit and activate more platelets from the blood. If the plaque becomes unstable, the fibrous cap ruptures leading to thrombosis and

occlusion of the artery. This process is eventually responsible for myocardial infarction, ischemic stroke or aortic aneurysm^{73,76,77} (Figure 1.3).

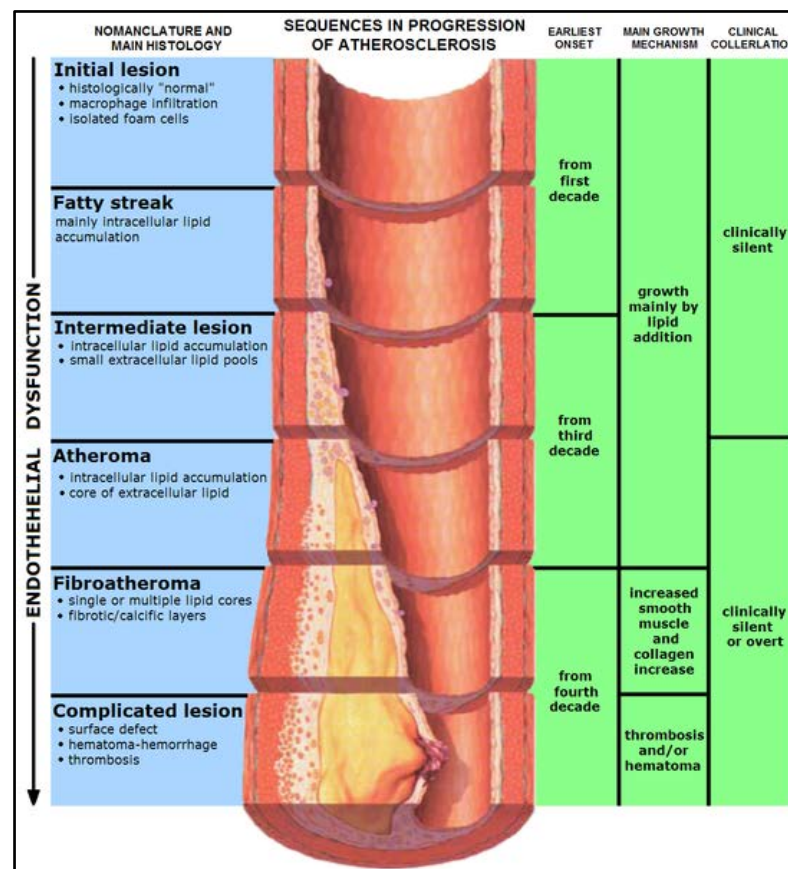


Figure 1.3 Atherosclerosis is a chronic inflammatory disease involving highly specific cellular and molecular responses and progresses through various stages leading to cardiovascular diseases. Source: Grahams Child at Wikimedia commons.

1.2.3 Monocytes and macrophages in atherosclerosis

Monocytes are considered to be the initiator cells in the immune progression of atherosclerosis. Monocytes develop in the BM and enter the blood stream. Patrolling blood monocytes are attracted to the site of endothelial dysfunction by chemo-attractants and adhesion molecules where they roll and adhere, then transmigrate through the endothelium⁷⁸. Macrophage colony stimulating factor (M-CSF) released by endothelial cells and SMCs converts the monocytes to macrophages and DCs which are potent phagocytic and antigen presenting cells^{79,80}. Macrophages up-regulate their scavenger receptors and TLRs and internalize modified LDL particles, leading

to accumulation of cholesterol and lipid deposits within the cell. Eventually these macrophages turn into lipid laden foam cells^{73,81}. Receptor activation and phagocytosis leads to release of a number of pro-inflammatory cytokines that help in recruitment, migration and activation of other cell types⁸². Macrophages that ingest lipids and other cellular debris have the potential to activate B and T cells at the vascular site or migrate to lymph nodes and present antigen to the lymphocytes there⁸³. At the plaque site, macrophages that develop into foam cells are responsible for increase in lesion size and occlusion of the vessel. These foam cells eventually undergo apoptosis owing to growth factor deprivation, oxidative stress and death receptor activation, forming necrotic cores⁸⁰. Mice lacking M-CSF have reduced numbers of macrophages and are protected from atherosclerosis, thus identifying a crucial pro-atherogenic role for macrophages^{84,85}

1.2.4 Dendritic cells in atherosclerosis

DCs bearing the CD11c marker have been detected in atherosclerosis prone areas of healthy arteries in both humans and mice⁸⁶⁻⁸⁸. These resident DCs are capable of accumulating lipids, forming foam cells, presenting antigens and initiating atherosclerosis⁸⁹. On the other hand, circulating DCs that patrol the body efficiently take up modified lipoproteins; migrate to lymph nodes and present antigens to T cells⁹⁰. With progression of atherosclerosis, the number of DCs in plaques increases due to proliferation of resident DCs, migration of circulating DCs which respond to chemokine signals from cells at the local site of inflammation and impaired egress of DCs from the plaque back into circulation^{91,92}. Simultaneously, certain macrophages have been shown to up-regulate the DC marker CD11c or convert to DCs under conditions of atherosclerosis making it difficult to identify and distinguish the two populations^{24,93}. The importance of DC migration and recruitment in atherosclerosis is evident from the fact that mice deficient in CX3CR1, CCL2 and CCR5 show reduced atherosclerotic burden due to impaired DC migration^{94,95}. Also, mice lacking CD74 - the invariant chain of MHCII necessary for DC motility and antigen presentation, show decreased atherosclerosis⁹⁶.

Oxidized LDL (oxLDL), the most commonly studied atherosclerosis antigen is shown to up-regulate HLA-DR, CD40, CD83, CD86 and CCR7 on DCs leading to DC maturation and activation⁹⁷. oxLDL has also been demonstrated to up-regulate scavenger receptors on DCs that are responsible for DC foam cell formation, cause enhanced secretion of pro-inflammatory cytokine IL-6 and decreased expression of anti-inflammatory IL-10 eventually aggravating vascular inflammation⁹⁸.

In bioengineered arteries, DCs were shown to stimulate CD4 T cells to produce IFN γ and infiltrate the arterial wall, thus initiating inflammation⁹⁹. Apart from the probable T_h1 modulating capacity of DCs in relation to atherosclerosis, DCs have also been shown to affect T_{reg} levels and subsequently influence atherosclerosis progression. In one study, CCL17 expressing DCs were shown to drive atherosclerosis by restraining T_{reg} homeostasis whereas in another paper, *Flt3*^{-/-} mice that lacked the classical CD103⁺ aortic DCs showed reduced numbers of T_{regs} and enhanced atherosclerosis indicating a protective role for Flt3 signaling dependent DCs^{100,101}. Another evidence for the protective role of DCs comes from a study where transfer of oxLDL loaded DCs led to protection rather than aggravation of atherosclerosis in *Ldlr*^{-/-} mice¹⁰². Despite such extensive research, the function and relevance of DCs in atherosclerosis remains poorly understood.

1.2.5 T cells in atherosclerosis

10% of the cells in the atherosclerotic plaque are T cells and the ratio of CD4⁺ to CD8⁺ cells is similar to that found in blood. Most T cells are $\alpha\beta$ type though a few $\gamma\delta$ T cells also exist in plaques⁷³. T cells are first activated in the lymph nodes in response to athero-specific antigens presented by migrating APCs. Here the T cells get activated and the CD8 cells become effector/memory cells whereas the CD4 cells polarize to helper subsets. Activated T cells home towards the plaque in response to adhesion molecules and chemokines. A further round of antigen presentation and stimulation takes place at the local site of inflammation where accumulated macrophages and DCs of the plaque enhance the immune activation of T cells. oxLDL in the plaque forms the major antigen for activation and T cells reactive to oxLDL

have been shown to be of the T_h1 phenotype¹⁰³. Systemically, T_h1 cells are the predominant subtype in atherosclerotic lesions of both humans and mice. Human plaques contain cells producing IFN γ , IL-12, IL-15, IL-18 and TNF α but few cells that produce the T_h2 cytokine IL-4^{104,105} giving further evidence to the hypothesis that atherosclerosis is a T_h1-mediated disease. In hypercholesteremic mice lacking IFN γ or its receptor, atherosclerosis was drastically reduced^{106,107}. Also, administration of recombinant IFN γ to mice led to enhanced atherosclerosis¹⁰⁸. IFN γ is known to activate macrophages, induce them to produce pro-inflammatory cytokines, pro-thrombotic and vasoactive mediators as also inhibit endothelial cell proliferation and decrease proliferation, differentiation and collagen production of VSMCs, thus making plaques unstable⁷³. Injection of IL-12 also promotes early lesion formation whereas deletion in mice leads to decreased atherosclerotic burden¹⁰⁹⁻¹¹¹, suggesting the importance of IL-12 in atherosclerosis progression and its importance in T_h1 polarization to generate IFN γ ⁺ cells. Other studies also observe decreased atherosclerotic plaque on deletion of IL-18, TNF α and T-bet proving a T_h1 mediated pathway for atherosclerosis¹¹²⁻¹¹⁴.

Studies targeting T_h2 cells see either pro-atherogenic effects, protective effects or no significant changes at all, making it difficult to assign a specific function to T_h2 cells in atherosclerosis progression^{76,109,115,116}. Contradictory data also exists for T_h17 cell functions in atherosclerosis¹¹⁷. IL-17 has been detected in human atherosclerotic plaque and studies in mice inhibiting IL-17 or with IL-17 deficiency show decreased plaque burden suggesting a pro-atherogenic role of the T_h17 subtype¹¹⁸⁻¹²³. On the other hand enhanced IL-17 in mice, due to a deletion of *Socs3* led to decreased atherosclerosis, hinting at a regulatory role for IL-17 in disease development¹²⁴. Some other studies also show no correlation between IL-17 and plaque phenotype^{125,126}. Low numbers of FoxP3⁺ cells have also been found in plaques and clear atheroprotective effects have been attributed to T_{regs} and their cytokines TGF β and IL-10¹²⁷⁻¹²⁹. All the extensive studies on T cells in atherosclerosis emphasize on the crucial role of T cells in atherosclerosis and specifically of the T helper subset T_h1 in progression of the disease^{73,76}.

1.2.6 Mouse models to study atherogenesis

Most clinical and retrospective studies in atherosclerosis involve non-invasive imaging or use of cells and tissues from symptomatic humans. Commonly, carotid artery endarterectomy or biopsy samples are used. Rabbits, pigs and non-human primates have also been used for experimental atherosclerosis studies, though genetically modified mice are commonly favored due to the ease of use and ethical regulations¹³⁰.

Two different mouse models have been commonly used to study atherogenesis. The *ApoE*^{-/-} mice lack Apolipoprotein E which is a key component in cholesterol metabolism. It helps in transport of lipids to the blood and is mainly synthesized in the liver, brain and macrophages. *ApoE*^{-/-} mice develop spontaneous cholesteremia and atherosclerotic disease, exacerbated by an atherogenic diet, which can progress to myocardial infarction and stroke^{131,132}. These mice show complex lesions that can progress from foam cell stage to fibro-proliferative stage with well-defined fibrous caps and necrotic core¹³³. On the other hand, *Ldlr*^{-/-} mice are deficient in the low-density lipoprotein receptor (LDLR) which mediates endocytosis of cholesterol rich LDL. These mice develop modest hypercholesterolemia when fed a normal diet but develop atherosclerotic lesions when fed a high fat diet¹³⁴. These lesions are predominantly made of lipid-laden macrophages and develop necrotic cores and calcification after prolonged feeding of high fat diets¹³⁵.

The *ApoE*^{-/-} mouse model has long been favored due to the spontaneous generation of complex atherosclerotic lesions. But the drawbacks with this mouse model are the extensive lesion formation leading to masking of smaller effects, dependency of disease progression on age of mice used and the dissimilarity in lipid metabolism and profile when compared with humans. Since the ApoE lipoprotein also plays a role in macrophage functions and adipose tissue biology, the effects seen in atherosclerosis could be attributed to this rather than a change in lipid profile. On the other hand, the *Ldlr*^{-/-} model is more closely comparable to human metabolism and lipid profile and hence gives better insight into atherosclerotic progression with respect to clinical studies. The lesion development is also slow and stable and can be

enhanced and controlled with appropriate diet and duration¹³⁶. The LDLR does not have any important functions apart from lipid metabolism and hence its deficiency does not interfere with any immune mechanisms under study. Also, unlike ApoE, LDLR is not present on BM cells, making it suitable for use in models of bone marrow transplantation (BMT)¹³⁰.

These mice models have been used to study disease progression or crossed with mice carrying deletions in target genes to study the role of such genes in atherosclerosis. Also, BMT of and spleen cell transfer to the *ApoE*^{-/-} and *Ldlr*^{-/-} mice has been used extensively to study the role of BM derived cells in disease development⁷³.

1.3 Hypoxia-inducible factor 1 α

1.3.1 Hypoxia and oxygen homeostasis in cells

In eukaryotic cells, oxygen acts as the final electron acceptor in the respiratory chain and as a substrate for energy production in aerobic organisms. The electrons transferred in the process interact with O₂ to form H₂O, but a fraction of electrons can combine with O₂ prematurely leading to the formation of reactive oxygen species (ROS). ROS react with biomolecules, change their properties and finally result in cellular dysfunction or death. In cases of decreased O₂ concentration, cells respond by enhanced release of ROS, hence setting a trigger to cope with the decreased O₂ levels. Reduced levels of O₂ also lead to deficient ATP production and hence energy deprivation of cells. As a result, cells have been equipped with highly elaborate mechanisms to maintain O₂ homeostasis^{137,138}. Even though environmental O₂ concentration is maintained at ~21% O₂, cellular O₂ levels are found to be about 16% in pulmonary alveoli and 6% in most other tissues. If the O₂ concentration falls below normal levels, as low as ~1% in some tissues, the resulting medical condition is termed hypoxia^{139,140}. Hypoxia is a common occurrence in the tumor microenvironment, transplanted organs, trauma, infection and inflamed tissues. In order to maintain oxygen homeostasis, hypoxic cells induce a set of molecules which are proficient in counteracting the harmful effects of hypoxia and returning the cells to a state

of normal oxygen stability¹⁴¹. The most important molecules in this process are the transcription factors called Hypoxia-inducible factors (HIFs).

1.3.2 Biology of the Hypoxia-inducible factors

The HIF protein complex was first discovered by Gregg Semenza in 1992 as a transcriptional inducer of the erythropoietin (EPO) gene under hypoxic conditions¹⁴². Later it was characterized to be a basic helix-loop-helix heterodimer whose expression is regulated by oxygen. The complex was made of a 120kDa HIF α subunit and a 91-94kDa HIF1 β subunit¹⁴³. The HIF1 β subunit is a constitutively expressed nuclear translocator that binds to a transcription factor or receptor subunit and aids in transport of the protein to the nucleus. It is also called Aryl hydrocarbon receptor nuclear translocator (ARNT) as it binds and activates the AhR ligand bound receptor¹⁴⁴. The HIF α subunits are only stable under hypoxic conditions and are continuously produced and degraded in the presence of O₂ via an ubiquitin proteasome pathway. In normoxia, the oxygen dependent Prolyl hydroxylases (PHDs) are active and cause hydroxylation of the HIF α subunits¹⁴⁵. The hydroxylated HIF α molecules are then polyubiquitinated by the von Hippel-Lindau tumor suppressor protein (VHL) and ultimately degraded by proteasomes¹⁴⁶. Under conditions of hypoxia, the O₂ requiring PHDs become inactive and cannot tag the HIF α molecules for degradation. This leads to increased abundance of HIF α molecules in the cytoplasm which then associate with the HIF1 β proteins and are transported to the nucleus. Here the HIF complex binds to target promoter sequences known as hypoxic response elements (HREs) (core sequence **5'-RCGTG-3'**), leading to transcription of various genes involved in response to hypoxic stress, metabolism, glycolysis, proliferation, angiogenesis, apoptosis and inflammation among many other pathways, leading to optimization of cell energetics and homeostasis for survival and function in hypoxic environments^{139,147,148} (**Figure 1.4**).

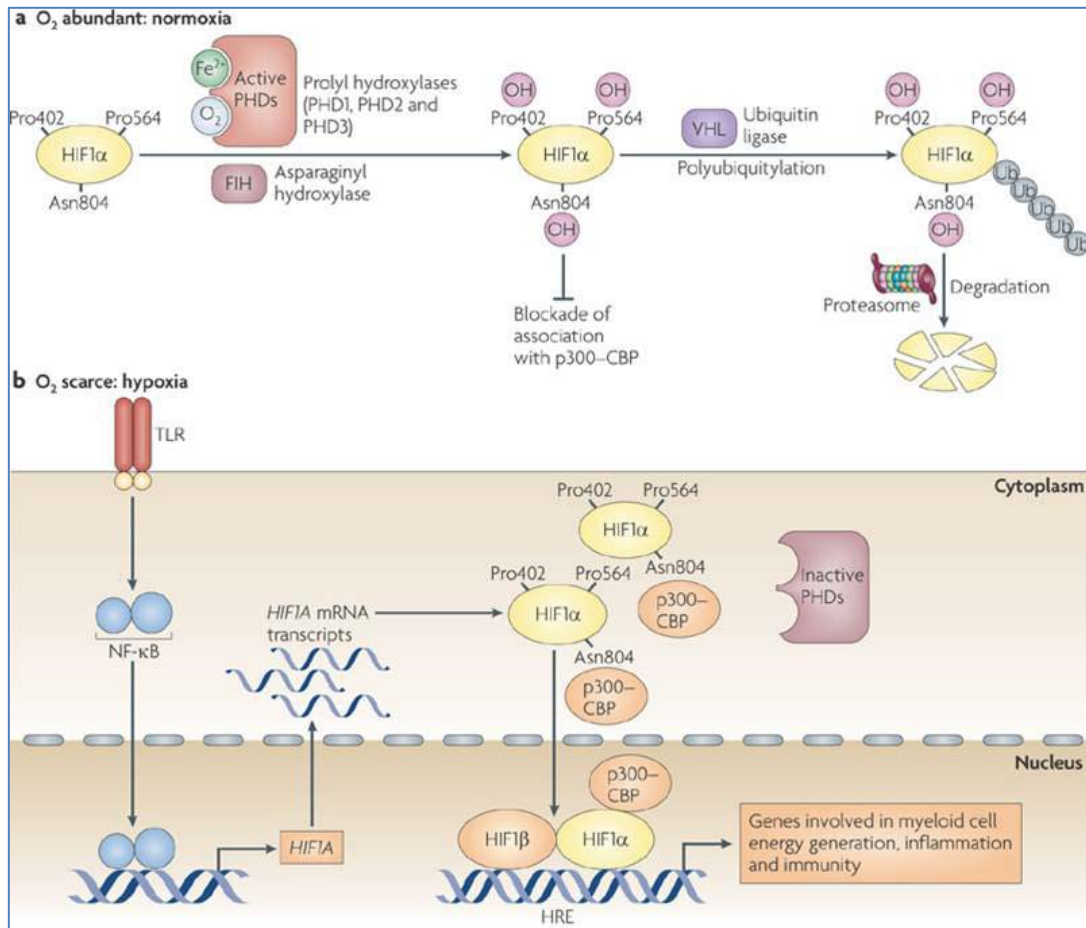


Figure 1.4 HIF1 α is continuously produced but degraded by oxygen dependent Prolyl hydroxylases under normoxia. In conditions of hypoxia, Prolyl hydroxylases become inactive and HIF1 α is stabilized. Source: Nizet and Johnson 2009¹³⁹.

The α subunits are of 3 types – HIF1 α , HIF2 α or HIF3 α . HIF1 α is the key molecule ubiquitously present in all cell types and has a general role in multiple physiological responses to hypoxia. Complete deletion of HIF1 α in mice leads to lethal embryonic defects in vascular development and morphology^{139,149-151}. HIF2 α on the other hand is predominantly present in the lung, endothelium and carotid body. It shares 48% amino acid sequence identity with HIF1 α and hence also shares some structural and biochemical similarities^{152,153}. HIF3 α is also expressed in a variety of tissues but is shown to act as a negative regulator of HIF1 α , thus contributing to a feedback loop activity^{148,154}. HIF1 α and HIF2 α are more extensively studied and research on HIF3 α is rare. Literature suggests that HIF1 α and HIF2 α show contradicting functions, though the detailed role of HIF2 α is still unclear and under

study^{155,156}. HIF1 α is a more established molecule and has proven to be an essential regulator in every cell type, and hence forms the basis of study of this thesis project.

1.3.3 Non-hypoxic regulation of HIF1 α

Further research on the activation and functions of HIF1 α proved that it can also be regulated under non-hypoxic conditions. In vascular smooth muscle cells; Angiotensin II, thrombin and platelet derived growth factor were shown to activate HIF1 α and in turn VEGF, implicating roles in angiogenesis. This activation was later revealed to be mediated via mitochondrial derived ROS^{157,158}. Other hormones and growth factors, like prostaglandin E2, insulin and insulin like growth factor have also been shown to activate HIF1 α ¹⁵⁹⁻¹⁶¹. Interestingly, HIF1 α is efficiently activated by a number of pro-inflammatory cytokines like IL-1 β , IFN γ and TNF α demonstrating an important role of HIF1 α in immune mechanisms¹⁶²⁻¹⁶⁸. Additionally, LPS was implicated to be a potent HIF1 α activator in macrophages, monocytes, DCs and fibroblasts acting via TLR4 and using the NF κ B pathway¹⁶⁹⁻¹⁷².

1.3.4 HIF1 α in immunity – lymphoid cells

The role of HIF1 α in both innate and adaptive immune responses is well studied. HIF1 α plays a consistently anti-inflammatory role in lymphoid cells. In B cells, HIF1 α is responsible for blocking B cell development in the BM along with accumulation of auto-antibodies and development of autoimmunity^{173,174}. In T cells, HIF1 α deficiency leads to higher levels of pro-inflammatory cytokines – mainly IL-2, IL-6, IFN γ and TNF α and stronger anti-bacterial effects and inflammatory responses in colitis¹⁷⁵⁻¹⁷⁷. Apart from inducing a T_h1 response in T cells, HIF1 α is also known to regulate the balance between T_h17 cells and T_{reg}s (**Figure 1.5**). It enhances T_h17 development through direct transcriptional activation of ROR γ t and attenuates T_{reg} development by binding to FoxP3 and targeting it for proteasomal degradation¹⁷⁸⁻¹⁸⁰.

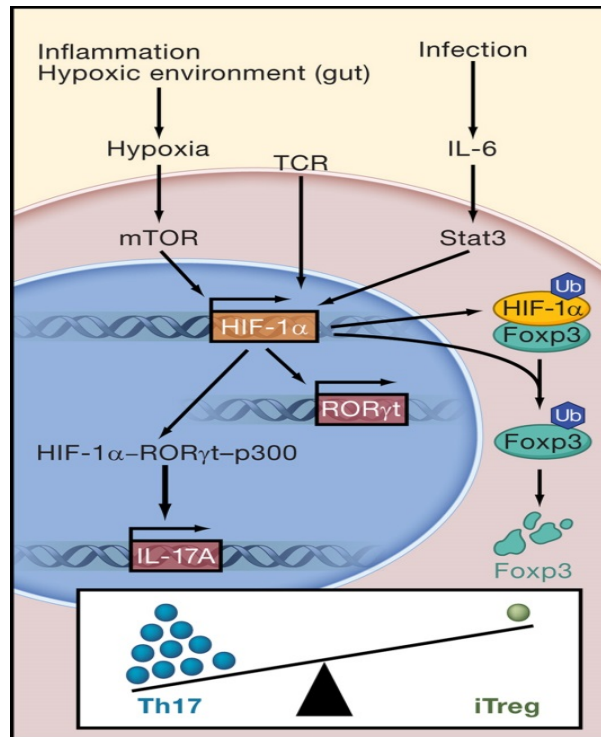


Figure 1.5 T cell expressed HIF1 α regulates T_h17 and T_{reg} balance by modulating transcription factors ROR γ t and FoxP3. Source: Nutsch and Hsieh 2011¹⁷⁸.

Another line of study has shown that HIF1 α enhances abundance of T_{regs} under hypoxic conditions. Hypoxia was seen to induce FoxP3 expression in Jurkat cells, human and murine mononuclear cells and *in vivo* mouse models in a HIF1 α dependent manner and increased the abundance and suppressive capacity of these cells^{181,182}. Further, HIF1 α deficient T_{regs} showed impaired functioning and failed to control T-cell mediated colitis¹⁸².

1.3.5 HIF1 α in immunity – myeloid cells

HIF1 α is mostly known to play a pro-inflammatory role in myeloid cells, of which macrophages and monocytes are the most widely studied^{139,183}. In a cell specific knockout model of HIF1 α in myeloid cells, the mice showed impaired myeloid cell aggregation, invasion and motility and therefore an inability to kill bacterial pathogens or develop arthritis¹⁸⁴. Using a similar mouse model, HIF1 α was shown to promote production of pro-inflammatory cytokines TNF α , IL-1, IL-4, IL-6 and IL-12 leading to sepsis¹⁸⁵. HIF1 α is induced by bacterial infection, even under normoxia, and regulates production of antimicrobial peptides, granule proteases, NO and TNF α in myeloid cells

thus aiding in their bactericidal activity¹⁸⁶ or by directly affecting phagocytic capacity^{187,188}. It also induces $\beta 2$ integrin expression and promotes epithelial binding in myeloid cells¹⁸⁹. It is known to extend survival and delay apoptosis in neutrophils¹⁹⁰⁻¹⁹². Thus, HIF1 α plays a pro-inflammatory role in myeloid cells, mainly affecting their phagocytic capacity. On the other hand, literature also mentions an anti-inflammatory role for HIF1 α in myeloid cells. In recent studies, myeloid HIF1 α was shown to prevent airway allergy by secretion of IL-10¹⁹³ whereas in a model of obstructive kidney injury, HIF was shown to suppress inflammation by down-regulating chemokine receptors¹⁹⁴.

1.3.6 HIF1 α in immunity – dendritic cells

Contradicting data is more common in DCs, another cell type of the myeloid lineage with overlapping yet distinct functions than monocytes and macrophages. Pro-inflammatory functions are commonly shown in literature where HIF1 α increased co-stimulatory molecule expression and T-cell proliferation capacity of both murine and human monocyte derived DCs. This effect was seen in cells stimulated by LPS, via TLR2 and TLR4 activation requiring MYD88 dependent NF κ B activity¹⁹⁵⁻¹⁹⁸. On the other hand, hypoxic human monocyte derived DCs were shown to down-regulate expression of co-stimulatory molecules, T-cell activation capacity, CCR7 and IFN γ expression but increase expression of TNF α and IL-1 β as also inflammatory chemokine receptors CCR5 and CXCR4. These DCs displayed defective DC homing to LNs but enhanced inflammation at subcutaneous sites of inflammation¹⁹⁹. In another research study, human monocyte derived DCs showed increased expression of co-stimulatory molecules but also CXCR4 and CCR5 under hypoxia, whereas expression of TNF α decreased with no effects on T-cell proliferation capacity, antigen presentation or IFN γ secretion²⁰⁰. A study using a DC specific *in vivo* model - CD11c cell specific knockout of HIF1 α – showed that hypoxic DCs have retarded cell growth but enhanced maturation states. While the pro-inflammatory cytokines TNF α , IL1 β and IL-12 are down-regulated, IL-22 and IL-23 show enhanced expression in HIF1 α deficient DCs²⁰¹.

The expression profile of immature DCs differentiated under hypoxic conditions is partly different compared to DCs experiencing hypoxia or an inflammatory stimulus only after maturation²⁰²⁻²⁰⁵. Also, effects seen are different in cells that mature under hypoxia but experience re-oxygenation later. Hypoxic BMDCs showed decreased expression of MHCII and co-stimulatory molecules or pro-inflammatory cytokines IL-1 β , IL-6 and TNF α but increased TGF β with poor ability to promote T-cell proliferation. On re-oxygenation, these DCs stimulated naive CD4⁺ T cells to T_h1 and T_h17 effector cells but not T_{regs}²⁰⁶. Hypoxia was also shown to skew human monocyte derived DCs to the T_h2 phenotype by secretion of IL-4 and IL-10 and down-regulation of IFN γ , IL-12 and TNF α ²⁰⁷. Apart from modulating the migration, antigen presentation and T-cell proliferation capacity of DCs, HIF1 α is also known to affect DC apoptosis and survival. Under hypoxic conditions, HIF1 α is up-regulated along with increased expression of pro-apoptotic molecule BAX and reduced expression of anti-apoptotic molecule BCL-2, leading to greater DC apoptosis²⁰⁸. Overall, the contradicting results of the functions of HIF1 α in DCs could be attributed to varying sources of DCs – human or mouse, BM derived or monocyte derived and varying isolation or culture protocols; different HIF1 α activation signals – hypoxia at varying stages of differentiation or different types of immune stimuli and experimental setups. It is thus clear that the role of HIF1 α in DCs is far from established unlike that in macrophages or monocytes where a consistent phenotype is observed.

1.3.7 HIF1 α in innate immunity

The phagocytic, apoptotic and bactericidal effects of myeloid cells and release of cytokines are evidence of the functions of HIF1 α in innate immunity. In addition, HIF1 α is known to induce expression of various genes which have roles in innate immune responses. The most well studied of all HIF targets is the vascular endothelial growth factor (VEGF), the interaction with which was first shown in the lab of Gregg Semenza in 1996²⁰⁹. VEGF plays a central role in angiogenesis and neovascularization and is implicated in cancer and ischemia²⁰⁹. VEGF is crucial for hematopoietic and endothelial cell development, endothelial and lymphocyte cell migration, signal transduction and vascular permeability²¹⁰⁻²¹². Expression of VEGF is commonly used to

analyze HIF1 α activity. Another common target of HIF1 α is NF κ B, an important regulator of innate immunity. HIF1 α mediates NF κ B activity and promotes expression of NF κ B regulated cytokines in neutrophils and macrophages stimulated by LPS in a TLR4 dependent manner^{185,192}. On the other hand NF κ B contributes to increased expression of *Hif1a* mRNA under hypoxia or infection via an IKK β pathway^{171,213,214}. But hypoxia itself can also activate NF κ B, independent of HIF1 α ²¹⁵. In mast cells, HIF1 α leads to release of pro-inflammatory cytokines IL-8 and TNF α , stimulates VEGF expression and facilitates production of inflammatory mediator histamine²¹⁶⁻²¹⁸.

1.3.8 HIF1 α in physiology and disease

Considering the prime role of HIF1 α in various cells, it is well accepted that HIF1 α plays an important role in physiology and disease. HIF1 α is shown to be crucial in embryonic development since knockout of HIF1 α leads to abnormal vascular development and death by embryonic day 11 in mice¹⁴⁹⁻¹⁵¹. Increased expression of HIF1 α was found in various cancers, owing probably to intra-tumoral hypoxia, angiogenesis or genetic alterations^{148,219-221}. HIF1 α was revealed to be a positive factor in tumorigenesis and a correlation between HIF1 α overexpression and patient mortality, poor disease prognosis and treatment resistance has been noted in studies^{151,222,223}. In individuals with hereditary erythrocytosis, a genetic mutation impairs hydroxylation and ubiquitination of molecules, leading to increased levels of HIF α . Affected individuals show altered responses to hypoxia, metabolism and exercise^{224,225}.

The role of HIF1 α in infections has been studied in numerous models using bacteria, viruses and parasites¹³⁹. Effects of HIF stabilization on viral infections results in mitigation of the disease as in the case of respiratory syncytial virus²²⁶ and vesicular stomatitis virus²²⁷ but contrastingly leads to pro-angiogenic effects and hence increased oncogenic potential in hepatitis B & C^{228,229} and papillomavirus²³⁰ as well as re-activation of herpes virus from latency²³¹. In the case of bacterial infections like *Streptococcus*, *Pseudomonas*, *Salmonella* and *Bartonella*, HIF1 α is responsible for phagocytic defenses against the pathogen^{184,186,232}. On the other hand, *Chlamydia* has evolved to release a protease-like activity factor which degrades accumulated

HIF1 α thus evading immune attack²³³. HIF1 α has also been exhibited to help survival and growth of the parasite *Toxoplasma gondii*²³⁴. HIF1 α has been implicated in sepsis where bacterial products provoke uncontrolled release of pro-inflammatory cytokines. Studies of LPS challenge in mice identified HIF1 α as a crucial determinant of sepsis. *Hif1a* deletion in macrophages protected animals against LPS induced mortality, thus blocking septic manifestations¹⁸⁵.

In addition, HIF1 α has also been well studied and associated with wound healing, organ transplant rejection, traumatic shock, sleep apnea, hypertension, colitis and other inflammatory diseases.

1.3.9 Hypoxia in atherosclerosis

The role of hypoxia and HIF1 α in atherosclerosis is an interesting topic of research and has been closely studied²³⁵. Atherosclerotic plaques become hypoxic due to the thickness of the plaque exceeding maximum oxygen diffusion distance and the accumulation of large number of cells with high metabolic demand²³⁶⁻²³⁸. In early studies, hypoxic areas have been detected *in vitro* and *in situ* in rabbit arteries using micro-electrode techniques²³⁹⁻²⁴². More recently, hypoxia was demonstrated *in vivo* using the hypoxia marker pimonidazole in symptomatic human biopsies, *ApoE*^{-/-} mice on a 16 week western diet and rabbits on a 6-8 week cholesterol-enriched diet^{236,243-246}. Pimonidazole is a 2-Nitroimidazole compound that undergoes intracellular nitroreduction forming reactive radicals, which bind to cellular constituents in the absence of oxygen, hence, a marker of hypoxia. The main advantage of pimonidazole is that it can be administered *in vivo* due to its low toxicity and high water solubility, making it possible to assess hypoxia in intact animals²⁴⁶. It is also essential to note that the hypoxia marker pimonidazole stains only viable, actively metabolizing cells, thus showing absence of hypoxic staining in the necrotic core regions²⁴⁷. Hypoxia increases the overall lipid content in macrophages by enhanced sterol synthesis and suppression of cholesterol efflux and induces formation of foam cells^{243,245,248,249}. Hypoxia stimulates plaque angiogenesis, glucose metabolism, proteolysis and inflammation in the plaque^{236,250}.

1.3.10 Role of HIF1 α in myeloid cells in atherosclerosis

The expression of HIF1 α has also been detected in atherosclerotic lesions. In human femoral endarterectomy specimens, human carotid artery sections and lesions of *ApoE*^{-/-} mice, nuclear HIF1 α expression was observed, co-localized with CD68 positive macrophages. While the femoral plaque sections showed HIF1 α expression in the shoulder, cap area and between the atheromatous lipid core and media; contradictory staining was seen for HIF1 α only in the central region of the plaque in mice^{236,243,251-253}. Significantly increased HIF1 α was also seen in *ApoE*^{-/-} arteries 6 hours after wire injury²⁵⁴. It was further also shown that the mRNA and protein expression of HIF1 α and its targets VEGF, GLUT3 and HK2 increases with progression of atherosclerosis in human carotid plaques and correlates with increasing angiogenesis²³⁶. HIF1 α induced foam cell formation in macrophages and monocytic cell lines of both mouse and human origin²⁵⁵⁻²⁵⁷. HIF1 α also regulated stromal derived factor (SDF) 1 α expression and mediated neo-intima formation in *ApoE*^{-/-} mice²⁵⁴. Apart from the pro-inflammatory capacity of HIF1 α in macrophages²³⁶, it was also shown to affect lipid metabolism in cells undergoing hypoxia in murine plaques²⁴³.

1.3.11 Role of HIF1 α in T cells in atherosclerosis

Though almost all the literature showing HIF1 α expression in plaques proves a macrophage source for this transcription factor, HIF1 α positive T cells were also detected in a murine model of cuff injury²⁴⁴. In another innovative experiment, mice were injected with plasmids overexpressing HIF1 α leading to increased IL-10 but decreased IFN γ expression in splenocytes. The mice showed a systemic shift towards a T_h2 phenotype and a significant reduction in plaque size was seen in the overexpressing mice. Since most overexpressing cells were found to be CD4⁺ T cells, it confirms the anti-inflammatory role of HIF1 α in T cells²⁵⁸. Adding to this hypothesis was the study in which T-cell specific HIF1 α deficient mice showed enhanced T-cell activation and proliferation and HIF1 α was implicated as a negative regulator in development of vascular remodeling²⁴⁴.

1.3.12 Non-hypoxic triggers of HIF1 α leading to atherosclerosis

Though hypoxia is a common occurrence in plaques and triggers HIF1 α in cells in local plaque areas, it is also essential to understand that HIF1 α activation by non-hypoxic regulators can take place both locally and systemically in atherosclerotic inflammation. The presence of various inflammatory markers, cytokines, vasoactive and thrombotic factors, pro-angiogenic hormones like Angiotensin II, oxidative stress, ROS, as also cell-cell contact and receptor mediated activation can lead to enhanced activation of HIF1 α in cells responsible for pathogenesis of atherosclerosis²⁵⁹. Amongst non-hypoxic regulators of HIF1 α is oxLDL, the well-known trigger for atherosclerosis, released in lipid rich areas on oxidative stress and transported to lymphoid organs by phagocytic cells. HIF1 α is activated by oxLDL in macrophages even under normoxia via ROS formation²⁶⁰. The effects of hypoxia and oxLDL in conjunction act as an additive boost for HIF1 α accumulation in macrophages and HIF1 α plays a crucial role in protecting oxLDL treated macrophages from apoptosis²⁶¹. oxLDL modulates pro-inflammatory and angiogenic functions in monocytes and macrophages via HIF1 α ²⁶².

1.4 Aim of this project

It is clear that HIF1 α and hypoxia play an important role in atherosclerosis. Most studies center around the role of hypoxic stimulation of HIF1 α and its activation in the plaque environment, rarely discussing systemic inflammation and its effects on HIF1 α mediated disease pathogenesis. Also, studies mainly focus on monocytes, macrophages and foam cells and the effects of HIF1 α in these cell types are clearly delineated. No studies have yet looked at the role of DC derived HIF1 α in atherosclerosis. Considering the important role of DCs in the initiation and progression of atherosclerosis and the controversial effects of HIF1 α in DCs, it would be essential to know how HIF1 α modulates the functions of this cell type. HIF1 α could behave in a pro-inflammatory manner like in other myeloid cells which are closer to the DCs morphologically and functionally but on the other hand an

anti-inflammatory role could also be expected considering the close interaction with T cells where HIF1 α is known to modulate anti-inflammatory functions. Hence, identifying the role of HIF1 α in DCs in the context of atherosclerosis forms the focus of this thesis.

2. MATERIALS

2.1 Chemicals

Glycerine	AppliChem (Darmstadt, Germany)
Magnesium chloride	
Sodium chloride	
Sodium hydroxide	
Tris	
LE agarose	Biozym (Hessisch Oldendorf, Germany)
Acetic acid	Carl Roth (Karlsruhe, Germany)
Agar-Agar Kobe I	
Ammonium chloride	
Citric acid	
Disodium phosphate	
Ethyl alcohol	
Glucose	
Hydrochloric acid	
Isopropanol	
LB medium powder (Lennox)	
Monopotassium phosphate	
Paraformaldehyde (PFA)	
Potassium bicarbonate	
Potassium chloride	
Sodium acetate	
Sodium citrate	
Sodium dodecyl sulphate (SDS)	
Triton X-100	
Tryptone	
Tween-20	
Xylene	
Yeast extract	
Eosin Y solution	Medite (Burgdorf, Germany)
Hematoxylin (Mayers hemalum)	Merck (Darmstadt, Germany)
Acetaldehyde	Sigma-Aldrich (Taufkirchen, Germany)
Basic Fuchsin	
Cobalt chloride hexahydrate	
Ethylenediaminetetraacetic acid (EDTA)	
Formaldehyde	
Gelatin (from bovine skin - type B)	
Glycine	
Hydrogen peroxide	
Lidocaine HCl	
Oil-Red O	
Picric acid	
Sirius red	

2.2 Kits and reagents

2.2.1 Kits

BD Cytotfix/Cytoperm kit	BD Biosciences (Heidelberg, Germany)
EnzyChrom Triglyceride assay kit	Biotrend (Cologne, Germany)
Foxp3/Transcription factor staining buffer set	eBioscience (Frankfurt am Main, Germany)
Hypoxyprobe Plus kit	Hypoxyprobe Inc (Burlington, USA)
Amplex Red Cholesterol assay kit	Life technologies (Darmstadt, Germany)
Purelink HiPure plasmid Maxiprep kit	
Amaxa P4 Primary Cell 4D-Nucleofector kit	Lonza (Basel, Switzerland)
Nucleospin RNA II kit	Macherey Nagel (Dueren, Germany)
NucleoBond PC 500 kit	
CD4 ⁺ CD62L ⁺ T-cell isolation kit	Miltenyi Biotec (Bergisch Gladbach, Germany)
CD4 ⁺ T-cell isolation kit II	
CD11c microbeads	
Lineage cell depletion kit	
IL-12 mini ELISA development kit	Peprtech (Rocky Hill, USA)
QIAquick DNA purification kit	Qiagen (Hilden, Germany)
QIAshredder	
RNeasy Mini kit	
RNeasy Micro kit	
ExactaChIP Human/Mouse HIF1 α chromatin immunoprecipitation kit	R&D Systems (Minneapolis, USA)
First strand cDNA synthesis kit	Thermo Scientific (St. Leon-Rot, Germany)
Avidin-Biotin blocking kit	Vector laboratories (Burlingame, USA)
DAB peroxidase substrate kit	

2.2.2 Molecular Biology reagents

GeneJammer transfection reagent	Agilent technologies (Santa Clara, USA)
OVA ₃₂₃₋₃₃₉ peptide	AnaSpec Inc. (Seraing, Belgium)
Ethidium bromide (EtBr)	AppliChem (Darmstadt, Germany)
Neomycin	Belapharm (Vechta, Germany)
10X Hanks Balanced Salt Solution (HBSS)	Life technologies (Darmstadt, Germany)
Goat serum	
Polymyxin B sulphate	
Vitro-Clud	R. Langenbrinck (Emmendingen, Germany)
Collagenase D	Roche (Mannheim, Germany)
OCT compound (Tissue-Tek)	Sakura (Staufen, Germany)
5(6)-Carboxyfluorescein diacetate N-succinimidyl ester (CFSE)	Sigma-Aldrich (Taufkirchen, Germany)

ABTS liquid substrate solution	Sigma-Aldrich (Taufkirchen, Germany)
Ampicillin sodium salt	
Aprotinin	
Bovine serum albumin	
Brefeldin A	
Fish skin gelatin	
Horse serum	
Ionomycin	
Leupeptin	
Mouse serum	
Phorbol-12-myristat-13-acetat (PMA)	
PMSF	
Rabbit serum	
Streptavidin agarose beads	
2X PCR mastermix	Thermo Scientific (St. Leon-Rot, Germany)
2X SYBR green mix	
GeneRuler 1 kb Plus DNA ladder	
Proteinase K	Vector laboratories (Burlingame, USA)
Vectashield with DAPI	
<i>Escherichia coli</i> XL10 and DH5 α	Kindly provided by Dr. Heike Hermanns, Rudolf Virchow Zentrum, Würzburg, Germany

2.2.3 Cell culture reagents

D-PBS	Life technologies (Darmstadt, Germany)
RPMI-1640 (with 2 mM L-Glutamine)	
Penicillin-Streptomycin	
β -Mercaptoethanol	
HEPES	
D-MEM	
Trypsin-EDTA	
FBS Gold	PAA Laboratories (Pasching, Austria)
DEAE-Dextran	Sigma-Aldrich (Taufkirchen, Germany)
LPS from <i>E.coli</i> 0111:B4	

2.3 Cytokines

murine GM-CSF	Peprotech (Rocky Hill, USA)
murine TNF α	
murine CCL19	

2.4 Antibodies

2.4.1 Fluorescent antibodies

Anti-mouse CD19 - FITC	1D3	BD Biosciences (Heidelberg, Germany)
Anti-mouse CD3 - FITC	17A2	
Anti-mouse CD3 – Pacific blue	500A2	
Anti-mouse CD45 - APCCy7	30-F11	
Anti-mouse CD8a - AmCyan	53-6.7	
Anti-mouse Gr1 - PerCP	RB6-8C5	
Anti-mouse IFN γ - APC	XMG1.2	
Anti-mouse MHCII - FITC	2G9	
Anti-mouse CD115 - PE	AFS98	
Anti-mouse CD11b - PerCP	M1/70	eBioscience (Frankfurt am Main, Germany)
Anti-mouse CD11c - PECy7	N418	
Anti-mouse CD4 - PE	RM4-5	
Anti-mouse CD4 – PECy7	GK1.5	
Anti-mouse CD25 - APC	PC61	
Anti-mouse CD44 - PerCP	IM7	
Anti-mouse CD62L - PECy7	MEL-14	
Anti-mouse CD80 - APC	16-10A1	
Anti-mouse CD86 - PE	GL1	
Anti-mouse F4/80 - APC	BM8	eBioscience (Frankfurt am Main, Germany)
Anti-mouse Foxp3 - PE	FJK-16s	
Anti-mouse IL-12 - PE	C15.6	
Anti-mouse IL-17a - PE	eBio17B7	
Anti-mouse Thy1.1 - APC	HIS51	
Anti-mouse α -Actin - Cy3	1A4	Sigma Aldrich (Taufkirchen, Germany)

2.4.2 Primary antibodies

Rat anti-mouse Mac-2	M3/38	Cedarlane (Burlington, Canada)
Rat anti-mouse Mac-3	M3/84	BD Biosciences (Heidelberg, Germany)
Rat anti-human CD3	CD3-12	AbD Serotec (Duesseldorf, Germany)
Armenian hamster anti-mouse CD11c - biotin	N418	Biologend (San Diego, USA)
Rabbit anti-mouse HIF1 α	poly-clonal	Novus Biologics (Littleton, USA)
Mouse anti-mouse STAT3	124H6	Cell Signaling (Danvers, USA)
Rat anti-mouse IL-12 p35	C18.2	eBioscience (Frankfurt am Main, Germany)

2.4.3 Secondary antibodies and detection reagents

Goat anti-rat IgG – Alexa Fluor 488	Life technologies (Darmstadt, Germany)
Streptavidin – Alexa Fluor 555	
Goat anti-rabbit IgG – Alexa Fluor 488	
Goat anti-mouse IgG2a – PE	Jackson ImmunoResearch (Suffolk, UK)

2.5 Primers

2.5.1 qPCR primers

Primers below were from Eurofins MWG Operon (Ebersberg, Germany)

Hprt	Fwd	5'-TCCTCCTCAGACCGCTTTT-3'
	Rev	5'-CCTGGTTCATCATCGCTAATC-3'
Hif1a	Fwd	5'-CAAGATCTCGGCGAAGCAA-3'
	Rev	5'-GGTGAGCCTCATAACAGAAGCTTT-3'
Cd80	Fwd	5'-TCGTCTTTCACAAGTGTCTTCAG-3'
	Rev	5'-TTGCCAGTAGATTCGGTCTTC-3'
Cd86	Fwd	5'-GAAGCCGAATCAGCCTAGC-3'
	Rev	5'-CAGCGTACTATCCCGCTCT-3'
Cd74	Fwd	5'-CACCGAGGCTCCACCTAA-3'
	Rev	5'-GCAGGGATGTGGCTGACT-3'
Il4	Fwd	5'-CAACGAAGAACACCACAAGAG-3'
	Rev	5'-ATGAATCCAGGCATCGAAAAGC-3'
Il6	Fwd	5'-GTGGCTAAGGACCAAGACCA-3'
	Rev	5'-ACCACAGTGAGGAATGTCCA-3'
Il10	Fwd	5'-TGCACTACCAAAGCCACAAGG-3'
	Rev	5'-TGGGAAGTGGGTGCAGTTATTG-3'
Tgfb	Fwd	5'-GACGTCACTGGAGTTGTACGG-3'
	Rev	5'-GGTTCATGTCATGGATGGTGC-3'
Tnfa	Fwd	5'-CTGTAGCCCACGTCTAGC-3'
	Rev	5'-GGTTGTCTTTGAGATCCATGC-3'
Nfkb1/p105	Fwd	5'-GAACTTCTCGGACAGCTTCG-3'
	Rev	5'-CGTAGTTCGAGTAGCCATACCC-3'

Rela/p65	Fwd	5'-CATGCGATTCCGCTATAAATG-3'
	Rev	5'-TCCTGTGTAGCCATTGATCTTG-3'
Stat3	Fwd	5'-CTACCTCTACCCCGACATTCC-3'
	Rev	5'-GATGAACTTGGTCTTCAGGTACG-3'
Nos2	Fwd	5'-GTTCTCAGCCCAACAATACAAGA-3'
	Rev	5'-GTGGACGGGTCGATGTCAC-3'
Igf1	Fwd	5'-TCGGCCTCATAGTACCCACT-3'
	Rev	5'-ACGACATGATGTGTATCTTTATTGC-3'
Mrc1	Fwd	5'-CACTCATCCATTACAACCAAAGC-3'
	Rev	5'-CAGGAGGACCACGGTGAC-3'
Cd88	Fwd	5'-GGGATGTTGCAGCCCTTATCA-3'
	Rev	5'-CGCCAGATTCAGAAACCAGATG-3'

<i>I12a</i> - Quantitect primer assay QT01048334	Qiagen (Hilden, Germany)
-----------------------------------------------------	--------------------------

2.5.2 Genotyping primers

Primers below were from Eurofins MWG Operon (Ebersberg, Germany)

<i>Hif1a</i> -flox	oIMR 7068	5'-TGCTCATCAGTTGCCACTT-3'
	oIMR 7069	5'-GTTGGGGCAGTATGGAAAG-3'
<i>Cd11c</i> -cre	oIMR 7841	5'-ACTTGGCAGCTGTCTCCAAG-3'
	oIMR 7842	5'-GCGAACATCTTCAGGTTCTG-3'
	oIMR 8744	5'-CAAATGTTGCTTGTCTGGTG-3'
	oIMR 8745	5'-GTCAGTCGAGTGCACAGTTT-3'
<i>Ldlr</i>	oIMR 0092	5'-AATCCATCTTGTTCAATGGCCGATC-3'
	oIMR 3349	5'-CCATATGCATCCCCAGTCTT-3'
	oIMR 3350	5'-GCGATGGATACACTCACTGC-3'
OT-II	oIMR 1825	5'-GCTGCTGCACAGACCTACT-3'
	oIMR 1826	5'-CAGCTCACCTAACACGAGGA-3'
	oIMR 1880	5'-AAAGGGAGAAAAAGCTCTCC-3'
	oIMR 1881	5'-ACACAGCAGGTTCTGGGTTC-3'

2.5.3 ChIP primers

Primers below were from Eurofins MWG Operon (Ebersberg, Germany)

Stat3 ChIP	Fwd	5'-GCCCTGATACGGCTCGCTTCTGC-3'
	Rev	5'-TGGGGACCGCCTAAGTGGCTG-3'
Socs3 ChIP set 1	Fwd	5'-CAAGCATCCCCTGCCAACC-3'
	Rev	5'-GTCTACAGGTAAATGTCGCGCATC-3'
Socs3 ChIP set 2	Fwd	5'-CAGCTCATCCGCCATTGCCTG-3'
	Rev	5'-TTCGCCACGCAGGTTGGGAG-3'

2.6 Plasmids

pCAGGS	Kindly provided by Dr. Heike Hermanns, Rudolf Virchow Zentrum, Würzburg, Germany
pEF-STAT3-YFP	
pCAGGS-STAT3D	
pLB2-FLIP-GFP	Kindly provided by Dr. Stephan Kissler, Joslin diabetes centre, Boston, USA
pLB2-FLIP-STAT3	
pMDL-gag/pol	
pCMV-vsvg	
pRSV-rev	
pAdvantage	
pIC-cre	Kindly provided by Dr. Bernhard Nieswandt, Rudolf Virchow Zentrum, Würzburg, Germany

2.7 Animals

C57BL6/J (B16)	Jackson laboratories (Maine, USA)
B6.129S7- <i>Ldlr</i> ^{tm1Her} /J (<i>Ldlr</i> ^{-/-})	
B6.129- <i>Hif1a</i> ^{tm3Rsjo} /J (<i>Hif1a</i> ^{flox/flox})	
B6.Cg-Tg(<i>Itgax-cre</i>)1-1Reiz/J (<i>Cd11c-cre</i>)	
B6.Cg-Tg(<i>TcraTcrb</i>)425Cbn/J (OT-II)	
<i>LysM-cre</i> ⁺ <i>Hif1a</i> ^{flox/flox}	Kindly provided by Dr. Randall Johnson, University of Cambridge, UK

2.8 Cell lines

HEK293F	Kindly provided by Dr. Stephan Kissler, Joslin diabetes centre, Boston, USA
L929	Kindly provided by Dr. Menno De Winther, Amsterdam medical centre, The Netherlands

2.9 Plasticware, glassware and other consumables

All general laboratory use plasticware (centrifuge tubes, microcentrifuge tubes, serological pipettes, microtips, cell culture dishes, plates) were from Sarstedt (Nümbrecht, Germany) or VWR (Darmstadt, Germany). All glassware (flasks, beakers, funnels, measuring cylinders, bottles) were from Schott-Duran, Mainz, Germany)

High fat diet (15% fat, 1.25% cholesterol)	Altromin (Lage, Germany)
70 µm cell strainer	BD Biosciences (Heidelberg, Germany)
FACS tubes	
Syringes	
Clear Ultracentrifuge tubes	Beckman Coulter (Brea, USA)
PCR tube strips	Biozym (Vienna, Austria)
Needles	Braun medical (Emmenbruecke, Switzerland)
Capillaries	Hirschmann Laborgeraete (Eberstadt, Germany)
8 µm ThinCert cell culture inserts	Greiner Bio-One GmbH (Frickenhausen, Germany)
Hemocytometer	Labor optic (Friedrichsdorf, Germany)
384-well plates	Life technologies (Darmstadt, Germany)
Poly-L-lysine glass slides	Menzel GmbH (Braunschweig, Germany)
LS columns	Miltenyi Biotec (Bergisch Gladbach, Germany)
MS Columns	
Pre-separation filters	
High fat diet (20% fat, 1.25% cholesterol)	Research Diets (New Brunswick, USA)
EDTA tubes	Sarstedt (Nümbrecht, Germany)
Serum gel tubes	
Stericup filters 0.2 µm	Sarstedt (Newton, USA)
PAP pen for immunostaining	Sigma Aldrich (Taufkirchen, Germany)
Filter tips	Starlab (Hamburg, Germany)
ELISA microplates (Nunc Maxisorp)	Thermo Scientific (St.Leon-Rot, Germany)
High speed centrifuge tubes (Nalgene Oakridge)	
Paraffin	Vogel Medizinische Technik und Elektronik (Giessen, Germany)
Star Frost glass slides	Waldemar Knittel Glasbearbeitung (Braunschweig, Germany)

2.10 Instruments

Sonicator (Sonoplus HD-2070)	Bandelin GmbH (Berlin, Germany)
FACS Canto II	BD Bioscience (Heidelberg, Germany)
Cell culture bench (SK12000)	BDK Luft- und Reinraumtechnik (Sonnenbühl, Germany)
High speed centrifuge (Avanti J-25)	Beckman Coulter (Brea, USA)
Ultracentrifuge (Optima L-80 XP)	
Cell culture Incubator	Binder (Tuttlingen, Germany)
Electrophoresis power supply (Powerpac)	Bio-Rad (München, Germany)
Electrophoresis units (Subcell GT)	
Thermal Cycler (S1000)	
Fluostar OPTIMA plate reader	BMG Labtech (Ortenberg, Germany)
Centrifuge (5430R)	Eppendorf (Hamburg, Germany)
Electronic dispenser (Multipette Xstream)	
Thermomixer	
Dissection tools	Fine Science Tools (Heidelberg, Germany)
Tissue floating waterbath	GFL (Burgwedel, Germany)
Gel documentation system (440K)	Herolab GmbH (Wiesloch, Germany)
Electronic pipette controller (Pipetus)	Hirschmann Laborgeraete (Eberstadt, Germany)
Slides shaker HS260 basic	IKA Werke GmbH (Staufen, Germany)
Bacterial incubator and shaker (ISF-1-W)	Kuehner (Birsfelden, Switzerland)
Cryotome (CM3050S)	Leica Microsystems (Nussloch, Germany)
Flattening table (HI1220)	
Fluorescence microscope DM4000B	
Microtome (RM2255)	
Tissue embedding station (EG1160)	
Tissue processing machine (ASP200S)	
Refrigerators and -20°C freezers	Liebherr (Bulle, Switzerland)
Real time PCR system (Applied Biosystems 7900HT)	Life technologies (Darmstadt, Germany)
4D Nucleofector system	Lonza (Basel, Switzerland)
Multichannel pipettes (Rainin)	Mettler Toledo (Giessen, Germany)
pH meter	
Cell culture microscope (CK-X31)	Olympus (Tokyo, Japan)
Dissecting microscope (SZX10)	
Waterbath	P-D Industriegesellschaft mbH (Dresden, Germany)
Microwave	Privileg (Stuttgart, Germany)
Cobas Fara centrifugal analyzer	Roche (Mannheim, Germany)
Weighing balance (TE3102S)	Sartorius (Goettingen, Germany)

Sysmex KX-21N	Sysmex (Norderstedt, Germany)
Autoclave (DX100)	System GmbH (Wettenberg, Germany)
-80°C freezers (Heraeus HERAFreeze)	Thermo Scientific (St.Leon-Rot, Germany)
Centrifuge (Heraeus Multifuge X3R)	
Dry air oven (Heraeus)	
Nanodrop ND-2000	
Minifuge (Galaxy ministar)	VWR (Darmstadt, Germany)
Single channel pipettes	
Vortex mixer	

2.11 Softwares

Diskus image analysis software	Hilgers (Koenigswinter, Germany)
FlowJo 7.6 software	Tree Star (Ashland, USA)
MatInspector software	Genomatix (Munich, Germany)
Primer BLAST tool	NCBI (Bethesda, USA)
Prism 4.0 software	GraphPad (La Jolla, USA)
SDS 2.4 software	Life technologies (Darmstadt, Germany)

2.12 Buffers, solutions and media

2.12.1 Buffers

Phosphate buffered saline (PBS)

- DDW
- 137 mM NaCl
- 2.7 mM KCl
- 18.61 mM Na₂HPO₄
- 1.8 mM KH₂PO₄
- pH adjusted to 7.4

Tris buffered saline (TBS)

- DDW
- 150 mM NaCl
- 50 mM Tris
- pH adjusted to 7.5

RBC lysis buffer

- DDW
- 155 mM NH₄Cl
- 10 mM KHCO₃
- 0.1 mM EDTA

MAC staining buffer

- 1 X PBS
- 2 % mouse serum
- 2 % rabbit serum
- 2 % horse serum
- 1 % BSA
- 0.1 % Triton X-100

DC staining buffer

- 1 X PBS
- 10 % goat serum
- 1 % fish skin gelatin
- 1 % Triton X-100

Tail lysis buffer

- DDW
- 10 mM Tris (pH 8.0)
- 10 mM EDTA (pH 8.0)
- 10 mM NaCl
- 0.5 % SDS

TAE buffer

- DDW
- 40 mM Tris
- 20 mM Acetic acid
- 1 mM EDTA

MACS buffer

- 1 X D-PBS
- 0.5 % BSA
- 2 mM EDTA

FACS staining buffer stock solution

- 1 X PBS
- 2 % mouse serum
- 2 % rabbit serum
- 1 % BSA

FACS staining buffer working solution

- 1 part HBSS
- 1 part FACS staining buffer stock solution

STAT3 blocking buffer

- 1 X PBS
- 0.5 % BSA
- 5 % goat serum
- 1:500 anti-mouse-biotin

Rinse buffer

- 1 X TBS
- 0.1 % Tween-20

2.12.2 Solutions

Heat inactivated FBS

- Frozen FBS thawed to RT, heated in a water bath at 56°C for 30 minutes, inverting the bottle every 10 minutes to mix

Aldehyde fuchsin stock Solution

- 70 % ethanol
- 5 g/l basic fuchsin

Aldehyde fuchsin Working Solution

- Aldehyde fuchsin stock solution
- 5 % acetaldehyde
- 2 % concentrated hydrochloric acid
- Solution incubated O/N at RT
- Filtered before use

Sirius Red Solution

- Saturated aqueous picric acid
- 0.1 % sirius red
- Thoroughly mixed and filtered

HBSS working solution

- 1 X HBSS (from 10 X commercial stock)
- 0.6 % BSA
- 300 μ M EDTA

Lidocaine-EDTA solution

- 1 X PBS
- 10 mM EDTA
- 4 mg/ml Lidocaine HCl

Oil-Red stock solution

- 99 % isopropanol
- 5 mg/ml Oil-Red O

Oil-Red O working solution

- 3 parts Oil-Red O stock solution
- 2 parts DDW
- Allowed to stand at RT for 1 hour. Filtered before use.

Kaiser's glycerin jelly stock solution

- 4 g gelatin
- 21 ml DDW
- 25 ml glycerin

Kaiser's glycerin jelly working solution

- 3 parts Kaiser's glycerin jelly stock solution
- 7 parts DDW

Antigen retrieval stock solution A

- DDW
- 2.101 % citric acid

Antigen retrieval stock solution B

- DDW
- 2.941 % sodium citrate

Antigen retrieval working solution

- 9 parts DDW
- 0.18 parts antigen retrieval stock solution A
- 0.82 parts antigen retrieval stock solution B
- 50 µl Tween-20

2.12.3 Media

DC medium

- RPMI-1640 (with 2 mM L-Glutamine)
- 10 % FBS (heat inactivated)
- 100 U/ml Penicillin-Streptomycin
- 50 µM β-Mercaptoethanol

L929 growth medium

- RPMI-1640 (with 2 mM L-Glutamine)
- 10 % FBS (heat inactivated)
- 100 U/ml Penicillin-Streptomycin
- 25 mM HEPES

HEK cell medium

- D-MEM
- 10 % FBS (heat inactivated)
- 100 U/ml Penicillin-Streptomycin

Transmigration medium

- RPMI-1640 (with 2 mM L-Glutamine)
- 0.5 % BSA
- 100 U/ml Penicillin-Streptomycin

L929 conditioned medium

- Cultured L929 cells in L929 growth medium for 10 days
- Collected spent medium at day 10
- Filtered supernatant through a 0.2 µm filter.

LB medium

- DDW
- 20 g/L LB medium powder (ready to use)
- medium autoclaved

LB agar

- LB medium
- 1.5 % bacto-agar
- Medium autoclaved

SOB medium

- DDW
- 20 g/L tryptone
- 5 g/L yeast extract
- 0.5 g/L NaCl
- 250 mM KCl
- pH adjusted to 7.0 and autoclaved
- 2 M MgCl₂ (added after autoclaving)

SOC medium

- SOB medium
- 1 M glucose

IL-17a/IFN γ stimulation medium (for intracellular staining)

- DC medium
- 50 ng/ml PMA
- 750 ng/ml ionomycin
- 2.5 µg/ml brefeldin A

IL-12 stimulation medium (for intracellular staining)

- DC medium
- 2.5 µg/ml brefeldin A
- 1 µg/ml LPS

3. METHODS

3.1 Animal work

3.1.1 Mice experiments

All mice were bred and maintained at the Zentrum für Experimentelle Molekulare Medizin (ZEMM), Würzburg or at the Rudolf Virchow Zentrum (RVZ), Würzburg. The mice were fed normal chow regularly apart from when placed on a high fat diet. All atherosclerosis inducing experiments (except for *LysM-cre⁺ Hif1a^{flox/flox} Ldlr^{-/-}* transgenic mice) were carried out by placing the mice on a high fat diet of 15 % fat and 1.25 % cholesterol for 8 weeks.

All transgenic mice were fertile and healthy and showed no phenotypic abnormalities. All studies with mice were approved by local authorities.

3.1.2 Generation of *Cd11c-cre⁺ Hif1a^{flox/flox} Ldlr^{-/-}* transgenic mice

Hif1a^{flox/flox} mice and *Cd11c-cre* mice were crossed to give heterozygous littermates. Appropriate littermates were crossed till *Cd11c-cre⁺ Hif1a^{flox/flox}* and *Cd11c-cre⁺ Hif1a^{+/+}* offspring were obtained. The *Cd11c-cre⁺ Hif1a^{flox/flox}* (henceforth referred to as CKO) mice were test mice lacking the *Hif1a* gene in CD11c⁺ cells whereas the *Cd11c-cre⁺ Hif1a^{+/+}* (henceforth referred to as WT) mice were used as controls.

To accelerate atherosclerosis progression, the CKO and WT mice were separately crossed with the *Ldlr^{-/-}* mice to give *Cd11c-cre⁺ Hif1a^{flox/flox} Ldlr^{-/-}* (henceforth referred to as CKO *Ldlr^{-/-}*) and *Cd11c-cre⁺ Hif1a^{+/+} Ldlr^{-/-}* (henceforth referred to as WT *Ldlr^{-/-}*). The genotypes of these mice were confirmed by conventional PCR methods using primers to the region of interest.

3.1.3 Generation of *LysM-cre⁺ Hif1a^{flox/flox} Ldlr^{-/-}* transgenic mice (done by Dr. Judith Sluimer, Maastricht, The Netherlands)

Recipient *Ldlr^{-/-}* mice were lethally irradiated (dose 10 Gy). BM cells were isolated from *LysM-cre⁺ Hif1a^{flox/flox}* and *LysM-cre⁺ Hif1a^{+/+}* donor mice. One day after irradiation, 10⁷ BM cells from the donor mice were injected i.v. per recipient *Ldlr^{-/-}* mouse. The recipient mice were given 0.1 g/L Neomycin

and 6×10^4 U/L polymyxin B sulphate in water for 4 weeks after BMT. They were placed on 6 weeks of high fat diet (20 % fat and 1.25 % cholesterol).

3.1.4 Generation of transgenic mice with STAT3 overexpression in DCs

Recipient *Ldlr*^{-/-} mice were lethally irradiated (dose 9.7 Gy). BM cells were obtained from CKO and WT donor mice and lineage depleted hematopoietic cells were isolated as mentioned later. These Lin⁻ cells were resuspended in DC medium at a concentration of 2×10^6 cells/ml and treated with 50 MOI control or STAT3 lentivirus in the presence of 10 µg/ml DEAE Dextran for 24 hours at 37 °C. One day after recipient irradiation, 10^6 virus-treated Lin⁻ BM cells were injected i.v. per recipient *Ldlr*^{-/-} mouse. The recipient mice were given 2 g/L Neomycin in water and normal chow for 2 weeks after BMT. Then they were placed on 4 weeks of high fat diet.

3.1.5 Sacrificing mice and harvesting organs

Mice were sacrificed by cervical dislocation. Blood was collected via the retro-orbital route or by cardiac puncture using a glass capillary into EDTA tubes or serum-separating tubes. The dead mice were perfused with 5 ml PBS to clear out blood from vessels. If organs were to be harvested for immunohistology by fixed paraffin sectioning, mice were also perfused with 1 % PFA after the PBS. Organs like the heart, aorta, spleen, peripheral lymph nodes (inguinal, axillary and brachial) and bones (femurs, tibias and hips) were harvested by general dissection techniques.

3.1.6 Processing of organs

Blood for FACS analysis was collected in EDTA tubes. Erythrocytes were lysed by treating each sample with 3 ml RBC lysis buffer for 5 minutes. The lysis reaction was stopped by adding 5 ml HBSS. The cell suspension was centrifuged at 350 g, 5 minutes, 4 °C to obtain blood leukocytes.

Serum was obtained by collecting blood in serum-separating tubes. The samples were allowed to stand at RT for at least 15 minutes and then spun at 10,000 g, 5 minutes, RT to obtain clear serum on the top. Serum was then aliquoted and frozen at -80 °C for future use.

Hearts were stored in 4 % PFA for fixed paraffin sectioning or flash frozen in OCT compound in a mold over dry ice for frozen sectioning.

Aortas were cleaned of extraneous fat. For RNA isolation, aortas were flash frozen in liquid nitrogen. For *en face* plaque analysis, aortas were harvested, cleaned of extraneous fat and stripped of adventitia. The aortas were then carefully pinned onto a slide for further staining.

Spleens were dissociated over a 70 µm cell strainer and washed with HBSS to obtain a single cell suspension for FACS analysis. Erythrocytes were lysed by treating each sample with 3 ml RBC lysis buffer for 5 minutes. The lysis reaction was stopped by adding 5 ml HBSS and spinning at 350 g, 5 minutes, 4 °C to obtain leukocytes. For isolating naive CD4⁺ T cells, total CD4⁺ T cells or CD11c⁺ cells, spleens were placed in sterile PBS and treated as described later.

LNs were dissociated over a 70 µm cell strainer and washed with HBSS to obtain a single cell suspension for FACS analysis. For isolating naive CD4⁺ T cells, LNs were placed in sterile PBS and treated as described later.

BM for *in vitro* cultures was obtained from femurs by flushing with sterile PBS using a 20 ml syringe and a 26 gauge needle and making a single cell suspension over a 70 µm cell strainer. For isolating Lin⁻ cells, BM cells from the femurs, tibiae and hips were obtained and treated as described later.

3.2 Histology

3.2.1 Oil-Red O staining of aortas for plaque analysis

En face aortas were prepared as above and treated as follows:

step	reagent	duration	conditions
1	PBS	5 minutes	RT
2	60 % isopropanol	Dip 10 times	RT
3	Oil-Red O working solution	15 minutes	RT
4	60 % isopropanol	Dip 10 times	RT
5	Running tap water	5 minutes	RT

The slides were mounted with Kaiser's gelatin jelly working solution and covered with a coverslip.

3.2.2 Analysis of aortic plaque area

The *en face* aortas were analyzed in 3 parts – aortic arch, thoracic aorta and abdominal aorta. The total aorta area and plaque area were marked using the Diskus image analysis software and quantitated.

3.2.3 Preparation of aortic roots for paraffin sectioning

Hearts were prepared as described above. For paraffin sectioning, the hearts were removed from 4 % PFA and processed in an automated processing machine as follows:

step	reagent	duration	conditions
1	70 % ethanol	1 hour	RT
2	70 % ethanol	1 hour	RT
3	96 % ethanol	1 hour	RT
4	96 % ethanol	1 hour	RT
5	100 % ethanol	1 hour	RT
6	100 % ethanol	1 hour	RT
7	100 % ethanol	1 hour	RT
8	xylene	1 hour	45 °C
9	xylene	1 hour	45 °C
10	xylene	1 hour	45 °C
11	paraffin	1 hour	62 °C
12	paraffin	1 hour	62 °C
13	paraffin	O/N	62 °C

The hearts were then embedded in paraffin at an embedding station and 5 µm sections were cut onto glass slides at a microtome. The slides were placed in a dry air oven at 56 °C, O/N to dry.

3.2.4 De-paraffinization of aortic roots

Appropriate slides (with intact valves starting close to each other) were chosen and de-paraffinized using the following protocol:

step	reagent	duration	conditions
1	xylene	15 minutes	RT
2	xylene	15 minutes	RT

3	xylene	15 minutes	RT
4	100 % ethanol	1 minute	RT
5	100 % ethanol	1 minute	RT
6	70 % ethanol	1 minute	RT
7	70 % ethanol	10 minutes	RT
8	DDW	10 minutes	RT

3.2.5 Collagen-elastin staining of aortic roots for plaque analysis

De-paraffinized sections were stained as below:

step	reagent	duration	conditions
1	70 % ethanol	Briefly	RT
2	Aldehyde fuchsin working solution	15 minutes	RT
3	70 % ethanol	Dip 5 times	RT
4	DDW	5 minutes	RT
5	Sirius red solution	90 minutes	RT
6	0.01 N HCl	1 minute	RT

The sections were then dehydrated as follows:

step	reagent	duration	conditions
1	DDW	Short dip	RT
2	70 % ethanol	1 minute	RT
3	96 % ethanol	1 minute	RT
4	96 % ethanol	1 minute	RT
5	96 % ethanol	1 minute	RT
6	100 % ethanol	1 minute	RT
7	100 % ethanol	1 minute	RT
8	100 % ethanol	1 minute	RT
9	Xylene	5 minutes	RT
10	Xylene	5 minutes	RT
11	Xylene	5 minutes	RT

The slides were mounted with Vitro-Clud and covered with coverslip.

3.2.6 Analysis of aortic root plaque area

3 sections (as far away from each other as possible) per mouse were analyzed. The total aortic root area and plaque area was marked using the Diskus image analysis software and quantitated.

3.2.7 Antigen retrieval of aortic roots

For immunofluorescence staining of aortic roots, the de-paraffinized sections were treated for antigen retrieval. 150 ml of antigen retrieval working solution was warmed in the microwave and the slides were placed in a slide holder and inserted into the warm solution. The solution was heated for 10 minutes in the microwave at medium-high setting. Then half the solution was discarded and fresh working solution was added. The solution, with the slides, was re-heated for 10 minutes. The solution was allowed to cool for 30 minutes. The slides were removed and washed twice in PBS for 5 minutes.

3.2.8 Macrophage-Smooth muscle cell staining of aortic roots

De-paraffinized and antigen-retrieval treated sections were dried and circled with a Pap-pen. The sections were stained with the following protocol:

step	reagent	volume	duration	conditions
Block	MAC staining buffer	30 – 50 µl	30 minutes	RT, humidifier chamber
1° Ab	1:600 anti-mouse Mac2 + 1:200 anti-mouse α -Actin - Cy3 (in MAC staining buffer)	30 – 50 µl	O/N	4 °C, dark
Wash	PBS	In wash jars	15 minutes	RT, shaker
Wash	PBS	In wash jars	5 minutes	RT, shaker
2° Ab	1:500 anti-rat IgG - Alexa Fluor 488 (in MAC staining buffer)	30 – 50 µl	1 hour	RT, dark
Wash	PBS	In wash jars	15 minutes	RT, shaker
Wash	PBS	In wash jars	5 minutes	RT, shaker

The slides were dried, mounted with Vectashield containing DAPI and covered with a coverslip. The slides were sealed with nail polish.

3.2.9 T-cell staining of aortic roots

De-paraffinized and antigen-retrieval treated sections were dried and circled with a Pap-pen. The sections were stained with the following protocol:

step	reagent	volume	duration	conditions
Block	1 % BSA in PBS	30 – 50 µl	30 minutes	RT, humidifier chamber
1° Ab	1:50 anti-human CD3 (in 1 % BSA in PBS)	30 – 50 µl	O/N	4 °C, dark
Wash	PBS	In wash jars	15 minutes	RT, shaker
Wash	PBS	In wash jars	5 minutes	RT, shaker
2° Ab	1:500 anti-rat IgG - Alexa Fluor 488 (in 1 % BSA in PBS)	30 – 50 µl	1 hour	RT, dark
Wash	PBS	In wash jars	15 minutes	RT, shaker
Wash	PBS	In wash jars	5 minutes	RT, shaker

The slides were dried, mounted with Vectashield containing DAPI and covered with a coverslip. The slides were sealed with nail polish.

3.2.10 Preparation of aortic roots for frozen sectioning

Hearts were prepared as described above. For frozen sectioning, hearts frozen in OCT compound were cut into 5 µm sections onto Poly-L-lysine coated glass slides at a cryotome. The slides were fixed in 95 % ethanol for 10 minutes and stored at -80 °C till further use.

3.2.11 CD11c⁺ cell staining of aortic roots

Ethanol fixed, fresh frozen sections were dried and circled with a Pap-pen. The sections were stained with the following protocol:

step	reagent	volume	duration	conditions
Wash	PBS + 0.05 % Tween-20	In wash jars	5 minutes	RT, shaker
Block	DC staining buffer	30 – 50 µl	30 minutes	RT, humidifier chamber
Biotin block	Avidin D solution	30 – 50 µl	15 minutes	RT, humidifier chamber
Wash	PBS + 0.05 % Tween-20	In wash jars	Briefly	RT, shaker
Avidin block	Biotin solution 18	30 – 50 µl	15 minutes	RT, humidifier chamber

Wash	PBS + 0.05 % Tween-20	In wash jars	Briefly	RT, shaker
1° Ab	1:50 anti-mouse CD11c - biotin (in DC staining buffer)	30 – 50 µl	1 hour	RT, dark
Wash	PBS + 0.05 % Tween-20	In wash jars	3 X 5 minutes	RT, shaker
2° Ab	1:1500 SAV - Alexa Fluor 555 (in DC staining buffer)	30 – 50 µl	1 hour	RT, dark
Wash	PBS + 0.05 % Tween-20	In wash jars	3 X 5 minutes	RT, shaker

The slides were dried, mounted with Vectashield containing DAPI and covered with a coverslip. The slides were sealed with nail polish.

3.2.12 Analysis of aortic root plaque cell content

3 sections (as far away from each other as possible) per mouse were analyzed for each staining. For MAC analysis; total plaque area, macrophage area (green stained area), number of macrophages (blue nuclei + green staining), number of other cells (blue nuclei without green staining) and total number of cells in plaque (number of macrophages + other cells) were analyzed using the Diskus image analysis software.

For SMC analysis, total plaque area, SMC area (red stained area), number of SMCs (blue nuclei + red staining), number of other cells (blue nuclei without red staining) and total number of cells in plaque (number of SMCs + other cells) were analyzed using the Diskus image analysis software.

For T-cell analysis, number of T cells (blue nuclei + green staining), number of other cells (blue nuclei without green staining) and total number of cells in plaque (number of T cells + other cells) were analyzed using the Diskus image analysis software.

For CD11c⁺ cell analysis, number of CD11c⁺ cells (blue nuclei + red staining), number of other cells (blue nuclei without red staining) and total number of cells in plaque (number of CD11c⁺ cells + other cells) were analyzed using the Diskus image analysis software.

For necrotic core analysis, total plaque area and necrotic core area (plaque area with no blue nuclei) were analyzed using the Diskus image analysis software.

3.2.13 CD11c⁺ cell and HIF1 α staining of aortic roots

Ethanol fixed, fresh frozen sections were dried and circled with a Pap-pen. The sections were stained with the following protocol:

step	reagent	volume	duration	conditions
Wash	PBS + 0.05 % Tween-20	In wash jars	5 minutes	RT, shaker
Block	DC staining buffer	30 – 50 μ l	30 minutes	RT, humidifier chamber
Biotin block	Avidin D solution	30 – 50 μ l	15 minutes	RT, humidifier chamber
Wash	PBS + 0.05 % Tween-20	In wash jars	Briefly	RT, shaker
Avidin block	Biotin solution 18	30 – 50 μ l	15 minutes	RT, humidifier chamber
Wash	PBS + 0.05 % Tween-20	In wash jars	Briefly	RT, shaker
1° Ab	1:50 anti-mouse CD11c - biotin + 1:250 anti-mouse HIF1 α (in DC staining buffer)	30 – 50 μ l	1 hour	RT, dark
Wash	PBS + 0.05 % Tween-20	In wash jars	3 X 5 minutes	RT, shaker
2° Ab	1:1500 SAV - Alexa Fluor 555 + 1:1000 anti-rabbit IgG – Alexa Fluor 488 (in DC staining buffer)	30 – 50 μ l	30 minutes	RT, dark
Wash	PBS + 0.05 % Tween-20	In wash jars	3 X 5 minutes	RT, shaker

The slides were dried, mounted with Vectashield containing DAPI and covered with a coverslip. The slides were sealed with nail polish.

3.2.14 Detection of hypoxia

Hypoxia was detected in atherosclerotic lesions using the Hypoxyprobe Plus kit according to the manufacturer's protocol. *Ldlr*^{-/-} mice on diet for 8 weeks or healthy *Ldlr*^{-/-} mice fed normal chow were injected with 60 mg/kg pimonidazole hydrochloride i.p. After 90 minutes, the mice were sacrificed, immediately flushed with PBS and 4% PFA and the hearts were stored in 4 % PFA. The hearts were embedded in OCT compound and cut into 5 µm sections onto Poly-L-lysine coated glass slides at a cryotome. The sections were fixed in 95 % ethanol for 10 minutes. The slides were then stored at -80 °C till further use. Fixed frozen sections were dried and circled with a Pap-pen. The sections were stained with the following protocol:

step	reagent	volume	duration	conditions
Peroxidase quenching	3 % H ₂ O ₂ in DDW	30 – 50 µl	5 minutes	RT
Wash	Rinse buffer	In wash jars	2 minutes	RT, shaker
Block	1 % BSA in TBS	30 – 50 µl	15 minutes	RT, humidifier chamber
Wash	Rinse buffer	In wash jars	2 minutes	RT, shaker
1° Ab	1:50 mouse anti-Hypoxyprobe-FITC (in rinse buffer)	30 – 50 µl	30 minutes	RT, dark
Wash	Rinse buffer	In wash jars	2 minutes	RT, shaker
2° Ab	1:100 rabbit anti-FITC-HRP (in rinse buffer)	30 – 50 µl	30 minutes	RT, dark
Wash	Rinse buffer	In wash jars	2 minutes	RT, shaker

HRP was detected using the DAB substrate kit for peroxidase according to the manufacturer's protocol. Substrate solution was prepared immediately before use by mixing 5 ml DDW, 2 drops buffer stock solution, 4 drops DAB stock solution and 2 drops Hydrogen peroxide solution.

step	reagent	volume	duration	conditions
Peroxidase reaction	Substrate solution	30 – 50 µl	10 minutes	RT
Wash	DDW	In wash jars	5 minutes	RT, shaker

The sections were counterstained and dehydrated as below:

step	reagent	duration	conditions
1	Hematoxylin	5 minutes	RT
2	DDW	Short dip	RT
3	Tap water	10 minutes	RT
4	DDW	Short dip	RT
5	Eosin	30 seconds	RT
6	DDW	Short dip	RT
7	70 % ethanol	1 minute	RT
8	96 % ethanol	1 minute	RT
9	96 % ethanol	1 minute	RT
10	96 % ethanol	1 minute	RT
11	100 % ethanol	1 minute	RT
12	100 % ethanol	1 minute	RT
13	100 % ethanol	1 minute	RT
14	Xylene	5 minutes	RT
15	Xylene	5 minutes	RT
16	Xylene	5 minutes	RT

The slides were mounted with Vitro-Clud and covered with coverslip.

3.3 Cell culture techniques

3.3.1 Bone marrow derived dendritic cell (BMDC) culture

To set up BMDC cultures, BM cells were obtained from mice aseptically as mentioned above and plated in 10 cm or 20 cm cell culture dishes in DC medium at a concentration of 2×10^6 cells/ml. The cultures were supplemented with 50 ng/ml murine GM-CSF. The plates were incubated at 37 °C, 5 % CO₂. The medium was changed on days 3, 5 and 7 and the cells were ready on day 8. Cells were used for RNA isolation, FACS analysis or further treatment.

3.3.2 Bone marrow derived macrophage (BMM) culture

To set up BMM cultures, BM cells were obtained from mice aseptically as mentioned above and plated in 10 cm or 20 cm cell culture dishes in DC medium supplemented with 15 % L929 conditioned medium at a concentration of 2×10^6 cells/ml. The plates were incubated at 37 °C, 5 %

CO₂. The medium was changed on days 3, 5 and 7 and the cells were ready on day 7. To harvest adherent macrophages, spent medium was discarded and the cell layer was washed lightly with PBS. 5 ml Lidocaine-EDTA solution was added to the plate and the cells were incubated at 37 °C for 2 to 5 minutes. The plate was flicked and tapped gently but thoroughly to dislodge all cells. More Lidocaine-EDTA solution was used if needed. The detached cells were added to a 50 ml Falcon tube containing DC medium. The cells were washed to remove all Lidocaine-EDTA and pelleted. Cells were used for RNA isolation, FACS analysis or further treatment.

3.3.3 Stimulation of cultured cells

BMDCs and BMMs were stimulated by treatment with 100 ng/ml murine TNF α for 24 hours. BMDCs were also treated with 1 μ g/ml LPS for 6 hours for some experiments.

3.3.4 Isolation of splenic DCs

For isolation of splenic DCs, CD11c microbeads were used following manufacturer's protocol. Spleens were obtained from mice as mentioned before. Each spleen was placed in 1 ml of 2 mg/ml Collagenase D solution in a well of a 24 well plate. Using a 26 gauge needle and a 1 ml syringe, the Collagenase D solution was perfused through the spleen. The spleen was then chopped into small pieces and incubated in the Collagenase D solution for 30 minutes at 37 °C. The spleens were then passed over a 70 μ m cell strainer to make a single cell suspension and washed with MACS buffer. The cells were tagged with CD11c microbeads and magnetically separated on MS columns to give CD11c⁺ cells.

3.3.5 Isolation of splenic CD4⁺ T cells

For isolation of splenic CD4⁺ T cells, CD4⁺ T-cell isolation kit II was used following manufacturer's protocol. Spleens were obtained from mice as mentioned before and passed over a 70 μ m cell strainer to make a single cell suspension and washed with MACS buffer. The cells were incubated with a Biotin-antibody cocktail to biotin-tag non-target cells using antibodies to CD8a, CD11b, CD11c, CD19, CD45R, CD49b, CD105, MHC class II, and Ter-119.

The cells were treated with anti-biotin microbeads and magnetically separated on MS columns to give untouched CD4⁺ T cells.

3.3.6 Isolation of naive CD4⁺ T cells

For isolation of naive CD4⁺ T cells, CD4⁺ CD62L⁺ T-cell isolation kit was used following manufacturer's protocol. Spleens and LNs were obtained from mice as mentioned before and passed over a 70 µm cell strainer to make a pooled single cell suspension and washed with MACS buffer. The cells were incubated with a Biotin-antibody cocktail to biotin-tag non-target cells using antibodies to CD8a, CD45R, CD11b, CD25, CD49b, TCRγ/δ, and Ter-119. The cells were treated with anti-biotin microbeads and magnetically separated on LS columns to give untouched CD4⁺ T cells. The cells were then tagged with CD62L (L-Selectin) microbeads and magnetically separated on MS columns to give naive CD4⁺ T cells.

3.3.7 Isolation of lineage depleted BM cells

BM cells were isolated as mentioned above and depleted for lineage cells using the Lineage cell depletion kit. The cells were incubated with a Biotin-antibody cocktail to biotin-tag lineage cells using antibodies to CD5, CD45R, CD11b, Gr-1 (Ly-6G/C), 7-4 and Ter-119. The cells were treated with anti-biotin microbeads and magnetically separated on LS columns to give untouched lineage depleted BM cells.

3.3.8 Antigen specific T-cell proliferation

Naive CD4⁺ T cells were isolated from OT-II mice as mentioned above. Cells were adjusted to 20 x 10⁶ cells/ml in DC medium and incubated with 1 µl/ml 5 mM CFSE for 10 minutes at 37 °C. Cells were then washed with DC medium and adjusted to 1 x 10⁶ cells/ml. In parallel, CD11c⁺ cells were isolated from spleens as mentioned above. Cells were adjusted to 1 x 10⁶ cells/ml and incubated with 1 µg/ml OVA₃₂₃₋₃₃₉ peptide in DC medium for 45 minutes at 37 °C. Cells were then washed with DC medium and adjusted to 1x10⁶ cells. The naive T cells and DCs were co-cultured in a ratio of 3:1 (T cell:DC) in a round bottom 96 well plate with final volume of 200 µl/well. Negative controls, where the DCs were not loaded with the OVA₃₂₃₋₃₃₉ peptide were also used. For IL-12 blocking experiments, wells were treated with

anti-IL-12 antibody at 1 µg/ml concentration. The cells were co-cultured for 48 hours at 37 °C. After this, the cells were pelleted and analyzed by FACS.

3.3.9 Antigen specific T-cell polarization

To analyze T-cell polarization, a co-culture assay was set up as above for the T-cell proliferation, but the naive T cells were not labeled with CFSE. The cells were co-cultured for 72 hours at 37 °C. After this, the cells were pelleted and analyzed by FACS.

3.3.10 BMDC transmigration assay

BMDCs were starved of serum by resuspending in transmigration medium O/N at 37 °C. The cells were washed and adjusted to 2×10^6 cells/ml in transmigration medium. 200 µl cell suspension was added to the top chamber of an 8 µm cell culture insert. The inserts were placed in wells of a 24 well plate which contained 600 µl transmigration medium with 100 ng/ml murine CCL19 or no cytokine (negative control) or 10 % serum (positive control). The plates were incubated for 2 hours at 37 °C. The inserts were then carefully removed and discarded. The cells in the bottom chamber were determined by counting in a hemocytometer.

3.3.11 Transfection of DCs with inhibition and overexpression plasmids

BMDCs were washed, counted and adjusted to 2×10^6 cells/ml. Per transfection reaction, 2.5×10^5 cells were mixed with 1.5 µg plasmid and 100 µl nucleofector solution from the P4 primary cell 4D-nucleofector kit. The cell suspension was added to nucleocuvette vessels without forming air bubbles. The cuvette was then placed in the retainer of the 4D-nucleofector X unit. The DK-100 program (for immature DCs with high efficiency) was run for each sample. Cells were then resuspended and added to 800 µl pre-warmed DC medium in a 24 well plate. Cells were incubated for 24 hours at 37 °C and then pelleted and used for RNA isolation.

3.3.12 Maintenance of HEK293F cells

HEK293F cells were cultured in 10 cm or 20 cm cell culture dishes in complete D-MEM. They were sub-cultured every 3rd day when they reached 80% confluency. To sub-culture cells, the spent medium was discarded and

the cell monolayer washed with PBS. 1 ml Trypsin-EDTA was added per 10 cm dish and incubated at 37 °C for 2 minutes. The cells were thoroughly dislodged by tapping gently. 9 ml fresh complete D-MEM was added to the plate to inactivate trypsin. A new culture was set up at 1:10 cell dilution of the old cell suspension.

3.4 Nucleic acid detection techniques

3.4.1 Genomic DNA isolation

To isolate gDNA for genotyping of mice, a 0.5 - 1 cm piece of the mouse tail was cut and incubated with 190 µl tail lysis buffer and 10 µl 1 mg/ml Proteinase-K at 56 °C, O/N with constant shaking at 1400 rpm. The tubes were centrifuged at 20,000 g for 10 minutes at RT and the supernatant transferred to a new microcentrifuge tube. To this tube, 300 µl tail lysis buffer, 50 µl 3M sodium acetate and 450 µl isopropanol were added, mixed well and centrifuged at 20,000 g for 30 minutes at RT. 500 µl 70 % ethanol was added to the pellet and centrifuged at 20,000 g for 20 minutes at RT. The pellet was dried thoroughly and resuspended in 75 µl 10 mM Tris, pH 8.0. This isolated gDNA was then used in conventional PCR reactions for genotyping analysis.

To isolate gDNA from isolated CD11c⁺ and CD4⁺ cells for deletion efficiency analysis, cells were incubated with 190 µl tail lysis buffer and 10 µl 1 mg/ml Proteinase-K at 56 °C for 1 hour with constant shaking at 1400 rpm. The isolation protocol was then continued as mentioned above for the tails.

3.4.2 Total RNA isolation

RNA was isolated with the RNeasy Mini kit or the Nucleospin RNA II kit for isolated splenic DCs, cultured BMDCs and BMMs and with the RNeasy Micro kit for flash frozen aortas according to manufacturer's protocol. RNA was eluted in a final volume of 30 – 50 µl nuclease free water and spectrometrically quantitated on the Nanodrop at wavelengths 260 nm and 280 nm.

3.4.3 cDNA synthesis

A cDNA synthesis reaction was set up as follows:

Total RNA	10 μ l
Random primers	1 μ l

The reaction was mixed and incubated at 65 °C for 5 minutes, chilled on ice, spun down briefly and the following components were added:

5 X Reaction Buffer	4 μ l
10 mM dNTP Mix	2 μ l
RiboLock RNase Inhibitor (20 U/ μ l)	1 μ l
M-MuLV Reverse Transcriptase (20 U/ μ l)	2 μ l
Total volume	20 μ l

The reaction was mixed and incubated at 25 °C for 5 minutes followed by 37 °C for 60 minutes. The reaction was terminated by heating at 70 °C for 5 minutes. The cDNA concentration was adjusted to 10 ng/ μ l with nuclease free water.

3.4.4 Conventional PCR for genotyping

A PCR reaction was set up as follows

10 ng/ μ l gDNA	3 μ l
2 X PCR master mix	12.5 μ l
Each 10 μ M primer	1.25 μ l
Nuclease free water	to make up volume to 25 μ l
Total volume	25 μ l

The PCR reaction tubes were closed, briefly spun and placed in a thermal cycler with the following conditions:

step	temperature	duration	cycle
1	94 °C	3 minutes	no
2	94 °C	30 seconds	35x
3	Varied (see below)	1 minute	
4	72 °C	1 minute	
5	72 °C	2 minutes	no
6	10 °C	∞	no

The annealing temperatures used were as follows:

<i>Hif1a</i> -flox	55 °C
<i>Cd11c</i> -cre	64 °C
<i>Ldlr</i>	61 °C
OT-II	56 °C

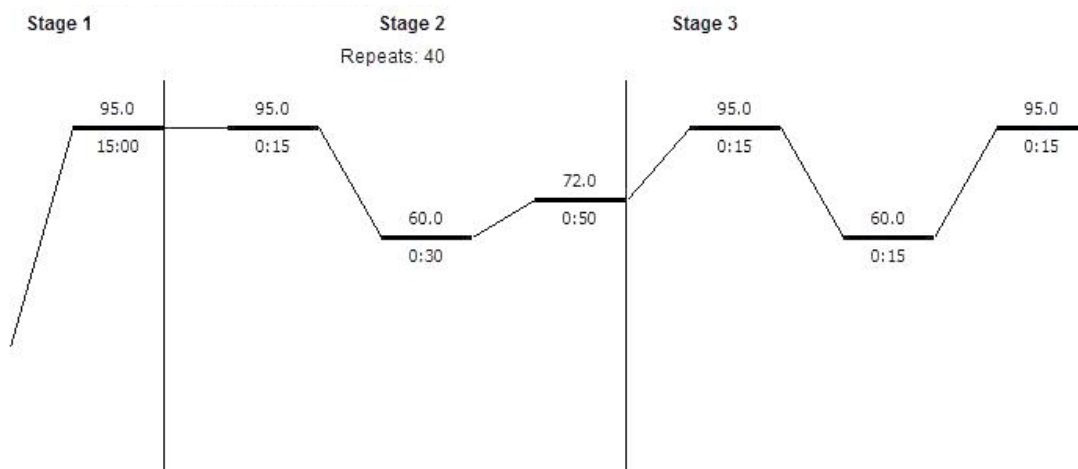
The PCR products were run on a 1.5 % or a 3 % agarose gel in 1 X TAE buffer.

3.4.5 Quantitative real time PCR

A PCR reaction was set up as follows

10 ng/ μ l cDNA or gDNA	2 μ l
2 X SYBR green master mix	5 μ l
10 μ M gene specific forward primer	0.5 μ l
10 μ M gene specific reverse primer	0.5 μ l
Nuclease free water	2 μ l
Total volume	10 μ l

The reaction was prepared in wells of a 384 well plate. The samples were also probed for a housekeeping gene (*Hprt*) to be used for normalization. No template controls were included for every primer pair. The plate was sealed, briefly spun and placed in a real time PCR system with the following conditions:



For the *I12a* qPCR, 1 μ l of the 10 X Quantitect primer was used in place of the forward and reverse primers. The annealing temperature was set at 55 °C. All the remaining conditions were same as above. Data was analysed using the SDS 2.4 software.

3.5 Protein detection techniques

3.5.1 Flow cytometry

For surface protein analysis by flow cytometry, cells were plated in a 96-well round bottom plate and centrifuged at 350 g, 5 minutes at 4 °C. The cells were washed once with HBSS. The pellet was stained with fluorescent antibodies at 1:300 dilution in 50 µl FACS staining buffer working solution and incubated at 4 °C for 30 minutes in dark. The cells were then washed twice with HBSS and resuspended in 50 µl HBSS per sample.

For intracellular IL-17a, IFN γ and IL-12 analysis by flow cytometry, cells were incubated at 37 °C for 4 hours with 200 µl of respective stimulation mix. After stimulation, cells were washed twice with HBSS and surface staining was carried out as mentioned above. After 2 washes with HBSS, the cells were pulse-vortexed and then fixed and permeabilized using 100 µl BD Cytotfix/Cytoperm buffer at 4 °C for 20 minutes in dark. The plate was centrifuged at 350 g, 4 °C, 5 minutes and washed twice with 1 X BD Perm/Wash buffer. The cells were then stained with the intracellular antibodies at 1:100 dilution in 50 µl 1 X BD Perm/Wash buffer and incubated at 4 °C for 30 minutes in dark. The cells were then washed twice with 1 X BD Perm/Wash buffer and resuspended in 50 µl HBSS per sample.

For intracellular FoxP3 analysis by flow cytometry, surface staining was carried out as mentioned above. After 2 washes with HBSS, the cells were pulse-vortexed and then fixed and permeabilized using 100 µl 1 X eBioscience Fixation/Permeabilization solution at 4 °C for 30 minutes in dark. The plate was centrifuged at 350 g, 4 °C, 5 minutes washed twice with 1 X eBioscience Permeabilization buffer. The cells were then stained with the FoxP3-PE antibody at 1:100 dilution in 50 µl 1 X eBioscience Permeabilization buffer and incubated at 4 °C for 30 minutes in dark. The cells were then washed twice with 1 X eBioscience Permeabilization buffer and finally resuspended in 50 µl HBSS per sample.

For intracellular STAT3 analysis by flow cytometry, surface staining was carried out as mentioned above. After 2 washes with HBSS, the cells were pulse-vortexed and then fixed and permeabilized using 100 µl 1 X eBioscience

Fixation/Permeabilization solution at 4 °C for 30 minutes in the dark. The plate was centrifuged at 350 g, 4 °C, 5 minutes and washed twice with 1 X eBioscience Permeabilization buffer. The cells were blocked with 50 µl STAT3 blocking buffer for 30 minutes at 4 °C and 1:100 Fc receptor block for 10 minutes at 4 °C. The plate was centrifuged at 350 g, 4 °C, 5 minutes to discard the blocking buffer. The cells were then stained with the STAT3 antibody at 1:200 dilution in STAT3 blocking buffer and incubated at 4 °C for 1 hour in dark. The cells were washed twice with 1 X eBioscience Permeabilization buffer and stained with anti-murine IgG2a-PE secondary antibody at 1:1000 dilution in STAT3 blocking buffer and incubated at RT for 30 minutes in dark. The cells were then washed twice with 1 X eBioscience Permeabilization buffer and finally resuspended in 50 µl HBSS per sample.

All samples were read in an HTS plate reader in the FACS Canto II and analyzed using the FlowJo software. Doublet cells were excluded using the FSC-H v/s SSC-H and FSC-W v/s SSC-W plots. Leukocytes were selected using the CD45 marker.

3.5.2 ELISA

IL-12 protein levels were detected in BMDC supernatants using the IL-12 Mini ELISA development kit according to the manufacturer's protocol. The final detection was done using ABTS liquid substrate solution and the protein levels were quantitated by comparing to a standard curve and extrapolating.

3.6 Lipid detection techniques

3.6.1 Cholesterol assay

Total cholesterol levels were measured in serum using the Amplex red cholesterol assay kit according to manufacturer's protocol and quantitated on the Fluostar OPTIMA plate reader or using standard enzymatic techniques automated on the Cobas Fara centrifugal analyzer.

3.6.2 Triglyceride assay

Triglyceride levels were measured in serum using the EnzyChrom triglyceride assay kit according to manufacturer's protocol and quantitated on the Fluostar OPTIMA plate reader.

3.7 Bacterial techniques

3.7.1 Eluting plasmids from filter paper spots

Spotted plasmids were cut and placed in a 1.5 ml microcentrifuge tube with 50 μ l nuclease free water for 1-2 hours. The eluted plasmids were pipetted out and aliquoted.

3.7.2 Preparation of LB plates

LB medium was supplemented with 15 % agar and autoclaved. When cooled to \sim 50 $^{\circ}$ C, 50 μ g/ml ampicillin was added and the medium poured into bacterial petri-plates. The plates were allowed to stand at RT O/N for the agar to set.

3.7.3 Transformation of bacterial cells

1 μ l plasmid (eluted from filter papers) was mixed with 50 μ l chemically competent *E.coli* XL10 or DH5 α cells and incubated on ice for 30 minutes. The cells were then incubated at 42 $^{\circ}$ C for 90 seconds and placed back immediately on ice for 2 minutes to provide heat shock. 800 μ l SOC medium was added to each tube and the cells incubated at 37 $^{\circ}$ C for 45 minutes. Various dilutions of the cells were plated on LB plates with 50 μ g/ml ampicillin. No-plasmid negative controls were also used. The plates were incubated O/N at 37 $^{\circ}$ C.

3.7.4 Growth of transformed cells for plasmid DNA isolation

A single bacterial colony was picked up from the incubated plates using a 200 μ l microtip and added to a tube containing 3 ml LB medium with 50 μ g/ml ampicillin. The tube was incubated at 37 $^{\circ}$ C for 6-8 hours at 200 rpm shaking. The 3 ml of culture was then added to 200 ml LB medium with

50 µg/ml ampicillin in a conical flask and incubated at 37 °C O/N at 200 rpm shaking.

3.7.5 Plasmid DNA isolation

Plasmid DNA was isolated from transformed bacterial cells using the NucleoBond PC 500 kit or the PureLink HiPure Plasmid Maxiprep Kit according to the manufacturer's protocol. DNA was resuspended in a final volume of 200 – 500 µl nuclease free water, and spectrometrically quantitated on the Nanodrop at wavelengths 260 nm and 280 nm.

3.7.6 Lentiviral vector – Cre vector co-transfection

HEK293F cells were plated onto 6 well plates and incubated at 37 °C for 24 hours to reach 80 % confluency. For each well, 1 ml serum-free D-MEM, 200 ng lentivirus vector, 600 ng pIC-cre vector and 2.5 µl Genejammer transfection reagent were mixed in a microcentrifuge tube and incubated at RT for 20 minutes. The mix was then added to the wells, dropwise over the medium. Some wells were treated only with 200 ng lentivirus vector to be taken as Cre-minus controls. The plates were incubated at 37 °C, 5 % CO₂. After 48 hours, the cells were stained for Thy1.1 and detected by FACS. Some cells were also pelleted and stored for RNA isolation.

3.8 Lentivirus techniques

3.8.1 Transfection of HEK293F cells for lentivirus production

HEK293F cells in 150 mm culture dishes at 80 % confluency were used for transfection. In a 15 ml tube, 2 ml serum-free D-MEM, 70 µl Genejammer transfection reagent, 20 µg lentiviral vector, 4 µg gag/pol vector, 3 µg vsvg vector, 3 µg rev vector and 5 µg pAdv vector were mixed for each 150 mm culture dish and incubated at RT for 20 minutes. The mix was then added to the 150 mm culture dish, drop wise over the medium. The plates were incubated at 37 °C, 5 % CO₂.

3.8.2 Harvesting of lentivirus

After 48 hours, the spent medium from transfected cells was removed into 50 ml tubes and centrifuged at 2,300 rpm, 7 minutes at 4 °C to remove

cell debris. The medium was then filtered through a 0.45 µm filter using a 30 ml syringe into another 50 ml tube. The filtered medium was added to clear ultracentrifuge tubes and the tubes were sealed with parafilm and placed in ultracentrifuge rotor buckets. The buckets were then placed in the pre-cooled rotor and the rotor adjusted into a pre-cooled ultracentrifuge. The tubes were centrifuged at 25,000 rpm for 90 minutes at 4 °C under vacuum. After centrifugation, the medium supernatant was aspirated and the ultracentrifuge tubes placed upside down on a tissue paper to allow excess supernatant to be absorbed. 50 µl D-PBS per 150 mm initial culture dish was added to the virus pellet and left O/N at 4 °C.

3.8.3 Virus titration

A day after harvesting virus, the virus particles were carefully resuspended and aliquoted into 1.5 ml micro centrifuge tubes. 1 µl virus suspension was kept aside for titration whereas the rest of the aliquots were snap frozen in LN₂ and stored at -80 °C. The 1 µl virus suspension was used to make 3 different dilutions (1, 1:10 and 1:100) in complete D-MEM. 1 ml of each dilution was added per well to HEK293F cells in a 6 well plate. One well was left untransfected. The cells were incubated at 37 °C for 48 hours. The virus was titrated by staining the cells for Thy1.1. The calculations were done as follows:

Since 200,000 HEK293F cells were plated in each well at day 0, it was assumed that on the day of transduction the number of cells would be 400,000.

If 1µl virus suspension led to x % Thy1.1⁺ cells,

Titer (virus particles/ml) = $x/100 \times 400,000$

Similarly, calculations for 1:10 and 1:100 dilutions were done after multiplying the dilution factor, and an average of the 3 titers was taken as the final viral titer.

3.8.4 Viral transduction of BM cells for *in vitro* analysis

BM cells from *Cd11c-cre* mice were plated onto 6 well plates in complete D-MEM. The cells were transduced with 50 MOI lentivirus (STAT3 or

control) in the presence of 10 µg/ml DEAE Dextran and incubated at 37 °C for 24 hours. Then, the cells were washed and cultured as per BMDC culture protocol in DC medium and 50 ng/ml GM-CSF for 7 days. The cells were stained for Thy1.1 and detected by FACS. Some cells were also pelleted and stored for RNA isolation.

3.8.5 Viral transduction of Lin- BM cells for *in vivo* transplantation

Lin- BM cells from CKO and WT mice were isolated as mentioned before and plated onto 6 well plates in complete D-MEM. The cells were transduced with 50 MOI lentivirus (STAT3 or control) in the presence of 10 µg/ml DEAE Dextran and incubated at 37 °C for 24 hours. Then, the cells were washed twice with sterile D-PBS and adjusted at a concentration of 1×10^6 cells/100 µl per recipient mouse. The cell suspension was loaded onto 1 ml syringes and injected retro-orbitally into irradiated *Ldlr*^{-/-} mice.

3.9 Transcription factor binding site analysis

3.9.1 Transcription factor binding site prediction

The transcription factor binding site prediction software MatInspector was used to predict HIF1α binding sites (HBS) and HIF1α ancillary sites (HAS) on SOCS1 (Gene ID: 12703), SOCS3 (Gene ID: 12702) and STAT3 (Gene ID: 20848) gene promoters²⁶³. The Entrez Gene ID for the particular gene was added to the input field and all the possible transcripts retrieved from the EIDorado database were selected. Default matrix parameters were used. The positions (if existing) of the HBS and HAS were noted. The HBS sequences were identified on the gene sequence and primers were designed around the HBS using NCBI Primer BLAST.

3.9.2 Chromatin immunoprecipitation assay

The commercially available ExactaChIP Human/Mouse HIF1α chromatin immunoprecipitation kit was used according to manufacturer's protocol. Day 7 BMDCs from C57BL6/J mice were treated with 150 µM CoCl₂ (to enhance HIF1α protein levels) for 16 hours. 5×10^6 cells per test were fixed and cross-linked with 37 % formaldehyde to obtain a final concentration of 1 %

and the samples were incubated on a rocker for 15 minutes at RT. The formaldehyde was quenched by adding 1 M glycine to a final concentration of 125 mM and incubated on a rocker at RT for 5 minutes. The cells were then pelleted and the supernatant discarded. Each pellet was resuspended in 500 μ l Lysis buffer (with 10 μ g/ml aprotinin, 10 μ g/ml leupeptin and 1 mM PMSF) and incubated on ice for 10 minutes. The samples were then sonicated at 45% output power for 6 cycles with 15 seconds pulse/cycle. The samples were placed on ice for 45 seconds between every cycle. After sonication, the cells were pelleted by centrifugation at 12,000 g for 10 minutes and the supernatant was collected. 25 μ l of this supernatant was stored at -20 °C as input DNA control. 10 μ l supernatant was run on a 1.5 % agarose gel to determine DNA fragment size and hence efficiency of sonication.

The supernatants were then diluted with 1 ml Dilution buffer (with 10 μ g/ml aprotinin, 10 μ g/ml leupeptin and 1 mM PMSF). To each test sample, 5 μ l anti-HIF1 α antibody was added. To each control sample, 20 μ l normal goat IgG was added as negative control. The samples were incubated on a rocker O/N at 4 °C. To precipitate the antibody tagged HIF1 α protein, along with the protein bound chromatin DNA fragments, the samples were incubated with 50 μ l Streptavidin beads on the rocker at 4 °C for 30 minutes. The beads were collected by centrifugation at 12,000 g for 1 minute. The beads were then washed twice with each of the 4 wash buffers provided with the kit. After the last wash, 100 μ l Chelating resin solution was added to each sample (and also to the input) to reverse crosslink and release the DNA and the samples were boiled for 10 minutes on a heat block. The DNA fragments were obtained in the supernatant by centrifugation at 12,000 g for 1 minute. The pelleted beads were washed with DDW to collect remaining DNA fragments in supernatant. The DNA fragments were cleaned and concentrated using the QIAquick DNA purification kit, following manufacturer's protocol. DNA was finally resuspended in 50 μ l nuclease free water.

Equal volumes of the samples (anti-HIF1 α , IgG and input) were taken in a qPCR reaction using primers against the HIF1 α binding region in the SOCS3 and STAT3 promoter regions (as predicted in the MatInspector software). The results were analyzed and presented as percent input. A conventional PCR

was also performed with the samples and the amplified products were separated on a 1 % agarose gel to visualize differences in band intensities.

3.10 Statistics

Statistical analysis was performed using the Graphpad Prism 4.0 software. Normality tests were performed to determine Gaussian distribution of data and accordingly either a parametric unpaired Student's t-test or a parametric Mann-Whitney test was used. To compare three or more groups, a one-way ANOVA test was used with a Tukey's post hoc test.

All data is presented as mean \pm SEM and p values below 0.05 are considered statistically significant (* = $p < 0.05$, ** = $p < 0.01$, *** = $p < 0.001$).

4. RESULTS

4.1 Presence of hypoxia and HIF1 α in atherosclerotic mice

Atherosclerotic plaques become hypoxic due to the thickness of the plaque, preventing optimal oxygen diffusion from the blood, and due to the high metabolic demand of accumulating cells. Hypoxia in the plaque has been demonstrated previously in human lesion specimens as well as mouse and rabbit models of atherosclerosis and to confirm the presence of hypoxia in our mouse model, the common hypoxia marker Hypoxyprobe (pimonidazole), which stains hypoxic but actively metabolizing cells, was used. In *Ldlr*^{-/-} mice fed a high fat diet for 8 weeks, Hypoxyprobe was injected i.p. and the mice were sacrificed after 90 minutes. The aortic root sections showed presence of hypoxia as marked by the brown DAB staining (**Figure 4.1.1a**). Atherosclerotic plaque sections from mice injected with PBS instead of Hypoxyprobe were used as negative controls for staining (**Figure 4.1.1b**). Additionally, C57BL6/J mice injected with Hypoxyprobe also did not show non-specific staining in the aortic root (data not shown).

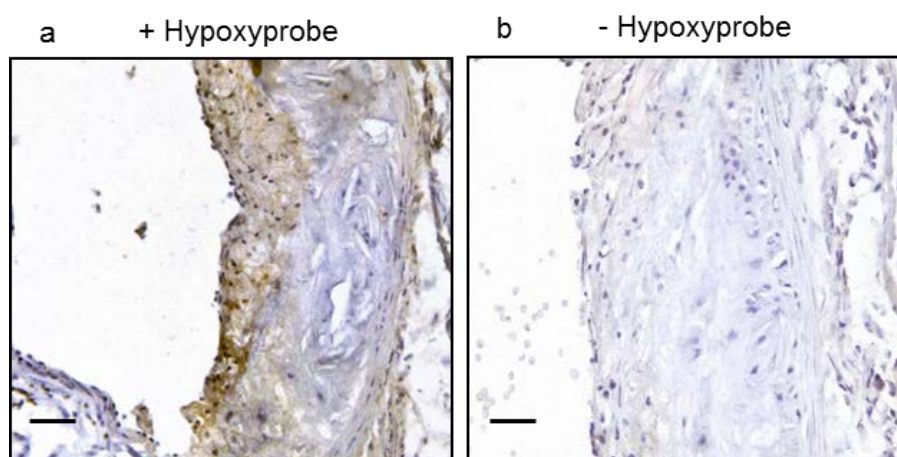


Figure 4.1.1 Presence of hypoxia in atherosclerotic plaques

(a) Sections of aortic root of *Ldlr*^{-/-} mice after 8 weeks of high fat diet injected with Hypoxyprobe and stained to detect presence of hypoxic regions (brown, scale bars: 50 μ m). **(b)** Sections of aortic root of *Ldlr*^{-/-} mice after 8 weeks of high fat diet injected with PBS and stained to detect presence of hypoxic regions (scale bars: 50 μ m).

Since the expression of *Hif1a* is known to increase in hypoxic tissues, it was essential to determine the change in expression of *Hif1a* in tissues from atherosclerotic mice. In whole aortas from *Ldlr*^{-/-} mice fed a high fat diet for 8 weeks, the mRNA expression of *Hif1a* was significantly up-regulated

compared to healthy 6 week old *Ldlr*^{-/-} mice fed normal chow (**Figure 4.1.2a**). Moreover, in CD11c⁺ cells isolated from spleens of *Ldlr*^{-/-} atherosclerotic mice, the expression of *Hif1a* was much higher compared to splenic CD11c⁺ cells from control healthy mice (**Figure 4.1.2b**). This clearly demonstrates that non-hypoxic conditions like inflammation in the spleen (due to atherosclerotic disease progression) are also responsible for increased *Hif1a* in cells leading to systemic changes, in addition to localized changes in hypoxic areas in the aorta.

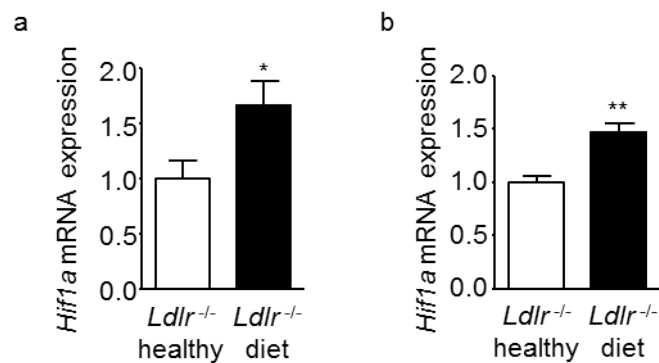


Figure 4.1.2 Increased mRNA expression of *Hif1a* in atherosclerosis

(a) Analysis of *Hif1a* mRNA expression by qPCR in aortic tissue of healthy *Ldlr*^{-/-} mice and *Ldlr*^{-/-} mice fed a high fat diet for 8 weeks, normalized to *Hprt* and relative to healthy *Ldlr*^{-/-} mice (n=8). **(b)** Analysis of *Hif1a* mRNA expression by qPCR in splenic DCs of healthy *Ldlr*^{-/-} mice and *Ldlr*^{-/-} mice fed a high fat diet for 8 weeks, normalized to *Hprt* and relative to healthy *Ldlr*^{-/-} mice (n=4). Data is presented as mean ± SEM; *p<0.05, **p<0.01.

In double immunofluorescence staining experiments, co-localization of lesional HIF1α protein with CD11c⁺ DCs could also be confirmed, indicating HIF1α expression in DCs in lesions of atherosclerotic mice (**Figure 4.1.3**).

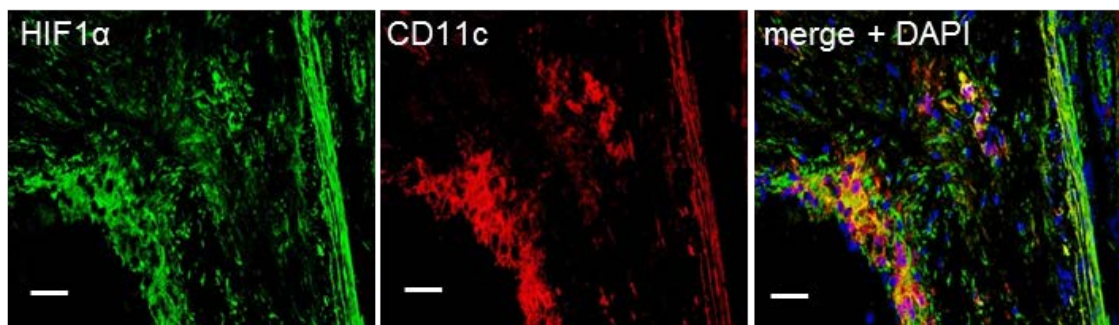
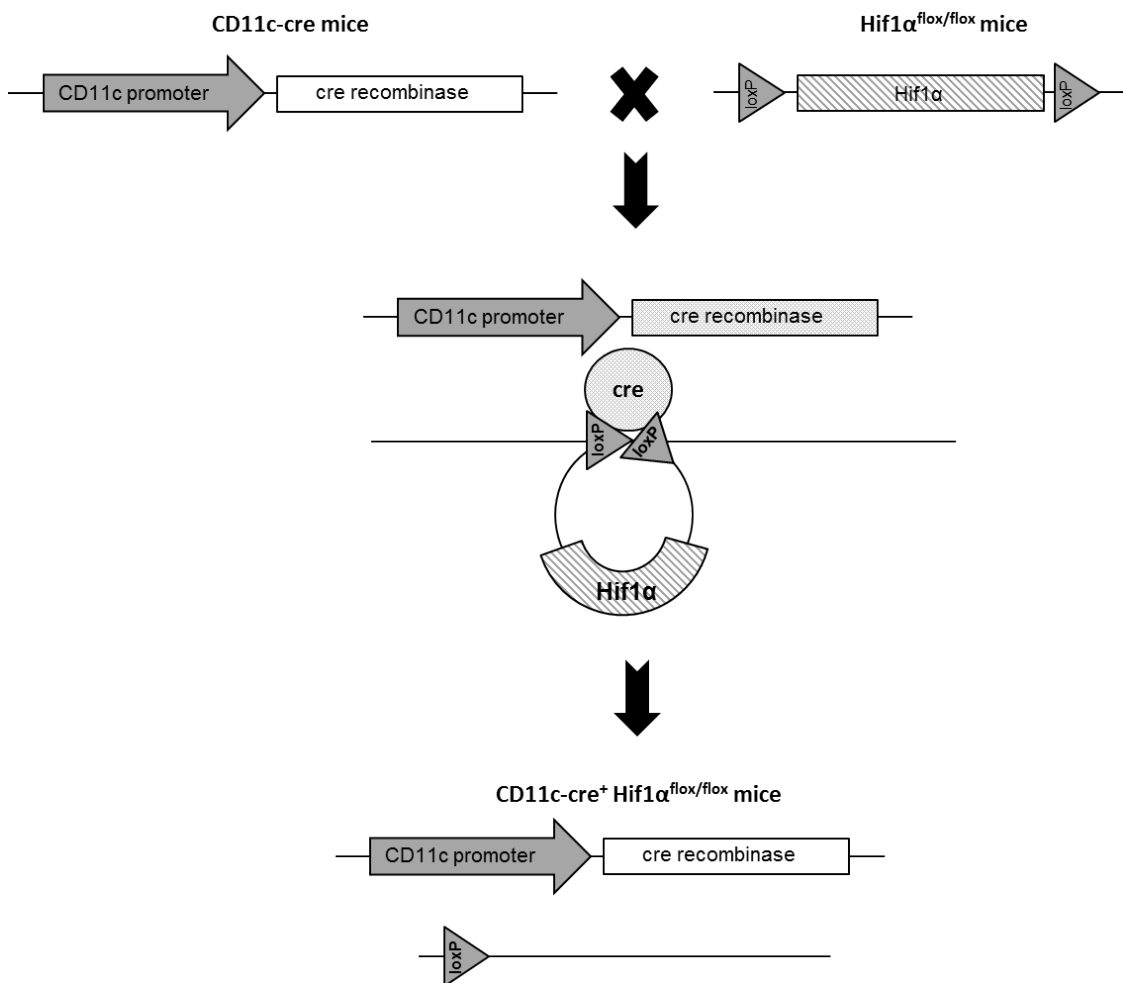


Figure 4.1.3 Co-expression of HIF1α and DCs in atherosclerotic plaques

Double-immunofluorescence staining of HIF1α (green) and CD11c (red) in atherosclerotic plaques of the aortic root of *Ldlr*^{-/-} mice fed a high fat diet for 8 weeks. Cell nuclei were counterstained with DAPI (blue) (scale bars: 50µm).

4.2 Generation of mice deficient for HIF1 α in CD11c⁺ cells

This project aimed at identifying the role of HIF1 α in DCs. Since CD11c is the most commonly used DC marker, the Cre-flox system under control of the CD11c promoter was used to generate mice lacking HIF1 α specifically in DCs. For this purpose, commercially available *Cd11c-cre* mice were crossed with *Hif1a*^{flox/flox} mice to generate *Cd11c-cre*⁺ *Hif1a*^{flox/flox} mice (termed CKO) which lack HIF1 α in CD11c positive cells, and controls *Cd11c-cre*⁺ *Hif1a*^{+/+} mice (termed WT) (**Figure 4.2.1**).



4.2.1 Cre-flox strategy

Cd11c-cre mice were crossed with *Hif1a*^{flox/flox} mice to generate *Cd11c-cre*⁺ *Hif1a*^{flox/flox} and *Cd11c-cre*⁺ *Hif1a*^{+/+} mice

In order to study the role of HIF1 α in DCs in the context of atherosclerosis, CKO and WT mice were separately crossed with *Ldlr*^{-/-} mice to generate *Cd11c-cre*⁺ *Hif1a*^{flox/flox} *Ldlr*^{-/-} mice (termed CKO *Ldlr*^{-/-}) and their

controls *Cd11c-cre⁺ Hif1a^{+/+} Ldlr^{-/-}* mice (termed WT *Ldlr^{-/-}*). *Ldlr^{-/-}* mice are a commonly used atherosclerosis model and lack the low-density lipoprotein receptor, making them highly susceptible to developing plaques. When they are fed a high fat diet, atherosclerosis progression is accelerated, making it easy to study the disease. Hence, these mice were fed a high fat diet for 8 weeks for all further experiments and analysis.

To confirm efficient deletion of the *Hif1a* gene from CD11c⁺ cells, CD11c⁺ and CD4⁺ cells from spleens of CKO *Ldlr^{-/-}* and WT *Ldlr^{-/-}* mice on 8 weeks of high fat diet, were isolated and presence of *Hif1a* gene copies in the gDNA of both cell types was determined by qPCR. An unrelated gene (*Cd88*) was used to set baseline expression. Decreased *Hif1a* (~80%) was observed in CD11c⁺ cells from CKO *Ldlr^{-/-}* mice and not from WT *Ldlr^{-/-}* mice or from CD4⁺ cells from either of the mice (**Figure 4.2.2**). This confirms efficient deletion of the *Hif1a* gene specifically in CD11c expressing cells.

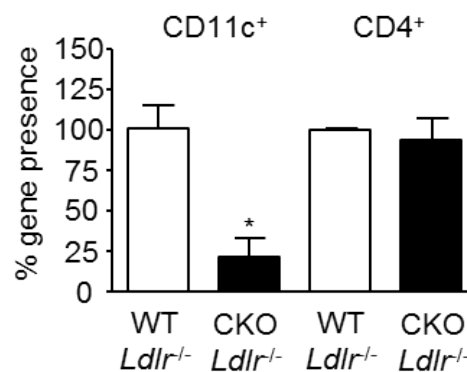


Figure 4.2.2 *Hif1a* gene is efficiently deleted from the genome of DCs in the CKO *Ldlr^{-/-}* mice
 CD11c⁺ DCs and CD4⁺ T cells were isolated from spleens of atherosclerotic WT *Ldlr^{-/-}* and CKO *Ldlr^{-/-}* mice, and *Hif1a* deletion from genomic DNA was analyzed by qPCR. The expression was normalized to an unrelated gene (*Cd88*) and expressed with WT as 100% (n=3). Data is presented as mean ± SEM; *p<0.05.

To also validate decreased expression of *Hif1a* on mRNA level, splenic DCs isolated from WT *Ldlr^{-/-}* and CKO *Ldlr^{-/-}* mice (after 8 weeks of high fat diet) as also *in vitro* cultured BMDCs from WT and CKO mice were analyzed by qPCR. The expression of *Hif1a* mRNA in both the splenic DCs (**Figure 4.2.3a**) and BMDCs (**Figure 4.2.3b**) from CKO mice was significantly decreased.

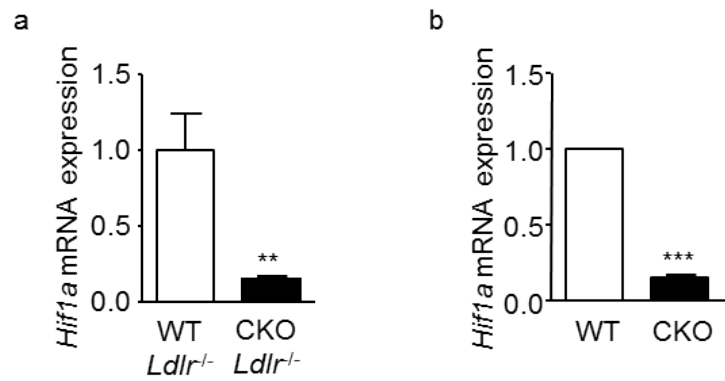


Figure 4.2.3 DCs from CKO mice show decreased *Hif1a* mRNA expression

Hif1a mRNA expression was analyzed in (a) WT *Ldlr*^{-/-} and CKO *Ldlr*^{-/-} splenic DCs and (b) WT and CKO BMDCs by qPCR (n=3 each). mRNA expression was normalized to *Hprt* and presented relative to WT *Ldlr*^{-/-} or WT controls. Data is presented as mean \pm SEM; **p<0.01, ***p<0.001.

4.3 Analysis of atherosclerosis progression in mice with DCs deficient for HIF1 α and fed a high fat diet

6 week old CKO *Ldlr*^{-/-} and WT *Ldlr*^{-/-} male mice were placed on a high fat diet for 8 weeks. The mice in the two groups did not show any physical differences. The total cholesterol, triglyceride levels and body weight were unchanged between groups (**Figure 4.3.1**).

	WT <i>Ldlr</i> ^{-/-}	CKO <i>Ldlr</i> ^{-/-}
Serum cholesterol (μ g/ml)	12,679 \pm 995	12,915 \pm 1,817
Serum triglycerides (mmol/L)	6.1 \pm 0.2	5.6 \pm 0.1
Body weight (g)	28.9 \pm 0.7	30.3 \pm 1.3

Figure 4.3.1 Lipid levels and body weight of atherosclerotic mice

Total serum cholesterol, serum triglycerides and body weight of atherosclerotic WT *Ldlr*^{-/-} and CKO *Ldlr*^{-/-} mice after 8 weeks of high fat diet. Values are expressed as mean \pm SEM.

In order to determine direct effects on atherosclerosis progression in the diet mice, *en face* aortas and aortic root cross sections were analyzed. In the aortic root, the total plaque area as well as the percent plaque area was significantly increased in the CKO *Ldlr*^{-/-} mice compared to controls (**Figure 4.3.2a**). Significantly increased plaque area (as % of total area) was also observed in the abdominal region of the aorta in the CKO *Ldlr*^{-/-} mice (**Figure**

4.3.2b). This data clearly indicates that the deficiency of HIF1 α in DCs leads to an enhanced plaque phenotype.

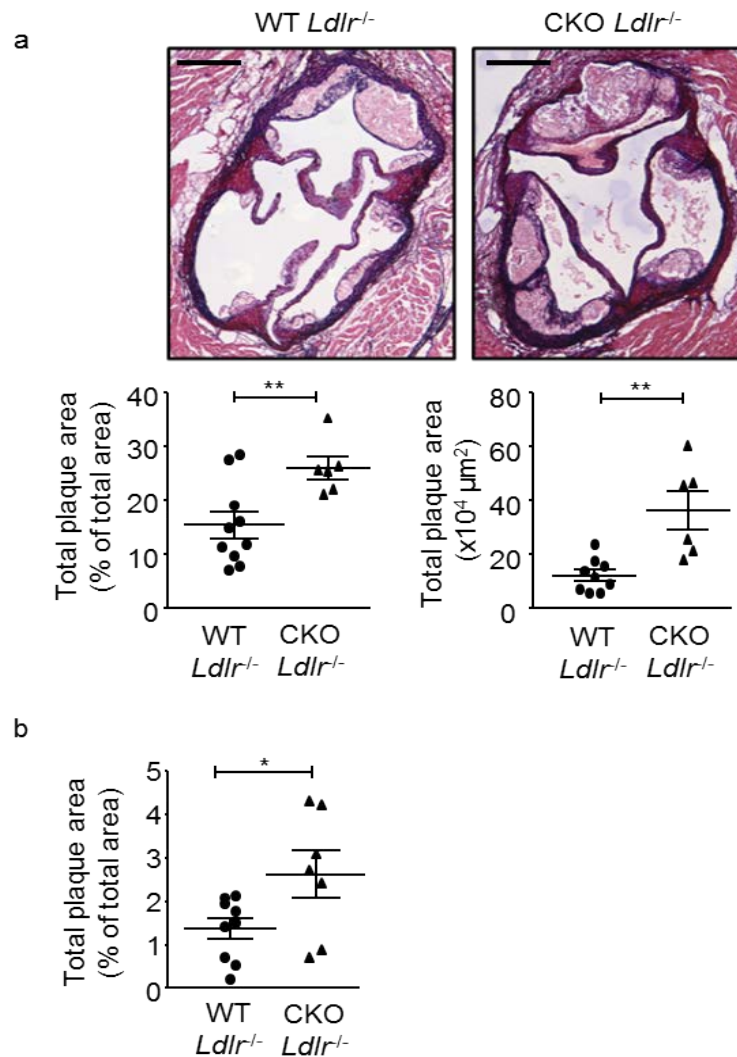


Figure 4.3.2 Mice with HIF1 α deficient DCs show increased atherosclerotic plaque area

Quantification of plaque area (a) as percent of total area and total area in μ m² in Aldehyde fuchsin stained aortic roots and (b) as percent of total area in Oil-Red O stained aorta of atherosclerotic WT *Ldlr*^{-/-} (n=10) and CKO *Ldlr*^{-/-} (n=7) mice fed a high fat diet for 8 weeks; representative sections of the aortic root are shown (scale bars: 250 μ m). Data is presented as mean \pm SEM; *p<0.05, **p<0.01.

In order to further characterize the plaque morphology, immunofluorescence staining on aortic root cross sections were performed to determine number of macrophages (Mac-2⁺), T cells (CD3⁺) and SMCs (α -Actin⁺) in the plaques. The total macrophage area and number showed no change but the area and numbers as percent of total plaque area and cells were significantly reduced (**Figure 4.3.3a**). It is important to note here that the

area occupied by the macrophages in the control plaques was converted to necrotic core areas in the CKO *Ldlr*^{-/-} mice plaques. Indeed, the necrotic core area (area of plaque without DAPI stained nuclei) in the aortic root sections was found to be significantly increased (**Figure 4.3.3b**) for the CKO *Ldlr*^{-/-} mice. The SMC area and SMC numbers in the CKO mice increased significantly (**Figure 4.3.3c**). Finally, the number and percent of T cells in the plaque also increased considerably (**Figure 4.3.3d**), pointing to enhanced infiltration of T cells into the plaque that would be suggestive of increased activation of T cells.

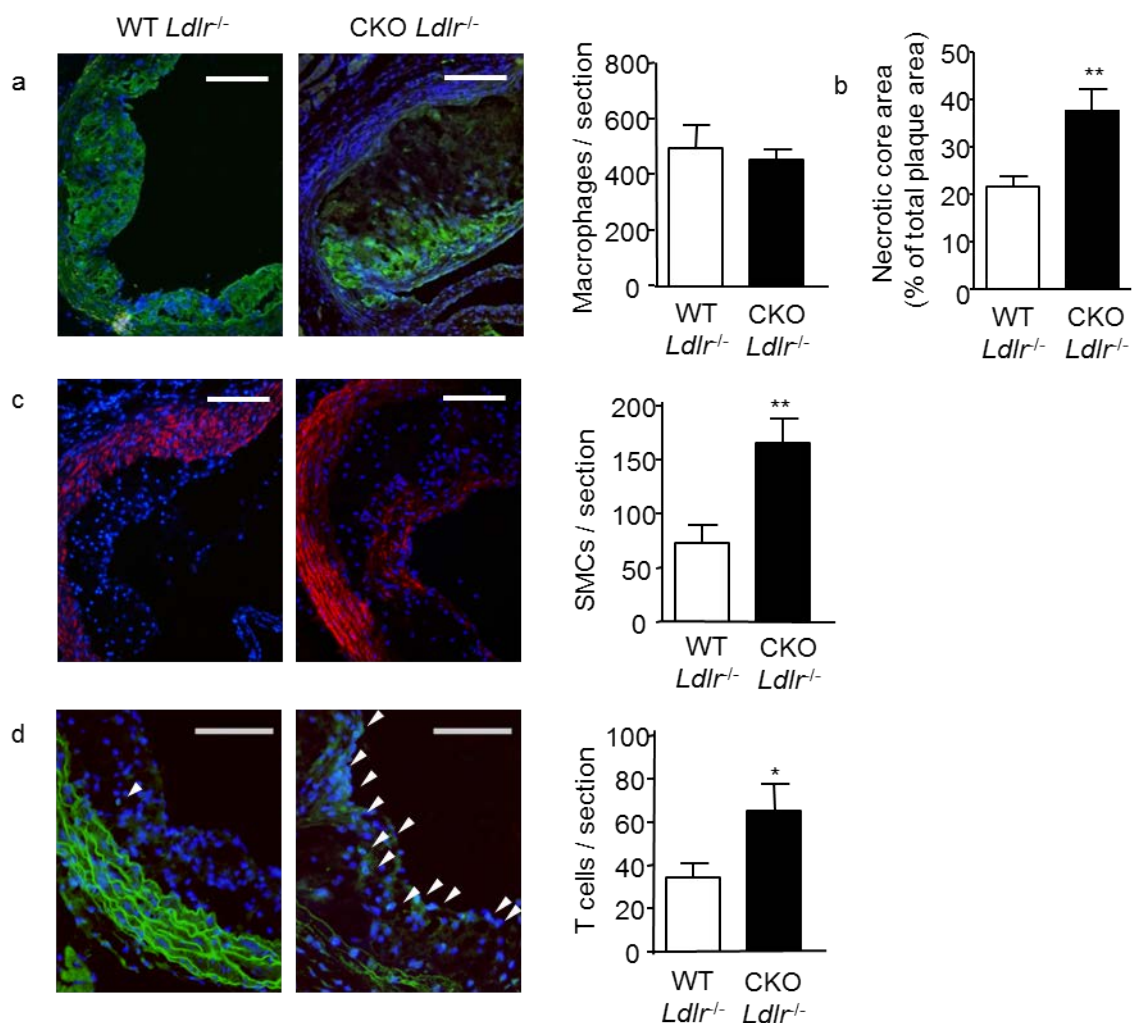


Figure 4.3.3 Mice with HIF1 α deficient DCs have a complex plaque phenotype

Quantification of the number of (a) Mac2⁺ macrophages (green, scale bars: 100 μ m), (b) acellular necrotic core area, (c) α -smooth muscle actin⁺ SMCs (red, scale bars: 100 μ m) and (d) CD3⁺ T cells (green, scale bars: 100 μ m) in aortic roots of atherosclerotic WT *Ldlr*^{-/-} (n=10) and CKO *Ldlr*^{-/-} (n=7) mice fed a high fat diet for 8 weeks; representative images of immunofluorescence staining are shown; cell nuclei were counterstained with DAPI (blue); arrow heads indicate T cells. Data is presented as mean \pm SEM; *p<0.05, **p<0.01.

As a whole, it is clear that the CKO *Ldlr*^{-/-} mice show a pro-atherogenic phenotype with enhanced plaque in the aortic roots and abdominal aorta and increased T-cell infiltration. These plaques are definitely more advanced and stable as the macrophages are transformed to necrotic cores. Increased SMCs also point to a more stable plaque phenotype.

It has been identified in previous publications that some macrophages express the CD11c marker, especially under inflammatory conditions in the atherosclerotic plaque. To determine whether the effects seen on atherosclerotic lesion development in CKO *Ldlr*^{-/-} mice are solely due to DCs or are a subsidiary effect of CD11c expressing macrophages, mice with HIF1 α deficient *LysM*⁺ cells, that are specific to the monocyte-macrophage lineage, were analyzed for atherosclerotic progression (done by Dr. Judith Sluimer, Maastricht, The Netherlands). *Ldlr*^{-/-} mice reconstituted with BM from *LysM-cre*⁺*Hif1a*^{flox/flox} mice or *LysM-cre*⁺*Hif1a*^{+/+} mice were placed on 6 weeks of high fat diet. The *Hif1a* deletion efficiency in *LysM*⁺ cells in these mice was ~70–80% and no differences in serum cholesterol were seen between the two groups (9,384 \pm 498 μ g/ml in *LysM-cre*⁺*Hif1a*^{+/+} \rightarrow *Ldlr*^{-/-} mice as opposed to 8,964 \pm 353 μ g/ml in *LysM-cre*⁺*Hif1a*^{flox/flox} \rightarrow *Ldlr*^{-/-} mice).

No changes were seen in the aortic root plaque area and percent macrophage area in mice lacking HIF1 α in *LysM*⁺ cells (**Figure 4.3.4**), stating that HIF1 α deficiency in CD11c⁺ cells causes no changes in macrophages in the context of atherosclerosis. This confirms the assumption that effects on atherosclerosis progression seen in *Cd11c-cre*⁺ *Hif1a*^{flox/flox} *Ldlr*^{-/-} mice (CKO *Ldlr*^{-/-}) are a result of CD11c⁺ DCs and not CD11c⁺ macrophages.

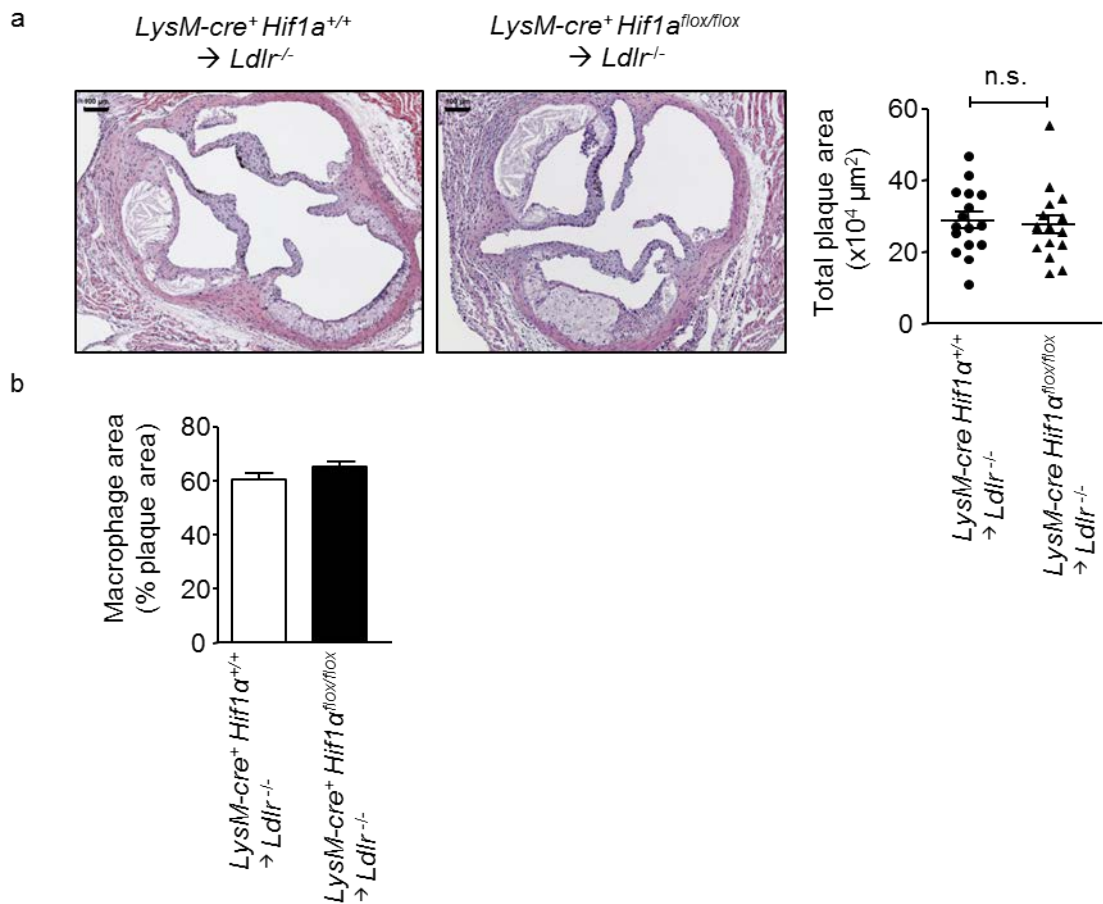


Figure 4.3.4 Deficiency of HIF1α in macrophages does not affect plaque growth

Quantification of (a) plaque area and (b) Mac3+ macrophage content in the aortic root of atherosclerotic *LysM-cre⁺ Hif1α^{+/+} → Ldlr^{-/-}* mice and *LysM-cre⁺ Hif1α^{flox/flox} → Ldlr^{-/-}* (n=16 mice each) fed a high fat diet for 6 weeks; representative H&E stained sections are shown (scale bars: 100μm). Data is presented as mean ± SEM.

4.4 Analysis of immune cell phenotype in mice with DCs deficient for HIF1α and fed a high fat diet

Since significant changes were seen in atherosclerotic plaque size and composition in CKO *Ldlr^{-/-}* mice as compared to the WT *Ldlr^{-/-}* controls, it was essential to determine the cellular phenotype in the periphery and secondary lymphoid organs. For this purpose, FACS analysis for various cell types was carried out in the blood, spleen and peripheral lymph nodes.

No changes were seen in the size and cell numbers of spleen and lymph nodes. Also, no changes were observed in the total numbers of lymphocytes (CD45⁺) and B cells (CD19⁺) (**Figure 4.4.1**) or T cells (TCRβ⁺) and ratios of CD4⁺ and CD8⁺ T cells (**Figure 4.4.2**) in any of the organs.

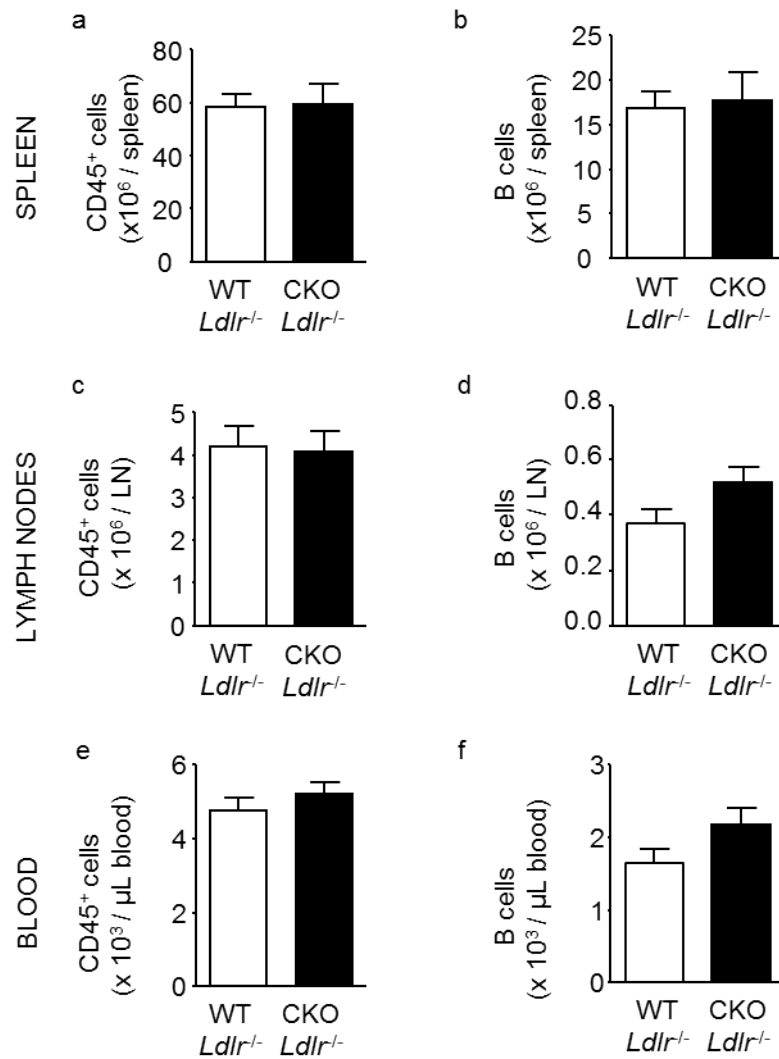


Figure 4.4.1 Mice with HIF1α deficient DCs do not show changes in lymphocyte or B cell numbers
 Flow cytometric analysis of CD45⁺ lymphocytes and CD19⁺ B-cells in (a,b) spleens, (c,d) peripheral LNs and (e,f) blood from atherosclerotic WT *Ldlr*^{-/-} (n=10) and CKO *Ldlr*^{-/-} (n=7) mice fed a high fat diet for 8 weeks. Data is presented as mean ± SEM.

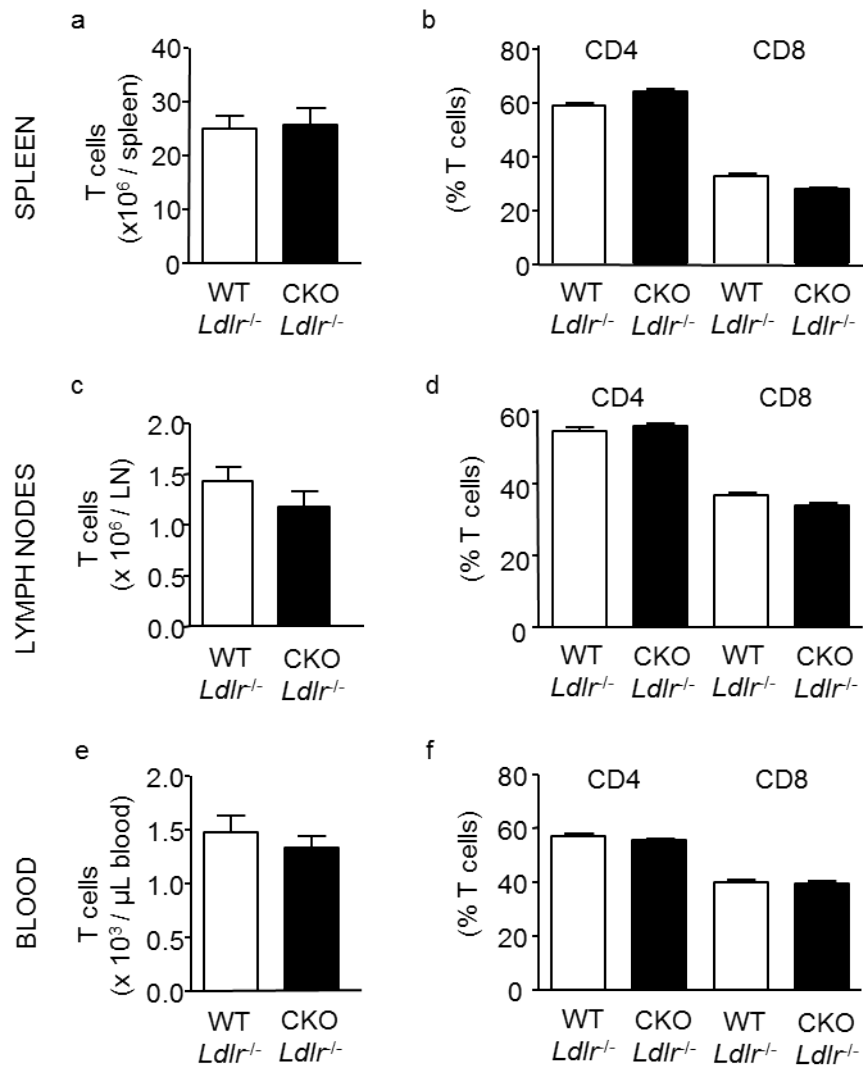


Figure 4.4.2 Mice with HIF1 α deficient DCs do not show changes in T cell numbers or frequencies
 Flow cytometric analysis of CD3⁺ T-cells and CD4-CD8 frequencies in (a,b) spleens, (c,d) peripheral LNs and (e,f) blood from atherosclerotic WT *Ldlr*^{-/-} (n=10) and CKO *Ldlr*^{-/-} (n=7) mice fed a high fat diet for 8 weeks. Data is presented as mean \pm SEM.

Interestingly, significantly increased frequencies of activated T cells and significantly decreased frequencies of naive T cells were found in the spleen, LNs and blood of CKO *Ldlr*^{-/-} mice compared to controls (**Figure 4.4.3**).

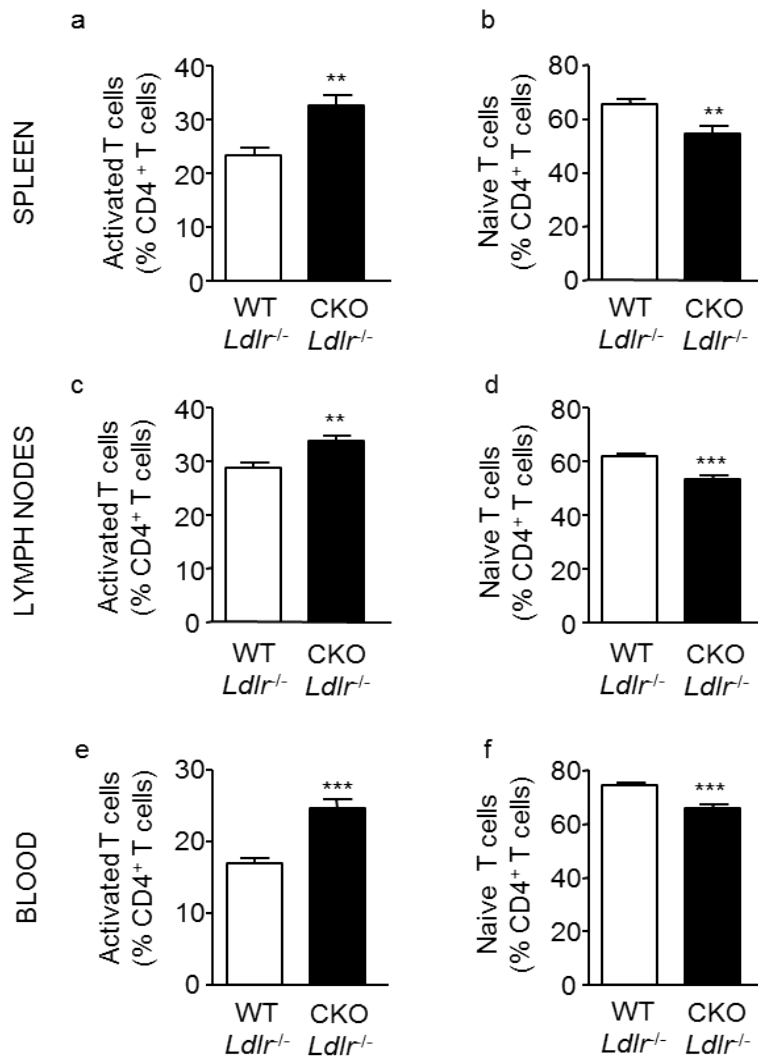


Figure 4.4.3 Mice with HIF1 α deficient DCs show greater T-cell activation

Flow cytometric analysis of activated and naive CD4⁺ T cells in (a,b) spleens, (c,d) peripheral LNs and (e,f) blood from atherosclerotic WT *Ldlr*^{-/-} (n=10) and CKO *Ldlr*^{-/-} (n=7) mice fed a high fat diet for 8 weeks. Data is presented as mean \pm SEM; **p<0.01, ***p<0.001.

Also, the percent of T_h1 cells, as represented by the IFN γ producing CD4⁺ T cells were significantly enhanced in spleen, LNs and blood of CKO *Ldlr*^{-/-} mice (**Figure 4.4.4**). No changes were seen in the T_h17 or T_{reg} populations (data not shown). This data suggests that the CKO *Ldlr*^{-/-} mice

have enhanced T-cell activation and pro-inflammatory phenotype supporting the increased T-cell infiltration in plaques and enhanced atherosclerosis.

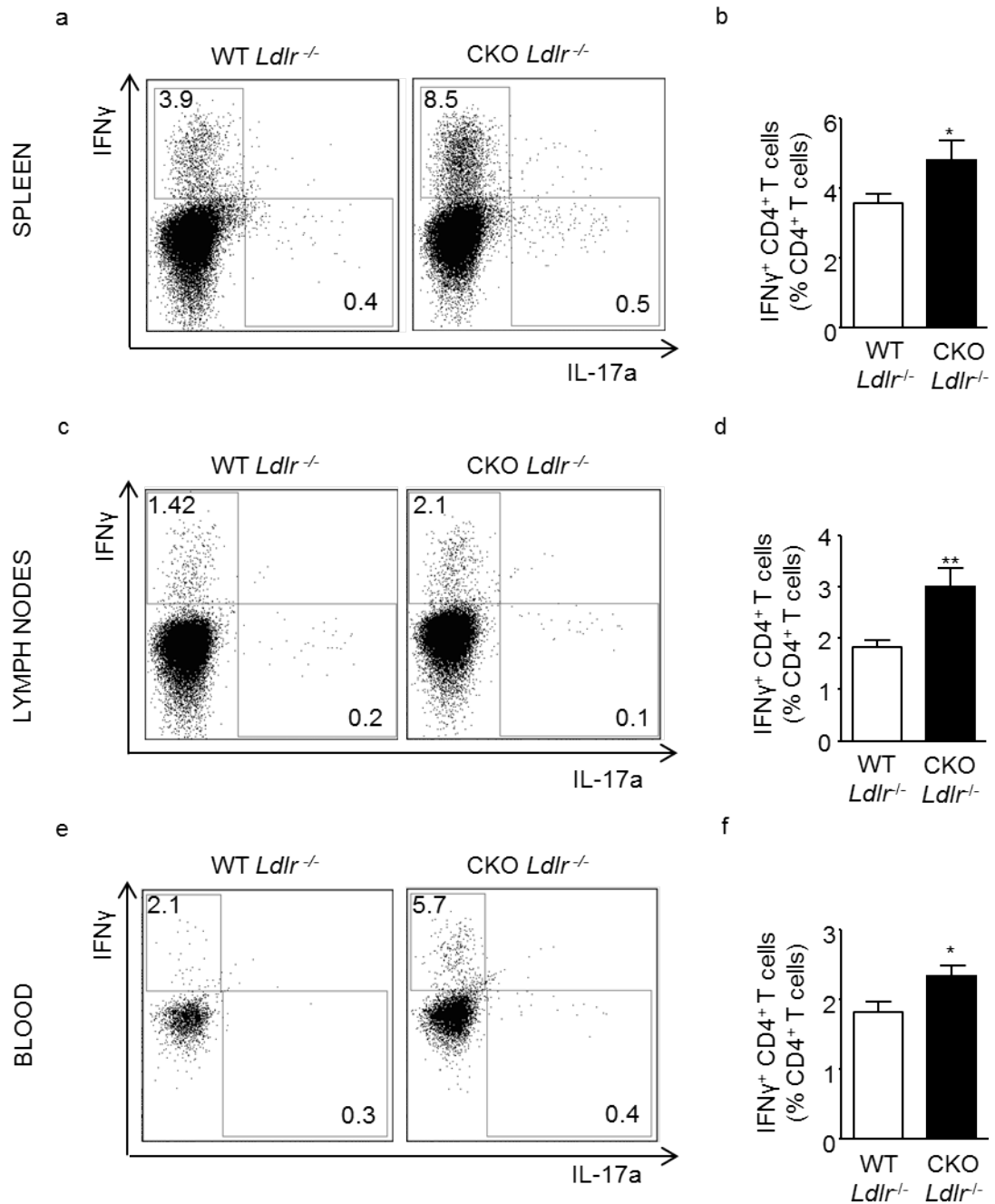


Figure 4.4.4 Mice with HIF1 α deficient DCs show a Th₁ phenotype

Intracellular staining for IFN γ and IL-17a and flow cytometric analysis of CD4⁺ T cells in (a,b) spleens, (c,d) peripheral LNs and (e,f) blood from atherosclerotic WT *Ldlr*^{-/-} (n=10) and CKO *Ldlr*^{-/-} (n=7) mice fed a high fat diet for 8 weeks. Figures a,c,e show representative dot plots for IFN γ versus IL-17a cell populations, values indicate gated events among CD4⁺ T cells. Figures b,d,f show percentage of IFN γ ⁺ cells among CD4⁺ T cells. Data is presented as mean \pm SEM; *p<0.05, **p<0.01.

Among the myeloid lineage, no changes were observed in percent of cDCs (CD11c⁺ MHCII^{hi}), neutrophils (CD11b⁺ CD115⁻ Gr1^{hi}), monocytes (CD11b⁺ CD115⁺ Gr1^{hi} and CD11b⁺ CD115⁺ Gr1^{lo}) or macrophages (CD11b⁺ F4/80⁺) (data not shown).

The systemic inflammatory status of the CKO *Ldlr*^{-/-} mice as seen by flow cytometry complements the pro-atherogenic phenotype of the mice analyzed by histology. These mice have more activated T cells of the T_h1 type that are known to be critical in progression of atherosclerosis. Thus it could be concluded that the HIF1 α deficient DCs have an enhanced capacity to activate T cells, polarize them to the T_h1 phenotype and mobilize them to the site of inflammation in the plaques.

4.5 Analysis of immune cell phenotype in mice with DCs deficient for HIF1 α at the baseline level

6 week old WT and CKO mice (not on the *Ldlr*^{-/-} background) on normal chow were analyzed for distribution of immune cell populations in the blood, spleen and peripheral lymph nodes by FACS. The body weight and cell numbers in spleen and lymph nodes did not vary between groups. No changes were observed in the total number of lymphocytes (CD45⁺), T cells (TCR β ⁺) or B cells (CD19⁺), or in the ratios of CD4⁺ and CD8⁺ T cells (**Figure 4.5.1a,b,f,g** and data not shown). Among the CD4⁺ T-cell population, the ratios of naive (CD62L^{hi} CD44^{lo}) cells and activated cells (CD62L^{lo} CD44^{hi}) remained unchanged (**Figure 4.5.1c,d,h,i** and data not shown). The CD4⁺ T cells did not show changes in polarization, as the percent of T_h1 cells (IFN γ ⁺), T_h17 cells (IL-17a⁺), or T_{reg} (CD25⁺ FoxP3⁺) cells were unchanged between groups (**Figure 4.5.1e,j** and data not shown).

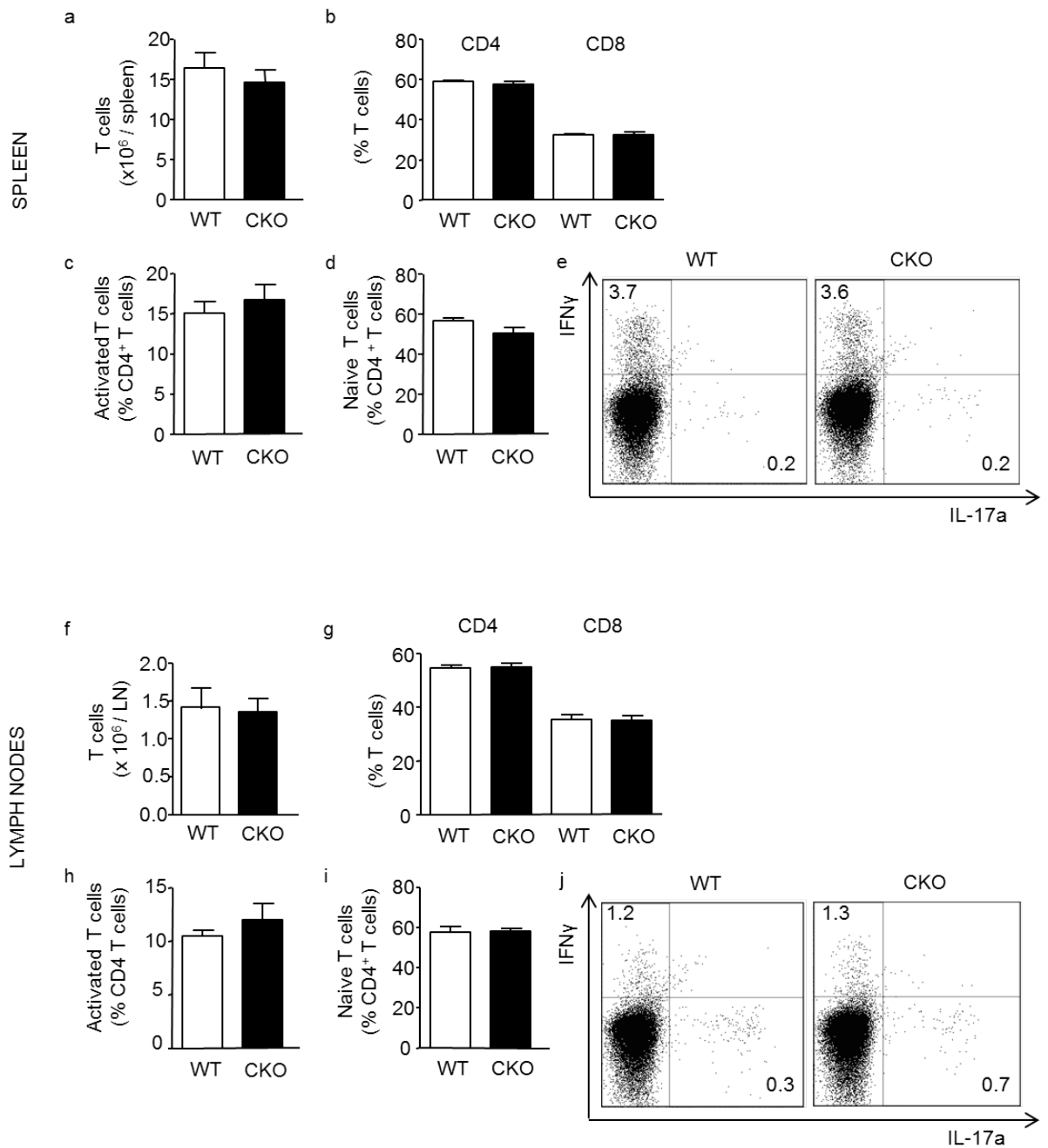


Figure 4.5.1 CKO mice under non-inflammatory conditions do not show changes in T-cell activation

Flow cytometric analysis of T-cell distribution in spleen (a-e) and lymph nodes (f-j) of 8 week old WT (n=8) and CKO (n=9 mice). CD3⁺ T cells (a,f), CD4⁺ and CD8⁺ T cells among CD3⁺ T cells (b,g), activated CD44^{high} CD62L^{low} (c,h) and naive CD62L^{high} CD44^{low} CD4⁺ T cells (d,i), IFN γ ⁺ CD4⁺ T cells and IL-17a⁺ CD4⁺ T cells (e,j) were quantitated. Figures e,f show representative dot plots for IFN γ versus IL-17a cell populations; values indicate gated events among CD4⁺ T cells. Data is presented as mean \pm SEM.

Among the myeloid lineage, no changes were observed in percent of cDCs (CD11c⁺ MHCII^{hi}), pDCs (CD11c⁺ PDCA1⁺ B220⁺), neutrophils (CD11b⁺ CD115⁻ Gr1^{hi}), monocytes (CD11b⁺ CD115⁺ Gr1^{hi} and CD11b⁺ CD115⁺ Gr1^{lo}) or macrophages (CD11b⁺ F4/80⁺) (data not shown).

4.6 Characterization of mature BMDCs deficient for HIF1 α

The *in vivo* data suggests that DCs deficient in HIF1 α are capable of activating and polarizing T cells better than control DCs. Hence, it was essential to study the DCs themselves to understand changes in their physical or functional characteristics. For this purpose, BMDCs were cultured from BM cells of CKO and WT mice. During the progress of the culture, no changes were observed in the physical appearance, growth or differentiation characteristics of the BMDCs from the different groups. At the end of the culture (day 9), both groups of BMDCs showed comparable numbers.

WT BMDCs were stimulated using 1 μ g/ml LPS and/or 0.1 μ g/ml recombinant murine TNF α for various time points and analyzed for increased HIF1 α expression by qPCR. The highest HIF1 α expression was seen at 24 hours of TNF α stimulation (**Figure 4.6.1**). Also TNF α is more physiological than LPS and a better stimulus with respect to atherosclerosis. Therefore, TNF α for 24 hours was used as an optimal treatment for maturation of DCs for all further *in vitro* experiments.

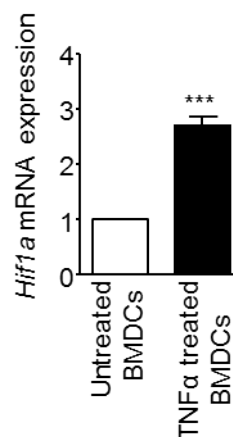


Figure 4.6.1 BMDCs up-regulate *Hif1a* on TNF α stimulation

Analysis of *Hif1a* mRNA expression by qPCR in BMDCs left untreated or treated with 0.1 μ g/ml TNF α ; normalized to *Hprt* and relative to untreated BMDCs (n=5). Data is presented as mean \pm SEM; ***p<0.001.

To determine changes in activation status of DCs, changes in MHCII and co-stimulatory molecules CD80 and CD86 were checked by qPCR and FACS analysis. No changes were seen in these molecules by either qPCR

(**Figure 4.6.2a**) or FACS (**Figure 4.6.2b**), suggesting that HIF1 α deficiency does not alter MHCII or co-stimulatory molecule expression of DCs.

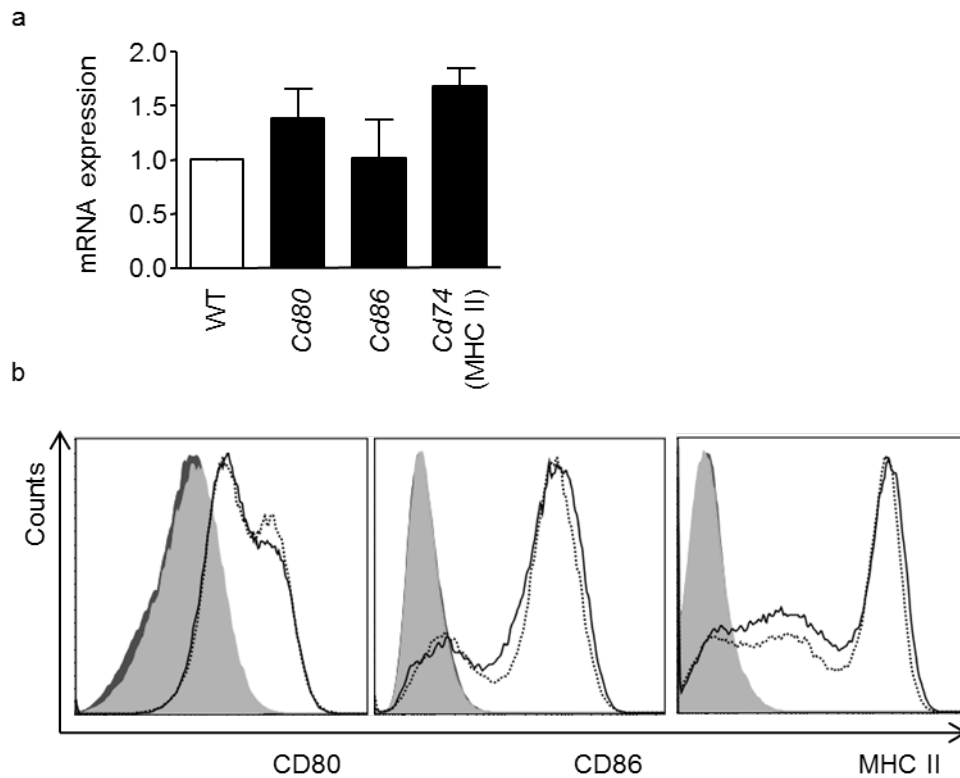


Figure 4.6.2 Co-stimulatory molecule expression remains unchanged in HIF1 α -deficient BMDCs
 (a) mRNA expression of indicated co-stimulatory molecules in TNF α treated mature BMDCs generated from WT and CKO mice (n=3). mRNA expression was normalized to *Hprt* and presented relative to WT controls. (b) Representative histogram depicting co-stimulatory molecule expression on WT and CKO BMDCs (solid line - WT, dotted line - CKO, filled dark grey line - WT FMO, filled faint grey line - CKO-FMO). Data is presented as mean \pm SEM.

To analyze changes in migratory capacity of HIF1 α deficient DCs, *Ccr7* mRNA expression was determined on mature BMDCs and their migratory capacity towards CCR7 ligand CCL19 or towards medium without cytokine (blank) was investigated *in vitro*. CKO BMDCs show no change in expression of *Ccr7* (**Figure 4.6.3a**) or migration towards CCL19 (**Figure 4.6.3b**) when compared to WT BMDCs.

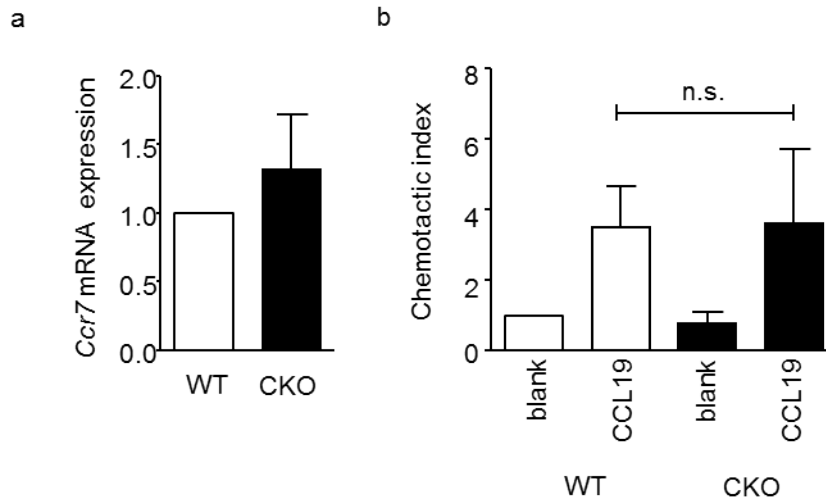


Figure 4.6.3 HIF1 α deficient BMDCs show no changes in *Ccr7* expression or migration towards CCL19

(a) *Ccr7* mRNA expression on mature BMDCs from WT and CKO mice, analyzed by qPCR (n=5 mice). mRNA expression was normalized to *Hprt* and presented relative to WT controls. (b) BMDCs from WT and CKO mice were analyzed for migration towards CCL19 in an *in vitro* migration assay. Values expressed as chemotactic index relative to migration of WT BMDCs towards a blank (n=3 experiments). Data is presented as mean \pm SEM.

DCs secrete different cytokines that are responsible for T-cell activation and polarization. To determine whether the cytokine profile of DCs changes due to knockout of HIF1 α , various pro- and anti-inflammatory cytokines were analyzed in mature BMDCs by qPCR. Though no changes were seen in the expression of *Il1a*, *Il4*, *Il6*, *Il10*, *Tgfb* or *Tnfa*, a significantly increased expression of *Il12* was observed (**Figure 4.6.4a**). IL-12 is secreted by APCs on antigenic stimulation and helps differentiate naive T cells into T_h1 cells, leading to production of IFN γ . Increased expression of IL-12 by HIF1 α deficient DCs hence fits with the enhanced IFN γ producing T cells seen *in vivo*. IL-12 protein secretion was also analyzed in culture supernatants from BMDCs. The HIF1 α deficient DCs secreted higher amounts of IL-12 protein in the culture supernatant as measured by ELISA (**Figure 4.6.4b**).

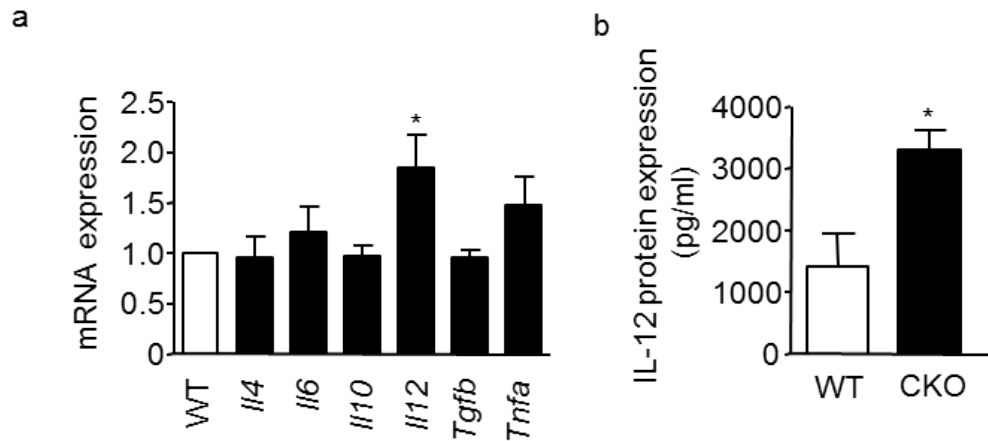


Figure 4.6.4 BMDCs deficient in HIF1 α show increased IL-12

(a) mRNA expression of indicated cytokines in TNF α treated mature BMDCs generated from WT and CKO mice, assessed by qPCR (3 independent experiments, n=3-4 mice per experiment). mRNA expression was normalized to *Hprt* and presented relative to WT controls. (b) IL-12 protein levels in culture supernatants of mature WT and CKO BMDCs, determined by ELISA (n=3). Data is presented as mean \pm SEM; *p<0.05.

It was essential to determine which molecules downstream of HIF1 α are responsible for the effects seen in IL-12 expression in DCs. An interesting candidate that could explain the effects seen was the SOCS family. SOCS are a family of proteins involved in inhibiting the JAK-STAT signaling pathway and particularly SOCS1 and SOCS3 in DCs have been shown to inhibit T_h1 differentiation capacities. Changes in expression of SOCS1 and SOCS3 were analyzed in TNF α matured BMDCs from CKO and WT. No changes were seen in either of the molecule expression (**Figure 4.6.5a**).

HIF1 α is also known to affect expression of NF κ B, an important immune mediator, in various cell types. Hence, mRNA expression of the 2 subunits of NF κ B – *Nfkb1* or *p105* and *Rela* or *p65* was analyzed. No changes in expression of either of the subtypes in BMDCs from CKO and WT were observed by qPCR (**Figure 4.6.5b**).

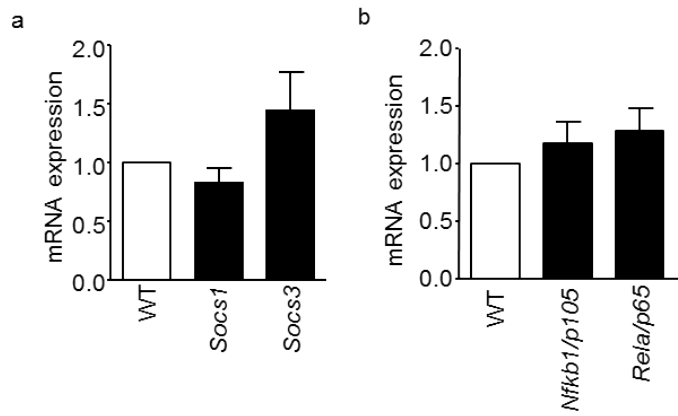


Figure 4.6.5 HIF1 α -deficient BMDCs show no changes in *Socs* or *Nfkb* expression

qPCR was performed to analyze mRNA expression of (a) *Socs1* and *Socs3*, (b) *Nfkb1/p105* and *Rela/p65* in mature BMDCs from WT and CKO mice (n=3); mRNA expression was normalized to *Hprt* and presented relative to WT controls. Data is presented as mean \pm SEM.

To once again rule out effects of HIF1 α deficiency on macrophages, bone marrow derived macrophages (BMMs) were cultured and probed for typical M1 and M2 markers by qPCR. Untreated and TNF α stimulated BMMs from CKO and WT mice did not display any consistent differences in pro-inflammatory *Il12*, *Nos2*, or anti-inflammatory *Mrc1* and *Igf1* mRNA expression (**Figure 4.6.6**), further corroborating that HIF1 α controls the functions of DCs at the interface with T cells, but not of macrophages.

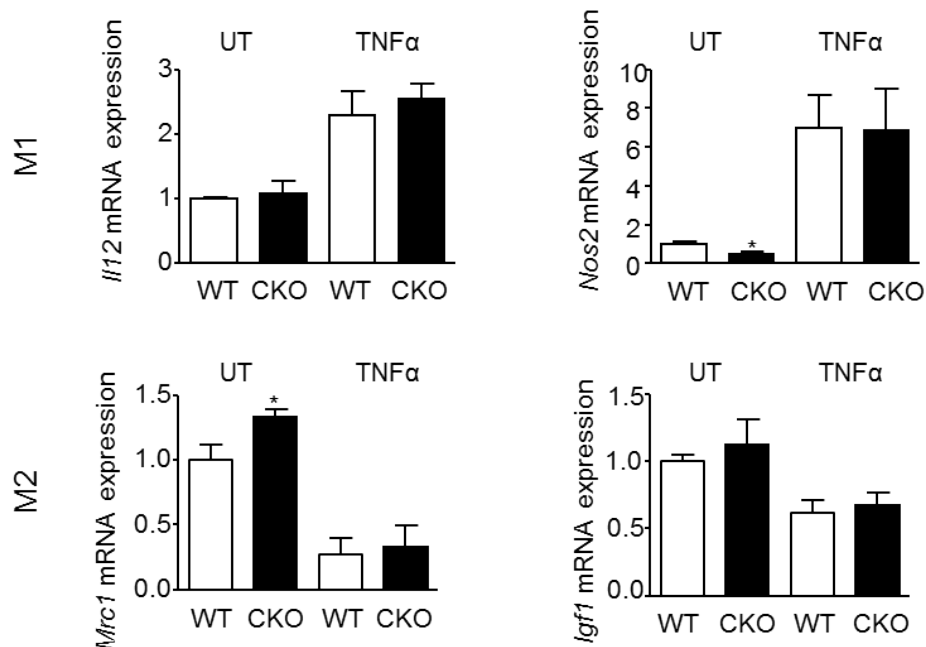


Figure 4.6.6 HIF1 α deficiency in CD11c cells does not affect macrophage polarization in a way that explains the pro-atherogenic phenotype

mRNA expression of M1 markers *Il12* and *Nos2* and M2 markers *Mrc1* and *Igf1* in untreated (UT) or TNF α treated BMMs from CKO mice and WT mice, as assessed by qPCR. mRNA expression was normalized to *Hprt* and presented relative to WT controls (n=5). Data is presented as mean \pm SEM; *p<0.05.

4.7 Characterization of splenic DCs isolated from atherosclerotic WT *Ldlr*^{-/-} and CKO *Ldlr*^{-/-} mice

Since significant changes were seen in mature BMDCs treated with TNF α with respect to IL-12 expression, it was interesting to track these changes in splenic DCs directly isolated from atherosclerotic WT *Ldlr*^{-/-} and CKO *Ldlr*^{-/-} mice placed on a high fat diet for 8 weeks. DCs directly isolated from these mice are the perfect model for studying changes in DCs deficient in HIF1 α under inflammatory conditions of atherosclerosis.

Splenic DCs isolated from atherosclerotic WT *Ldlr*^{-/-} and CKO *Ldlr*^{-/-} mice were analyzed for expression of MHCII and co-stimulatory molecules CD80 and CD86. Similar to results in mature BMDCs, these splenic DCs showed no changes in mRNA expression of *Cd74* (MHCII), *Cd80* or *Cd86* by qPCR (Figure 4.7.1).

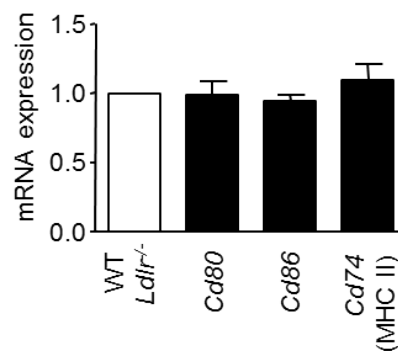


Figure 4.7.1 Co-stimulatory molecule expression remains unchanged in HIF1 α deficient splenic DCs from atherosclerotic mice

mRNA expression of indicated co-stimulatory molecules in splenic DCs from WT *Ldlr*^{-/-} and CKO *Ldlr*^{-/-} mice (n=12) fed a high fat diet for 8 weeks; mRNA expression was normalized to *Hprt* and presented relative to WT *Ldlr*^{-/-} controls. Data is presented as mean \pm SEM.

The migratory capacity of DCs from atherosclerotic WT *Ldlr*^{-/-} and CKO *Ldlr*^{-/-} mice was analyzed by counting the number of CD11c⁺ DCs in the atherosclerotic plaque to understand whether plaque changes are due to differences in migration of DCs into or out of the plaque. The number of DCs in the plaque was comparable between the two groups (Figure 4.7.2), indicating no changes in DC migration due to HIF1 α deficiency, similar to results from BMDCs.

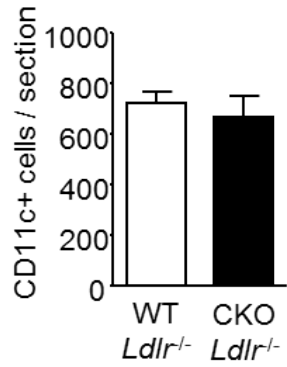


Figure 4.7.2 HIF1 α deficient DCs do not show changes in DC migration to plaque
 Quantification of the number of CD11c⁺ cells in aortic roots of atherosclerotic WT *Ldlr*^{-/-} (n=10) and CKO *Ldlr*^{-/-} (n=7) mice fed a high fat diet for 8 weeks. Data is presented as mean \pm SEM.

When atherosclerotic splenic DCs were probed for cytokine expression, increased expression of IL-12 was seen in DCs deficient for HIF1 α by both qPCR (**Figure 4.7.3a**) and FACS (**Figure 4.7.3b**).

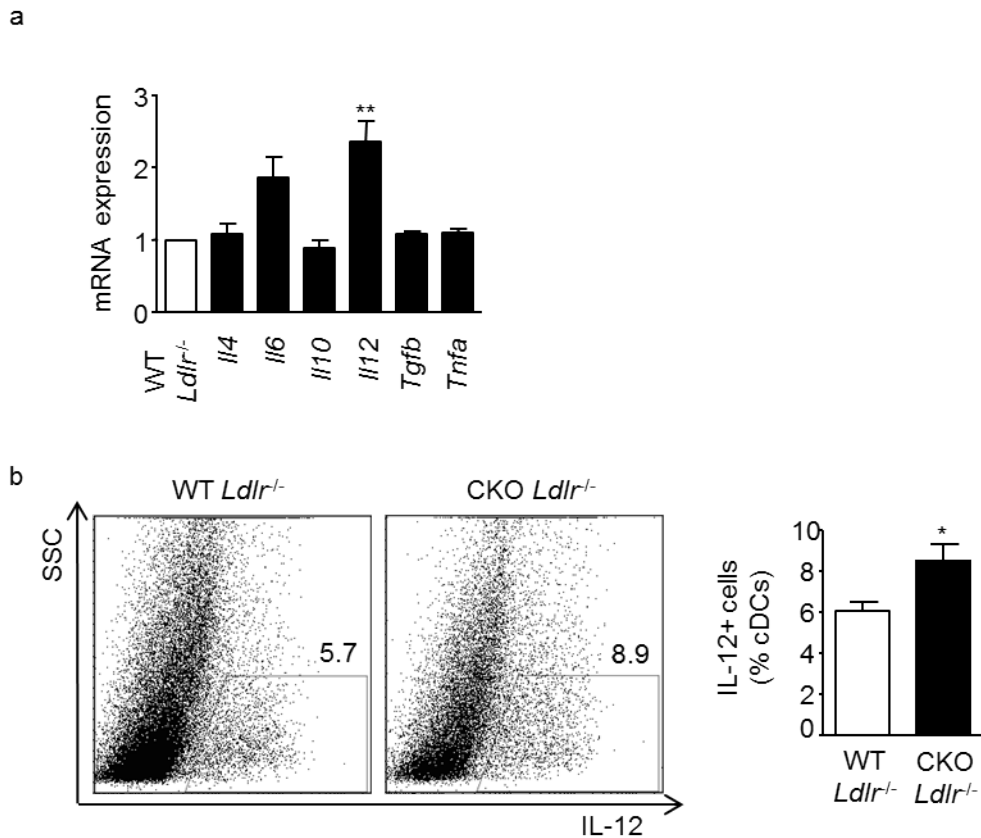


Figure 4.7.3 Atherosclerotic splenic DCs deficient in HIF1 α also show increased IL-12
 (a) mRNA expression of indicated cytokines in splenic DCs from atherosclerotic WT *Ldlr*^{-/-} and CKO *Ldlr*^{-/-} mice, assessed by qPCR (3 independent experiments, n=3-4 mice per experiment). mRNA expression was normalized to *Hprt* and presented relative to WT *Ldlr*^{-/-} controls. (b) Percent of IL-12⁺ cells among the cDC population analyzed by flow cytometry (n=6). Representative dot plots are shown, values indicate gated events among cDCs. Data is presented as mean \pm SEM; *p<0.05, **p<0.01.

Since CKO *Ldlr*^{-/-} mice showed enhanced T-cell activation and T_h1 polarization *in vivo*, it was essential to determine whether similar effects were also seen *in vitro* when splenic DCs from atherosclerotic mice were co-cultured with naive CD4⁺ T cells in an antigen specific assay. Indeed, splenic DCs isolated from atherosclerotic CKO *Ldlr*^{-/-} mice and loaded with OVA₃₂₃₋₃₃₉ antigen showed an enhanced capacity to proliferate naive CD4⁺ T cells isolated from OT-II mice and polarize them to the T_h1 phenotype as compared to splenic DCs from atherosclerotic WT *Ldlr*^{-/-} mice (**Figure 4.7.4**). This proves that the activation and polarization effects seen *in vivo* are undeniably DC mediated and possible take place via enhanced IL-12 production.

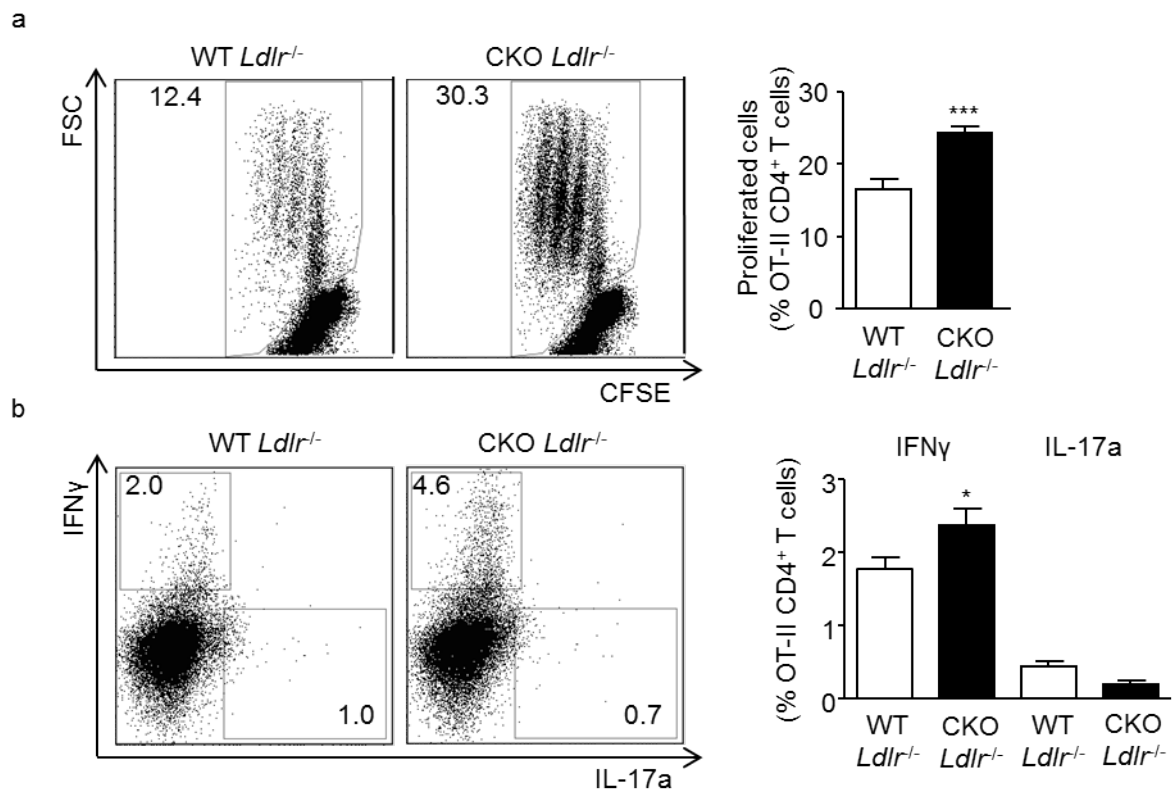


Figure 4.7.4 HIF1 α deficient DCs have higher proliferation and polarization potential

DCs isolated from spleens of atherosclerotic WT *Ldlr*^{-/-} and CKO *Ldlr*^{-/-} mice fed a high fat diet for 8 weeks and pulsed with OVA₃₂₃₋₃₃₉ peptide were co-cultured with naive CD4⁺ OT-II T cells for 3 days. (a) Proliferation of CD4⁺ T cells was analyzed by CFSE dilution by flow cytometry. Quantitation and representative dot plots are shown, values indicate gated events among CD4⁺ T cells. (b) T-cell polarization was determined by intracellular staining for IFN γ and IL-17a. Quantitation and representative dot plots are shown, values indicate gated events among CD4⁺ T cells, (3 independent experiments, n=3-5 mice per experiment). Data is presented as mean \pm SEM; *p<0.05, ***p<0.001.

To provide a final confirmation to the fact that T-cell proliferation and polarization is mediated by IL-12 produced from DCs, the *in vitro* DC – T-cell co-culture assay was repeated with OVA₃₂₃₋₃₃₉ loaded DCs from CKO *Ldlr*^{-/-} mice and naive CD4⁺ T cells from OT-II mice in the presence of an IL-12 blocking antibody. The anti-IL-12 antibody blocked proliferation and polarization of T cells *in vitro* (**Figure 4.7.5**) and fits with already seen data in literature as to the T-cell proliferating and T_h1 polarizing role of IL-12^{264,265}.

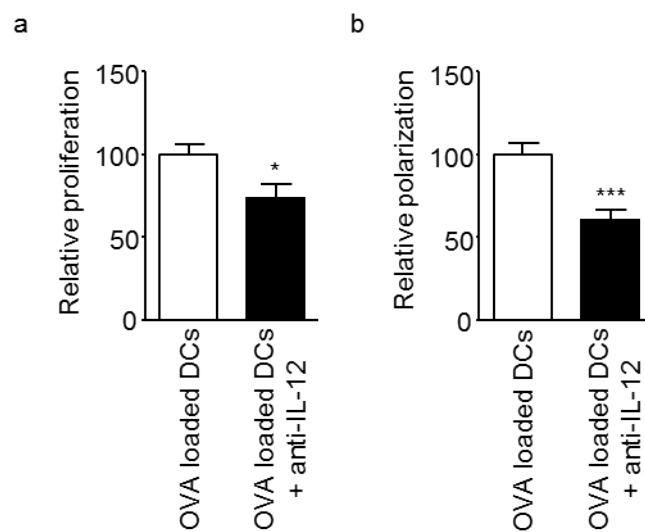


Figure 4.7.5 DC released IL-12 is responsible for T-cell proliferation and polarization to the T_h1 phenotype

DCs isolated from spleens of atherosclerotic CKO *Ldlr*^{-/-} mice fed a high fat diet for 8 weeks and pulsed with OVA₃₂₃₋₃₃₉ peptide were co-cultured with naive CD4⁺ OT-II T cells for 3 days without or with an anti-IL-12 antibody. (a) Proliferation of CD4⁺ T cells was analyzed by CFSE dilution and (b) polarization to the T_h1 phenotype was assessed by staining for IFN γ ⁺ cells by flow cytometry. Quantitation is shown relative antibody untreated cells. Data is presented as mean \pm SEM; *p<0.05, ***p<0.001.

Unlike BMDCs, the atherosclerotic splenic DCs showed a significant decrease in *Socs1* and *Socs3* mRNA expression (**Figure 4.7.6a**) although no changes in mRNA expression of *Nfkb1/p105* or *Rela/p65* (**Figure 4.7.6b**).

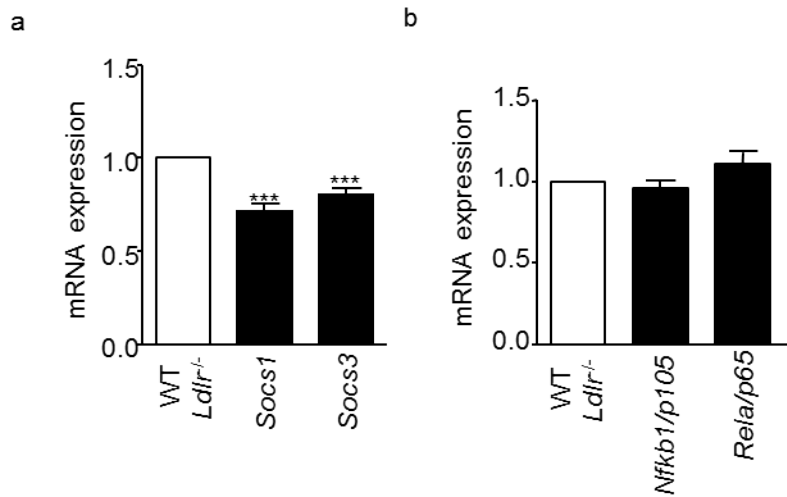


Figure 4.7.6 HIF1 α deficient splenic DCs show no changes in *Socs* or *Nfkb* expression.

qPCR was performed to analyze mRNA expression of (a) *Socs1* and *Socs3*, (b) *Nfkb1/p105* and *Rela/p65* in splenic DCs from WT *Ldlr*^{-/-} and CKO *Ldlr*^{-/-} mice (n=12) mRNA expression was normalized to *Hprt* and presented relative to WT *Ldlr*^{-/-} controls. Data is presented as mean \pm SEM; ***p<0.001.

4.8 Expression of STAT proteins in DCs deficient in HIF1 α

Signal transducers and activators of transcription (STAT) proteins play a critical role in directing the function of different cytokines²⁶⁶. Among these, STAT3 is unique as it has been shown to exert anti-inflammatory activities in DCs²⁶⁷. Moreover, STAT3 deficient DCs were previously shown to display an enhanced IL-12 cytokine production^{267,268}. Since HIF1 α lacking DCs showed enhanced IL-12 secretion with pro-inflammatory properties, it was interesting to analyze STAT3 expression in these DCs. Notably, a significant reduction in *Stat3* mRNA and protein expression could be detected in mature CKO *versus* WT BMDCs, as assessed by qPCR analysis (**Figure 4.8.1a**) and flow cytometric analysis (**Figure 4.8.1b**) as also in atherosclerotic WT *Ldlr*^{-/-} and CKO *Ldlr*^{-/-} splenic DCs (**Figure 4.8.2a,b**), suggesting that HIF1 α dependent changes in STAT3 expression may regulate IL-12 production. No changes in *Stat3* mRNA expression were seen in BMDCs not treated with TNF α (data not shown) hinting at the essential role of an inflammatory stimulus in the process.

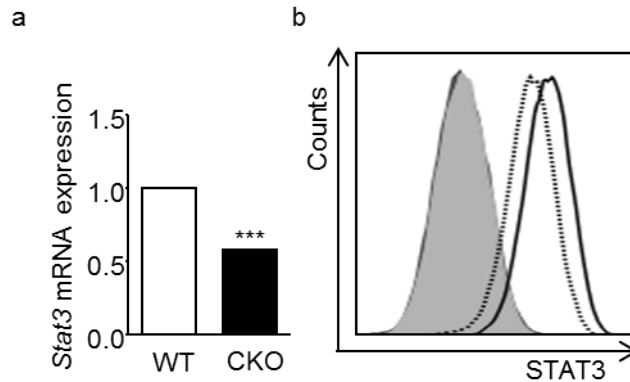


Figure 4.8.1 STAT3 expression decreases in HIF1 α deficient BMDCs treated with TNF α

(a) mRNA expression of *Stat3* in TNF α treated mature BMDCs generated from WT and CKO mice (n=3). mRNA expression was normalized to *Hprt* and presented relative to WT controls. (b) Representative histogram depicting STAT3 protein expression in WT and CKO BMDCs (solid line - WT, dotted line - CKO, filled dark grey line - WT FMO, filled faint grey line - CKO FMO). Data is presented as mean \pm SEM; ***p<0.001.

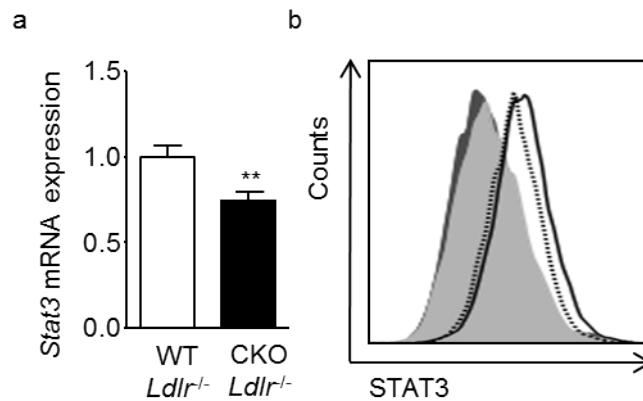
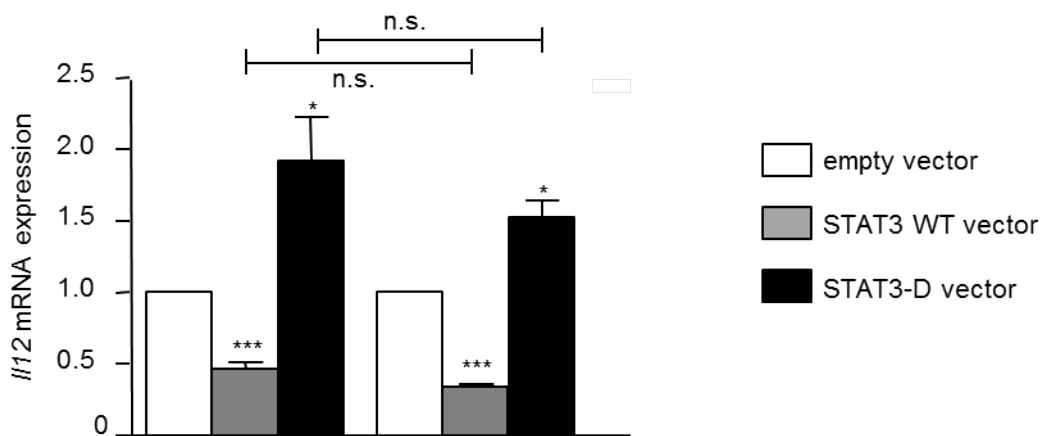


Figure 4.8.2 STAT3 expression decreases in HIF1 α deficient splenic DCs from atherosclerotic mice

(a) mRNA expression of *Stat3* in atherosclerotic splenic DCs from WT *Ldlr*^{-/-} and CKO *Ldlr*^{-/-} mice (n=3). mRNA expression was normalized to *Hprt* and presented relative to WT *Ldlr*^{-/-} controls. (b) Representative histogram depicting STAT3 protein expression in WT *Ldlr*^{-/-} and CKO *Ldlr*^{-/-} DCs (solid line - WT *Ldlr*^{-/-}, dotted line - CKO *Ldlr*^{-/-}, filled dark grey line - WT *Ldlr*^{-/-} FMO, filled faint grey line - CKO *Ldlr*^{-/-} FMO). Data is presented as mean \pm SEM; **p<0.01.

4.9 A HIF1 α -STAT3-IL-12-IFN γ pathway in atherosclerosis

To determine a link between STAT3 and IL-12, mature BMDCs were transfected with either a STAT3 overexpressing plasmid (called STAT3-WT vector) or a STAT3 dominant negative mutant plasmid (called STAT3-D vector) which has a mutation in the DNA-binding domain²⁶⁹. Vector overexpression was confirmed by observing dramatically increased *Stat3* mRNA expression in mature WT and CKO BMDCs transfected with STAT3-WT vector (2,982 \pm 756, and 1,186 \pm 490 fold increase, respectively, n=3 each) and STAT3-D vector (3,221 \pm 1,045, and 3,530 \pm 2,425 fold increase, respectively, n=3 each). Indeed, overexpression of STAT3 in BMDCs decreased *Il12* mRNA levels, whereas inhibition of STAT3 via the STAT3-D vector enhanced *Il12* expression in both WT and CKO BMDCs (**Figure 4.9.1**). It is noteworthy that the effects on IL-12 were seen in both the WT and CKO BMDCs indicating that STAT3 modulates IL-12 independently of HIF1 α .



4.9.1 STAT3 modulates IL-12 independently of HIF1 α

Il12 mRNA expression was analyzed in WT and CKO BMDCs transfected with pEF-STAT3 wild type vector (grey bars), pCAGGS-STAT3D dominant negative mutant vector (black bars), or empty vector (white bars) by qPCR, normalized to *Hprt* and expressed relative to respective empty vector controls, (3 independent experiments, n=3 mice per experiment). Data is presented as mean \pm SEM; *p<0.05, ***p<0.001.

Since a clear link between STAT3 and IL-12 expression was seen in BMDCs *in vitro*, further the effects on atherosclerosis progression *in vivo* after STAT3 overexpression were determined. For this purpose, a novel technique of Cre-dependent expression using the lentiviral vector pLB2-Ubi-FLIP was

employed^{270,271}. The pLB2-Ubi-FLIP-Stat3 vector contained *Stat3* cDNA cloned in the reverse orientation and flanked by inverted loxP sequences, such that Cre-induced recombination irreversibly flipped *Stat3* to a sense orientation, resulting in expression of *Stat3* under the ubiquitin promoter in all Cre-expressing cells.

The specificity of the Cre system was validated in HEK293F cells co-transfected with the pLB2-Ubi-FLIP-Stat3 vector and a Cre-producing pIC-cre vector, demonstrating significantly increased *Stat3* mRNA expression compared to cells transfected without the pIC-cre vector (**Figure 4.9.2a**). The pLB2-Ubi-FLIP-Stat3 vector was then incorporated into lentiviral particles. Transduction of BM cells from *Cd11c-cre*⁺ mice with lentivirus carrying the pLB2-Ubi-FLIP-Stat3 vector confirmed significantly elevated *Stat3* mRNA expression in differentiated BMDCs (that would also up-regulate Cre under the CD11c promoter) after 7 days (**Figure 4.9.2b**).

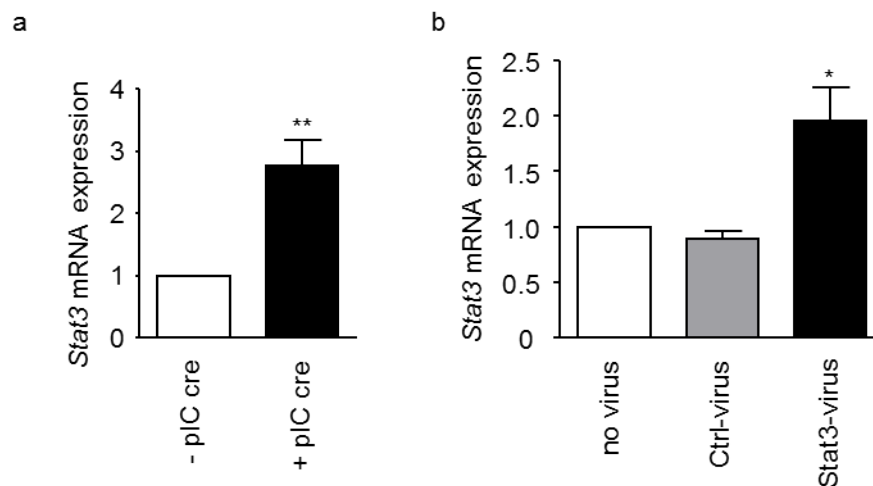


Figure 4.9.2 *Stat3* mRNA expression is enhanced in presence of Cre protein

(a) qPCR analysis of *Stat3* mRNA expression in HEK293F cells co-transfected with the STAT3 overexpressing vector pLB2-Ubi-FLIP-Stat3 and with or without a Cre producing pIC-cre vector (n=6) (b) qPCR analysis of *Stat3* mRNA expression in BMDCs differentiated from BM of *Cd11c-cre* mice, transduced with control or pLB2-Ubi-FLIP-Stat3 lentivirus (n=3). Values normalized to *Hprt* and expressed relative to respective -pIC-cre or no virus controls. Data is presented as mean ± SEM; **p<0.01.

WT and CKO BM cells were transduced with lentivirus containing control or pLB2-Ubi-FLIP-Stat3 vector and transplanted into lethally irradiated *Ldlr*^{-/-} mice. Increased lesion formation was seen in *Ldlr*^{-/-} mice carrying control virus-transduced CKO BM (CKO-BM+Ctrl-virus→*Ldlr*^{-/-} **black bar**) versus WT BM (WT-BM+Ctrl-virus→*Ldlr*^{-/-} **white bar**) in the aortic root after 4 weeks of

high fat diet, complementing the original plaque data from WT *Ldlr*^{-/-} and CKO *Ldlr*^{-/-} mice. Notably, this increase was completely nullified by transduction with the pLB2-Ubi-FLIP-Stat3 vector in CKO BM (CKO-BM+Stat3-virus→*Ldlr*^{-/-} **dark gray bar**) (Figure 4.9.3). Also of note is that there was no difference between WT-BM transduced with Stat3-virus (WT-BM+Stat3-virus→*Ldlr*^{-/-} **light gray bar**) and CKO-BM transduced with Stat3-virus (**dark gray bar**). This again, like the STAT3 overexpression experiment in BMDCs, confirms that STAT3 functions independent of HIF1α and mostly lies downstream of the transcription factor.

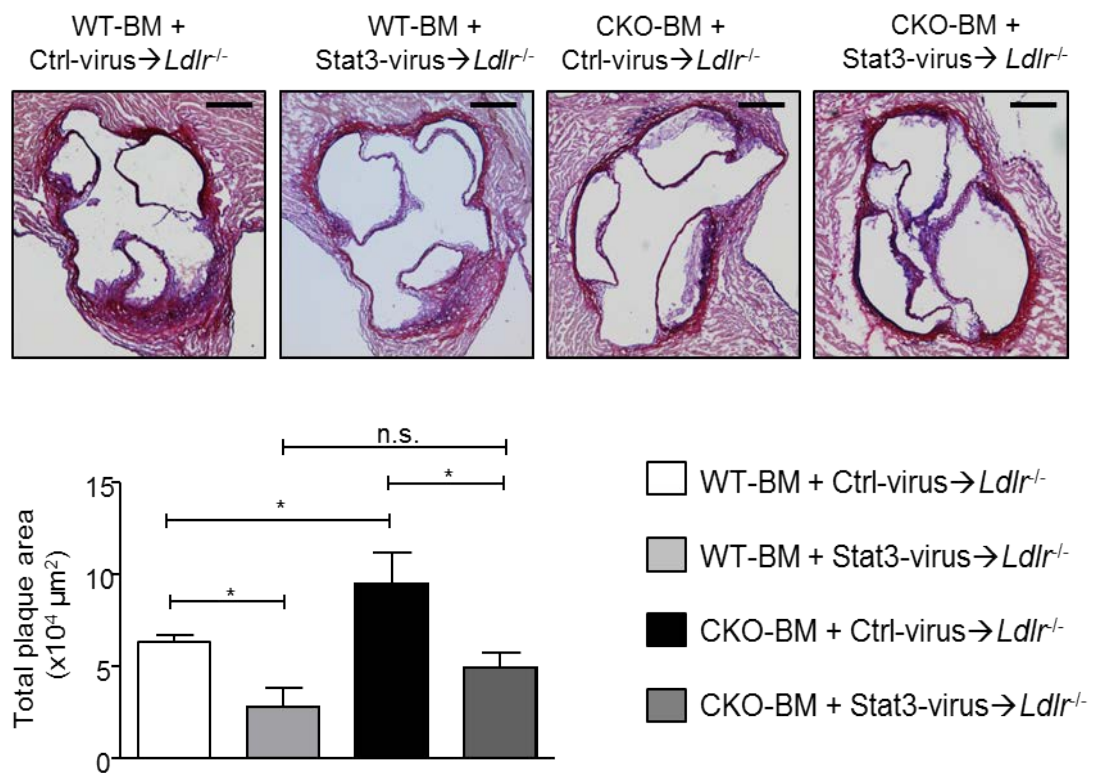


Figure 4.9.3 DC-intrinsic effects of HIF1α on plaque development are STAT3-mediated

Quantification of plaque area in Aldehyde fuchsin stained aortic roots of *Ldlr*^{-/-} mice transplanted with control-lentivirus transduced WT BM (WT-BM+Ctrl-virus→*Ldlr*^{-/-}) or CKO BM (CKO-BM+Ctrl-virus→*Ldlr*^{-/-}) and *Ldlr*^{-/-} mice transplanted with Stat3-overexpressing-lentivirus transduced WT BM (WT-BM+Stat3-virus→*Ldlr*^{-/-}) or CKO BM (CKO-BM+Stat3-virus→*Ldlr*^{-/-}) and fed a high fat diet for 4 weeks (n=5 mice each), representative sections of the aortic root are shown (scale bars, 250μm). Data is presented as mean ± SEM; *p<0.05.

4.10 Determination of HIF1 α binding sites on gene promoters and evidence of direct transcription factor activity by ChIP

HIF1 α , being a transcription factor, binds to the promoters of various genes at specific regions called the Hypoxia response element (HRE). All genes whose transcription is controlled by HIF1 α have the HRE in their promoter region. The HRE consists of the binding sequence (HBS) or the core sequence and the downstream ancillary sequence (HAS) which helps in full activation of the gene. To determine whether the changes in expression of genes *Socs1*, *Socs3* and *Stat3* were direct effects of HIF1 α binding to the promoters of these genes and modulating their expression, a transcription factor binding software was used to determine whether these genes have the HRE sequences in their promoters. *Socs1* did not show the core HRE sequence but only the HAS which hints that *Socs1* is not directly controlled by HIF1 α . *Socs3* had the core HRE sequence in the promoter without the HAS, which points towards partial gene activation by HIF1 α . Interestingly, the *Stat3* gene promoter displayed both the HBS and the HAS which proves that it is a suitable candidate for direct gene transcriptional activation by HIF1 α (**Figure 4.10.1**).

Accession no.	GeneID	Matrix Family	Start position	End position	Anchor position	Strand	Matrix sim.	Evidence
SOCS1								
GXP_18168	12703	V\$HASF	185	195	190	-	0,947	tgaCACGcctc
GXP_419291	12703	V\$HASF	217	227	222	+	0,921	tgcCACGcctc
SOCS3								
GXP_252332	12702	V\$HIFF	141	157	149	+	0,889	tggtcctACGTcccttt
GXP_3066430	12702	V\$HIFF	42	58	50	-	0,982	gtgacagaCGTGggtgc
GXP_3066430	12702	V\$HIFF	226	242	234	+	0,889	tggtcctACGTcccttt
GXP_3066431	12702	V\$HIFF	109	125	117	+	0,970	gatactcaCGTGaccag
GXP_3066431	12702	V\$HIFF	110	126	118	-	0,966	cctggtcaCGTGagtat
STAT3								
GXP_219849	20848	V\$HIFF	109	125	117	+	0,983	gattccaCGTGgtaag
GXP_219849	20848	V\$HIFF	110	126	118	-	0,975	ccttaccaCGTGggaat
GXP_219849	20848	V\$HIFF	139	155	147	+	0,989	cgcccccaCGTGgtgcc
GXP_219849	20848	V\$HIFF	140	156	148	-	0,975	tggcaccaCGTGggggc
GXP_219849	20848	V\$HASF	512	522	517	-	0,934	agaCACGcctc

Figure 4.10.1 Determination of HRE in promoters of *Socs1*, *Socs3* and *Stat3* genes

Details of binding sites of HIF1 α on *Socs1*, *Socs3* and *Stat3* gene promoters, showing start, end and anchor positions and sequence of the HRE with the core sequence marked in capital letters (Matrix family V\$HASF is for the ancillary site HAS and matrix family V\$HIFF is for the binding site HBS).

The position of HIF1 α binding on the *Socs3* and *Stat3* gene promoters was determined for different versions of the genes and primers were designed around these sequences (**Figure 4.10.2**).

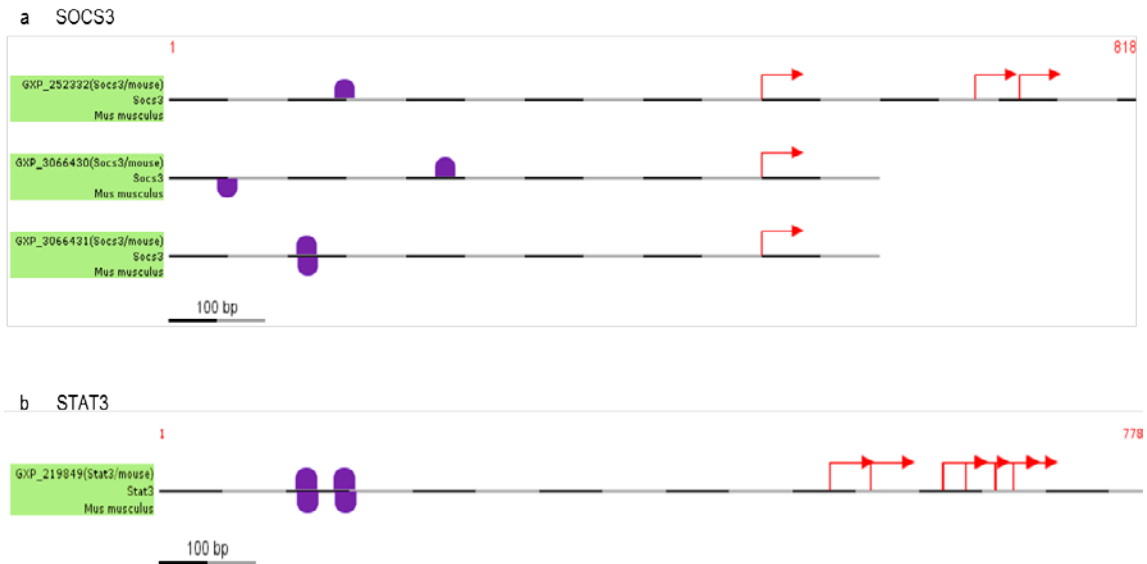


Figure 4.10.2 Determination of HIF1 α transcription factor binding sites

HIF1 α binding sites (marked as violet hemispheres) on different promoter versions of the genes (a) *Socs3* and (b) *Stat3* in relation to the transcription start site (marked as red arrow).

Finally, in order to experimentally confirm direct binding of HIF1 α to the gene promoters of *Stat3* and *Socs3*, a chromatin immunoprecipitation assay was carried out. A HIF1 α specific antibody or control IgG antibody was incubated with cross-linked and sheared chromatin from CoCl₂ treated BMDCs. The anti-HIF1 α antibody precipitates the transcription factor, pulling down along with it any DNA fragments that it binds. When these precipitated DNA fragments were analyzed in qPCR using primers against the HBS of *Socs3* promoter and compared to input DNA, no signal differences were seen between the anti-HIF1 α and IgG antibodies, suggesting that HIF1 α does not directly bind to the *Socs3* gene promoter (data not shown). On the other hand it was interesting to note that the precipitated DNA fragments were positive for the *Stat3* gene promoter HBS, evident from the significantly higher percent input amplification in the anti-HIF1 α samples compared to the IgG control by qPCR (**Figure 4.10.3a**) as well as the high band intensity on agarose gel

(**Figure 4.10.3b**). This confirms that HIF1 α directly binds to and influences transcription of *Stat3* but not *Socs3*.

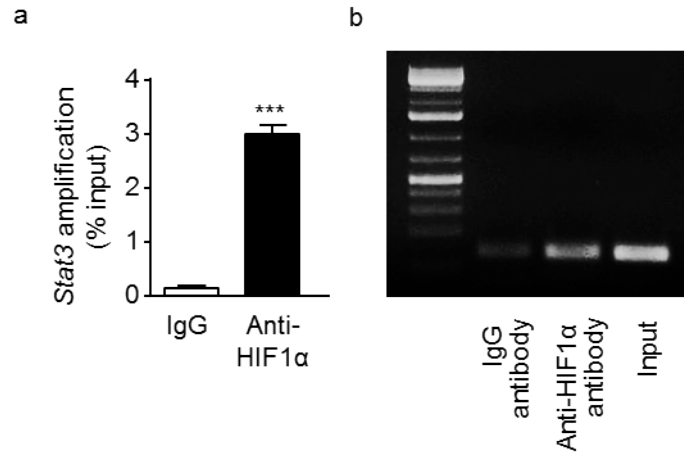


Figure 4.10.3 ChIP assay provides evidence that HIF1 α binds directly to the *Stat3* gene promoter
ChIP assay was performed using anti-HIF1 α antibody or respective IgG control antibody for HIF1 α precipitation from C57BL/6J BMDCs treated with CoCl₂. (a) Immunoprecipitated chromatin was analyzed by qPCR using primers to HIF1 α binding sites on the *Stat3* promoter. Results were normalized to input chromatin (n=3 mice from 2 independent experiments). (b) A representative agarose gel of conventional PCR-amplified samples is shown (Ladder: 1 kB). Data is presented as mean \pm SEM; ***p<0.001.

5. DISCUSSION

Atherosclerotic lesions are areas of accumulated cells that undergo continuous and enhanced metabolism and finally cell death to form necrotic cores. These areas are covered with a fibrous cap and with progression of disease, plaque area increases to such a large extent that the thickness exceeds maximum oxygen diffusion distance²³⁶. The plaque area exhibits high oxygen demand due to increased metabolic activity and reduced oxygen availability as a result of impaired oxygen diffusion. Hence, the cells in the plaque experience periods of chronic hypoxia owing to the imbalance between oxygen supply and demand^{238,246}. Hypoxia has been experimentally demonstrated in atherosclerotic vessels in literature. The first studies involved *in vitro* or *in situ* analysis of oxygen consumption and pressure using micro-electrodes in diet fed rabbit aortas²³⁸⁻²⁴². Recently, more accurate and easy to perform immunohistochemical methods using the hypoxia marker pimonidazole have become the gold-standard method for detecting hypoxia. Hypoxia has thus been shown *in vivo* in atherosclerotic rabbits and *ApoE*^{-/-} mice as well as in carotid lesions of symptomatic individuals^{236,243-246}.

Along the same lines, in this project, pimonidazole was used to test for presence of hypoxia in the aortic plaque of *Ldlr*^{-/-} mice fed a high fat diet for 8 weeks. The cross-sections of the aortic root clearly showed DAB stained areas indicating presence of hypoxia in these mice. The pimonidazole stained hypoxic but actively metabolizing cells that experience O₂ concentrations below 1% but did not stain anoxic cells or apoptotic cells. Hence, it is clear that the staining for hypoxia seen is present in the cellular part of the plaque closer to the lumen that contains actively metabolizing and O₂ consuming cells and not in the acellular necrotic core of the plaque which lacks metabolizing cells even though the distance of this area from the O₂ providing lumen is much higher. Additionally, no DAB staining was seen in atherosclerotic mice that were not treated with pimonidazole or in C57BL6/J mice treated with pimonidazole, indicating specificity of the hypoxia marker.

With the clear indication of presence of hypoxia in atherosclerotic plaques, it becomes essential to understand how immune cells accumulating in lesions behave under conditions of low O₂. To counteract the effects of hypoxia, these cells would have to up-regulate hypoxia inducible genes and show high expression of HIF proteins. Previously, enhanced expression of HIF1α was shown in atherosclerotic lesions of humans^{251,272} as well as mice and was associated with an inflammatory plaque phenotype^{243,245}. HIF1α expression has also been shown to increase from early to stable lesions, associated with increasing hypoxia, but at the same time to be up-regulated in luminal plaque macrophages by inflammatory stimulation even in the absence of hypoxia²³⁶. Similarly, in this study the expression of HIF1α in the aortas of atherosclerotic *Ldlr*^{-/-} mice was determined. In line with previous reports, an up-regulation of *Hif1a* mRNA expression in atherosclerotic aortas of *Ldlr*^{-/-} mice was detected when compared to healthy controls, showing that HIF1α is increased and stabilized in the hypoxic environment of plaque.

Literature which investigates HIF1α expression in the atherosclerotic plaque also mentions that HIF1α co-localizes with CD68 positive macrophages in the plaque^{243,251,272} but no data exists as to the co-localization of HIF1α with other cell types, specifically DCs in the plaque. Since the focus of this project was to elucidate the role of HIF1α in DCs, plaque sections from atherosclerotic *Ldlr*^{-/-} mice were co-stained for HIF1α and the DC marker CD11c and a clear co-localization was seen. This staining also correlates to the location of hypoxia in the plaque. Apart from the fact that lesional DCs experience hypoxia and up-regulate HIF1α, it is also important to consider that these DCs engulf modified lipoproteins to initiate early lesion formation⁸⁹ and are stimulated by pro-inflammatory cytokines like TNFα, IFNγ or IL-1β in the plaque environment which may thus instigate HIF1α expression, independently of, or in addition to hypoxia. It is clear from previous reports that HIF1α is also stabilized under non-hypoxic conditions like stimulation by oxLDL²⁶⁰ and pro-inflammatory cytokines¹⁶²⁻¹⁶⁸ supporting the idea that HIF1α increase in DCs is not only hypoxia dependent but could also involve non-hypoxic stimuli. Along these lines, it was necessary to determine whether DCs from secondary lymphoid organs like the spleen would also up-regulate

HIF1 α under inflammatory conditions of atherosclerosis but in absence of hypoxia as seen in the plaque. Interestingly, splenic CD11c⁺ cells from atherosclerotic mice also up-regulated HIF1 α compared to healthy controls confirming the hypothesis that up-regulation of HIF1 α in DCs during atherosclerosis progression is evident locally in the plaque as a result of hypoxia and non-hypoxic mediators as well as systemically in secondary lymphoid organs as a result of inflammatory stimuli independent of hypoxia.

Since HIF1 α is up-regulated in DCs during atherosclerosis and immune responses as whole, it must play an essential role in helping the cells to survive and adapt to hypoxia and modulate their functions, thus affecting the immune response. Limited studies exist to determine the role of HIF1 α in DCs and the data provided by these is contradictory¹⁹⁵⁻²⁰⁰. Though HIF1 α is consistently known to play a pro-inflammatory role in macrophages, monocytes and neutrophils¹⁸⁴⁻¹⁹² but an anti-inflammatory role in T cells¹⁷³⁻¹⁷⁷, its role in DCs is still unresolved. Specifically, no studies have focused on the role of HIF1 α in DCs in the context of atherosclerosis, which formed the aim of this particular research project.

To investigate the role of HIF1 α deficient DCs in atherosclerosis progression, CKO *Ldlr*^{-/-} and WT *Ldlr*^{-/-} mice were generated. Earlier, time point based diet study was performed in the lab where *Ldlr*^{-/-} mice were fed high fat diet for various durations to determine the best time point to study atherosclerotic development. At 8 weeks of diet, the atherosclerotic lesions are big enough to study differences between groups but not so large that any small changes are masked. Also, at 8 weeks of high fat diet, the plaques are in the initial stages of advancement where various cell types are active and can be appropriately studied. Hence in this study, the CKO *Ldlr*^{-/-} and WT *Ldlr*^{-/-} mice were placed on 8 weeks of high fat diet to accelerate atherosclerotic lesion formation. After 8 weeks, body weights and serum lipid levels were analyzed in these mice. Both the groups showed comparable levels of body weight, total cholesterol and triglycerides, thus eliminating any effects due to changes in lipid metabolism itself. In order to ascertain efficient deletion of *Hif1a* from the DCs in these mice, isolated splenic DCs were analyzed for gDNA deletion of *Hif1a* gene as also mRNA expression of *Hif1a* was

determined in both splenic DCs as well as *in vitro* cultured BMDCs. The expression of *Hif1a* in both cases was significantly diminished in DCs from CKO *Ldlr*^{-/-} mice as compared to WT *Ldlr*^{-/-} mice.

In comparison to the controls, CKO *Ldlr*^{-/-} mice displayed enhanced plaque development in both the aortic root and the aortas, on staining with Aldehyde fuchsin or Oil-Red O to discern plaque area. Thus, mice with HIF1 α deficiency in DCs have a pro-atherogenic phenotype suggesting an inhibitory role of DC-HIF1 α in atherosclerosis development. Interestingly, the plaque composition in these mice, when analyzed by immunofluorescent staining, showed no changes in total numbers or area of macrophages but a significant decrease as percent of total plaque cells or area. On closer analysis, it was found that the acellular necrotic core area of the plaque was significantly enhanced in the CKO *Ldlr*^{-/-} mice. Also, the smooth muscle cell content showed an increase in the CKO *Ldlr*^{-/-} mice. This phenotype is typical of more advanced plaques where the macrophages form foam cells and undergo cell death leaving an acellular necrotic core area in the plaque and the plaques acquire a fibrous cap where SMCs multiply^{73,80}.

T cells play an important role in progression of atherosclerosis. It is known that a pro-atherogenic response is equivalent to a pro-inflammatory phenotype where T cells show increased activation and mobilization to the plaque area^{73,273,274}. The CKO *Ldlr*^{-/-} mice revealed highly enhanced numbers of T cells in the plaques and on FACS analysis of the blood, spleen and peripheral lymph nodes, it was evident that there were significantly increased numbers of activated CD4⁺ T cells and decreased numbers of naive CD4⁺ T cells in circulating blood as well as in the lymphoid organs. This suggests that, in CKO *Ldlr*^{-/-} mice, there is enhanced activation of CD4⁺ T cells which are abundant in the periphery and then start to migrate to the site of inflammation in the atherosclerotic lesions. Since total numbers of CD3⁺ T cells and the ratio of CD4⁺ and CD8⁺ T cells in the periphery did not change, it can be ruled out that the enhanced migration of T cells to the plaque is due to enhanced production of T cells in the BM.

On closer analysis of the polarization status of these CD4⁺ T cells, it was revealed that the CKO *Ldlr*^{-/-} mice have increased percentage of IFN γ producing T_h1 cells but no changes in IL-17a producing T_h17 cells or FoxP3⁺ T_{regs}. T_h1 cells have been closely linked to atherosclerotic development and IFN γ is shown to be a prime cytokine in eliciting a pro-atherogenic response²⁷⁵⁻²⁷⁸. On the other hand, studies concerning other T helper subsets identify T_{regs} to play a protective role in atherosclerosis²⁷⁹⁻²⁸¹ whereas the exact role of T_h2 and T_h17 cells still remains controversial^{76,117,282}. Therefore, a rise in IFN γ producing T_h1 cells in mice with HIF1 α deficient DCs explains the pro-atherogenic phenotype seen. In studies of HIF1 α deficiency in CD4⁺ T cells, HIF1 α has been shown to enhance FoxP3 expression and result in T_{reg} abundance in mice^{181,182}. On the other hand, some studies identify the role for HIF1 α in maintaining a balance between T_h17 and T_{reg} differentiation where HIF1 α induces CD4⁺ T cells to differentiate into T_h17 cells and inhibits T_{reg} cell generation^{179,180}. Along these lines, no changes were observed in the T_h17 or T_{reg} populations in any of the organs. This is expected as the HIF1 α deficiency is only in the CD11c⁺ cell compartment and the CD4⁺ cells show only a marginal non-significant HIF1 α deletion in their genome. The HIF1 α deficiency of DCs clearly does not affect T cell polarization to the T_h17 or T_{reg} phenotype but specifically to T_h1, which proves that HIF1 α is responsible for polarization-specific changes in DCs which affects their interaction with T cells.

Furthermore, no changes were seen in numbers of B cells, monocytes, neutrophils, macrophages and the ratio of Gr1^{high} and Gr1^{low} monocytes in the periphery between the groups. Importantly the numbers of CD11c⁺ DCs and ratio of MHCII^{hi} and MHCII^{lo} DCs did not change with deletion of HIF1 α in CD11c⁺ cells. In addition, no changes were observed in the numbers of CD11c⁺ DCs in the plaque. The migratory capacity towards CCL19 and the expression of *Ccr7* also remained unchanged in HIF1 α deficient DCs. Literature is contradictory with regards to the effects of hypoxia and HIF1 α on the expression of CCR7 and the migration of DCs. In one study, hypoxia was shown to enhance expression of CCR7 on DCs and their migration towards CCL19 in a HIF1 α dependent manner²⁰¹, while in another study, CCR7 was up-regulated on hypoxia, even though migratory capacity of DCs was reduced compared to normoxic DCs²⁸³. Conversely, CCR7 expression decreased in

hypoxic DCs, reducing the migratory capacity towards CCL19^{199,207,284}. Also, no effects on CCR7 were seen in hypoxic DCs in line with findings seen in this project²⁰⁰. These data stress on the fact that HIF1 α is not essential for generation and development of DCs or their circulation and migration to inflammatory sites. The pro-atherogenic phenotype seen in the CKO *Ldlr*^{-/-} mice is not affected by these factors and is a result of HIF1 α deficient DCs modulating the T cell response towards a more activated, T_h1 mediated phenotype.

Monocytes and macrophages have also been known to express CD11c under inflammatory conditions without converting to DCs²³. Especially under conditions of hypercholesteremia, blood monocytes have been shown to up-regulate CD11c which helps in recruitment and development of atherosclerosis²⁴. It was essential to determine whether the effects seen on atherosclerosis development and T-cell activation in the CKO *Ldlr*^{-/-} mice were indeed due to deletion of HIF1 α in DCs and not in macrophages or monocytes. For this purpose, a similar atherosclerosis study was carried out in a *LysM-cre*⁺*Hif1a*^{flox/flox} mouse model by Dr. Judith Sluimer at Maastricht. *LysM* is a myeloid lineage specific marker present on monocytes, macrophages and neutrophils. If the effects seen due to HIF1 α depletion in CD11c⁺ cells are due to monocytes and macrophages, similar effects would be expected after deletion of HIF1 α in the *LysM*⁺ cells. Interestingly, no changes in atherosclerotic lesions were seen in these *LysM-cre*⁺*Hif1a*^{flox/flox} mice. Also, cultured macrophages from the CKO (*Cd11c-cre*⁺ *Hif1a*^{flox/flox}) mice did not show required changes in their M1 and M2 markers that could explain the atherosclerotic phenotype seen *in vivo*. Thus, the effects seen in CKO *Ldlr*^{-/-} mice can clearly be attributed to DCs rather than monocytes or macrophages. Additionally, literature that has exclusively considered the role of HIF1 α in the myeloid lineage has seen a pro-inflammatory role for this transcription factor¹⁸⁴⁻¹⁸⁶. Especially in regards to atherosclerosis, myeloid cells have been shown to be responsible for induction of foam cell formation, neo-intima formation and enhanced angiogenesis^{236,254,256}. This clearly delineates separate functions for macrophages or monocytes and DCs. Even though they share certain properties, it is clear that the most important function of DCs, which is T-cell polarization, defines its significance and distinguishes it from

other APCs. This also confirms the fact that effects seen in the CKO *Ldlr*^{-/-} mice are DC specific without influence of other myeloid cells.

It was clear that HIF1 α plays an anti-inflammatory role in DCs in the context of atherosclerosis due to the increased lesion size, advanced plaque phenotype and enhanced numbers of activated and IFN γ producing CD4⁺ T cells in CKO *Ldlr*^{-/-} mice. Similarly, FACS analysis was carried out in CKO mice (which were not crossed to *Ldlr*^{-/-} mice, were fed normal chow and hence did not develop atherosclerosis) to check for effects of HIF1 α on T cells at the baseline non-inflammatory levels. No differences were seen between the WT and CKO mice under such circumstances. This stresses on the fact that HIF1 α is only up-regulated under inflammatory or hypoxic conditions, when its effects are visible and hence comparable. Under non-inflammatory conditions HIF1 α is absent and hence no effects on T-cell activation or polarization were seen. Up-regulation of *Hif1a* mRNA seen in aortas and spleens after high fat diet also supports this fact.

It is known that DCs polarize T cells to a T_h1 response by presenting antigen on the MHCII complex, overexpressing co-stimulatory molecules and releasing pro-inflammatory cytokines, the most potent of which is IL-12^{44,285,286}. IL-12 plays an important role in cell-mediated immune responses by differentiating naive CD4⁺ T cells to the T_h1 phenotype and inducing production of IFN γ which regulates a pro-inflammatory response^{46,264,287}. IL-12 has also been shown to be an essential mediator of atherosclerotic development and deficiency of IL-12 has clearly been associated with decreased lesion development in mice¹⁰⁹⁻¹¹¹. In this project, an enhanced production of IL-12 in the CKO BMDCs as well as splenic DCs from atherosclerotic CKO *Ldlr*^{-/-} mice was observed on both the mRNA and protein level. This clearly explains the enhanced T-cell activation and T_h1 polarization and finally the pro-atherogenic phenotype. No other cytokines showed changes on HIF1 α deletion stating that HIF1 α primarily regulates IL-12 expression in DCs. Along these lines, when the CKO *Ldlr*^{-/-} splenic DCs isolated from atherosclerotic mice were co-cultured with naive CD4⁺ T cells in an antigen specific co-culture assay, the naive T cells showed enhanced proliferation and polarization to the T_h1 phenotype than when co-cultured with

WT *Ldlr*^{-/-} DCs as seen by flow cytometry analysis of CFSE⁺ and IFN γ ⁺ CD4⁺ cells in the culture. This excess proliferation and polarization was successfully inhibited by using an anti-IL-12 blocking antibody. This data provides further proof that HIF1 α deficient DCs have higher capabilities to proliferate and polarize naive CD4⁺ T cells and this activation is mediated by increased expression of IL-12 on these DCs and reaffirms the phenotype seen in CKO *Ldlr*^{-/-} mice.

Previously, studies have shown that in human monocyte-derived DCs, hypoxia-induced HIF1 α activation inhibits LPS-induced co-stimulatory molecule expression and T-cell proliferation¹⁹⁹, whereas it was also shown that hypoxia or HIF1 α stabilization do not alter DC maturation without additional pro-inflammatory stimuli²⁸⁸. In contrast, LPS-stimulation of murine BMDCs in combination with hypoxia enhanced co-stimulatory molecule expression and T-cell proliferation²⁸⁹. In this project, no changes were observed in the expression levels of MHCII and co-stimulatory molecules, thus affirming that enhanced activation of T cells is a result of IL-12 secretion and not due to increased signaling by MHCII or co-stimulatory molecules.

It was essential to understand the molecular pathway that associates HIF1 α and IL-12. The most common modulators of HIF1 α that would affect immune responses would be NF κ B subunits^{213,214}. But no changes in NF κ B subunits p105 or p65 were seen in the HIF1 α deficient BMDCs or atherosclerotic splenic DCs suggesting that HIF1 α does not modulate IL-12 via NF κ B signaling or that the pro-inflammatory responses in CKO *Ldlr*^{-/-} mice are not a result of changes in NF κ B. Additionally, the suppressors of cytokine signaling (SOCS) 1 and 3 molecules would easily explain the phenotype seen in DCs as SOCS1 and SOCS3 are responsible for suppressing expression of pro-inflammatory cytokines and modulating immune responses^{290,291}. Also, SOCS1 in DCs is shown to restrict DC immune functions, especially production of IL-12 and T_h1 cell induction. In studies where SOCS1 was silenced in BMDCs, the cells were shown to be more responsive to LPS and IFN γ and secreted higher amounts of pro-inflammatory cytokines. SOCS1 silenced DCs also showed enhanced capacity to proliferate antigen-specific T cells and induce a hyper T_h1 immune response both *in vitro* and

in vivo^{292,293}. Thus, if the effects seen in the CKO DCs could be attributed to a reduction of SOCS molecules, it could be possible that HIF1 α controls the expression of SOCS by binding to its promoter and affecting mRNA expression. In the CKO BMDCs, no changes in *Socs1* or *Socs3* expression were observed but in splenic DCs from atherosclerotic CKO *Ldlr*^{-/-} mice a slight but significant decrease in the mRNA expression of both molecules was seen, suggesting that an atherosclerotic immune response was responsible for modulating expression of the SOCS molecules but not clearly stating whether these molecules were responsible for the effects seen in the DCs and whether they lie between the HIF1 α -IL-12 pathway.

To explain if HIF1 α activates SOCS molecules directly, a transcription factor binding analysis was carried out to determine presence of hypoxia responsive elements on the promoters of these genes. The HRE consists of a HIF1 α binding site (HBS) with the sequence 5'-RCGTG-3' and a HIF1 α ancillary site (HAS) with the sequence 5'-CAGGT-3'. Absence of both HBS and HAS is a clear indication that the gene is not modulated by the transcription factor. In the absence of an HAS, HIF1 α binding to the HBS is affected and leads to a transcriptionally inactive or non-functional state. Hypoxia responsive genes consist of both the HBS and HAS sequences for complete binding of the HIF1 α protein to the promoter site and full activation of gene transcription²⁹⁴. The *Socs1* gene promoter had neither the HBS nor the HAS sequence clearly indicating that HIF1 α does not activate *Socs1* by direct binding to its promoter. The *Socs3* gene had an HBS sequence suggesting a possible binding of the transcription factor. But a ChIP assay and qPCR analysis for *Socs3* gene promoter region in chromatin fragments pulled down by a HIF1 α antibody proved that HIF1 α did not bind to the *Socs3* gene promoter. Thus the changes seen in mRNA expression of SOCS molecules in CKO *Ldlr*^{-/-} splenic DCs could be attributed to an indirect effect of HIF1 α deletion or a reverse effect of inflammation or atherosclerosis mediated changes on SOCS expression.

To further elucidate the identity of the molecule activated by HIF1 α that is responsible for modulating IL-12 expression, a detailed literature search revealed STAT3 to be a probable candidate. STAT3 is a member of the signal

transducers and activators (STAT) family of proteins and is induced mainly by IL-6 type cytokines but also by receptor tyrosine kinases and members of the IFN and IL-2 family of cytokines. On receptor activation, STAT3 is phosphorylated by kinase JAK2 and translocates to the nucleus where it affects the expression of a variety of genes in response to the stimulus, thus playing essential roles in cell growth apoptosis and inflammation. STAT3 deficient mice do not exist as the embryos die prior to gastrulation due to an essential role of STAT3 in embryogenesis²⁹⁵.

In literature, STAT3 deficient T cells show impaired proliferative responses to IL-6 and IL-2 whereas STAT3 deficient macrophages show enhanced production of inflammatory cytokines with a capacity to polarize T cells to the T_h1 phenotype^{296,297}. In DCs, STAT3 has been clearly shown to be a negative regulator of DC functions. In a study where STAT3 was deleted in CD11c cells using the Cre-flox system, CKO mice showed inflammatory responses like lymphadenopathy and ileo-colitis with enhanced levels of circulating pro-inflammatory cytokines. The STAT3 deficient DCs demonstrated enhanced immune activity by releasing increased levels of IL-12 and IL-23 in addition to IL-6 and TNF α and showed increased capacity to stimulate T-cell proliferation and IFN γ secretion in OVA antigen specific assays, though a pathway explaining the effects was not elucidated²⁶⁷. In another study, the JAK2/STAT3 pathway was inhibited using a chemical inhibitor JSI-124. DCs treated with this inhibitor, showed dramatic activation seen as up-regulation of MHCII and co-stimulatory molecules as well as ability to stimulate T cells. The authors attributed this activation to the transcription factor NF κ B²⁶⁸. Other studies showed that STAT3 activation was required for suppression of LPS induced DC maturation and that STAT3 deficiency in the hematopoietic lineage via an inducible system led to enhanced activation of not just DCs but also neutrophils, T cells and NK cells^{298,299}. In line with these studies, STAT3 changes were observed in the CKO DCs in this project, which could explain the enhanced DC activation status. CKO DCs, both mature BMDCs and atherosclerotic splenic DCs, showed decreased levels of STAT3 on mRNA and protein levels. This is in conjunction with the negative regulatory role of STAT3 in DCs as seen in literature.

To further confirm whether these changes in STAT3 are responsible for changed levels of IL-12, BMDCs were transfected with a STAT3 overexpressing vector (STAT3-WT) or a STAT3 dominant negative mutant vector (STAT3-D) which has a mutation in its DNA binding domain and hence inhibits STAT3 activity³⁰⁰. In cells transfected with the STAT3 overexpressing vector, *Il12* mRNA levels were reduced as compared to cells transfected with an empty vector. On the other hand, cells transfected with the STAT3 dominant negative mutant vector, showed greatly enhanced levels of *Il12* mRNA. This proves that STAT3 is responsible for negatively modulating IL-12 levels and likewise DC activation status. Interestingly, the STAT3 – IL-12 changes seen were similar in both WT and CKO DCs which states that the STAT3 – IL-12 pathway is HIF1 α independent. But since reduced STAT3 levels were seen in CKO DCs as compared to WT, it becomes clear that the STAT3 – IL-12 pathway lies downstream of HIF1 α and very likely HIF1 α affects STAT3 which further modulates IL-12.

To determine whether the STAT3 effects seen *in vitro* also have *in vivo* relevance, an innovative approach of STAT3 overexpression was used. *Stat3* cDNA was cloned in the antisense orientation under an Ubiquitin promoter into the lentivirus vector pLB2-FLIP. The cDNA is between two antiparallel loxP sites. This leads to a Cre mediated inversion of the cDNA which is irreversibly flipped to the sense orientation for transcription. This is different from genes that are placed between parallel loxP sites where Cre-mediated deletion occurs in lieu of inversion³⁰¹. Such a vector was packaged into lentiviral particles and transduced into BM cells of WT (*Cd11c-cre⁺ Hif1a^{flox/flox}*) and CKO (*Cd11c-cre⁺ Hif1a^{+/+}*) mice; the DCs thus generated (either cultured *in vitro* or naturally differentiated *in vivo*) up-regulate CD11c and start production of the Cre protein. Hence, the Cre plays a dual role in these cells – to delete the *Hif1a* gene between two parallel loxP sites in the genome and additionally to invert the *Stat3* cDNA between two antiparallel loxP sites in the stably incorporated lentiviral vector. Thus only CD11c expressing cells (DCs) that delete the HIF1 α also start overexpression of STAT3. This is a highly specific and stable method of gene expression, successfully used in many studies before^{270,271}. When such a STAT3 overexpressing vector was transduced into lineage negative BM cells and transplanted into recipient *Ldlr^{-/-}*

mice, the mice with STAT3 overexpressing BM showed reduced atherosclerotic lesions in the aortic root compared to mice with a control vector BM, irrespective of whether the BM was from WT or CKO mice. Thus, the presence or absence of HIF1 α did not affect the downstream STAT3 functions in atherosclerosis, similar to the *in vitro* STAT3 overexpression experiment, confirming that the STAT3-IL-12 pathway is independent of and lies downstream of HIF1 α .

Literature has shown that STAT3 affects expression of HIF1 α by directly binding to its promoter^{179,302}. The results seen in both the *in vitro* and *in vivo* STAT3 overexpression experiments clearly elucidate that the effects seen on IL-12 levels as well as atherosclerotic lesions as a whole are not a result of STAT3 affecting HIF1 α and further the immune response in some other downstream signaling pathway since CKO DCs or the recipient *Ldlr*^{-/-} mice bearing such DCs also show the same effects as WT DCs or the respective control recipient mice. Thus, these effects do not involve STAT3-mediated circuitries reinforcing HIF1 α effects but occur independently and downstream of HIF1 α .

Using a transcription factor binding analysis software it became clear that the *Stat3* gene promoter has both the HBS (with sequence CGTG) and HAS (with sequence CACG), making *Stat3* a potential HIF1 α target gene. To determine whether HIF1 α modulates *Stat3* levels by directly binding to the promoter, a ChIP assay was performed to pull down HIF1 α and analyze chromatin fragments bound to the transcription factor. The chromatin fragments when analyzed by qPCR and primers specific to the *Stat3* gene promoter HBS showed presence of the *Stat3* gene and hence undeniably confirmed that *Stat3* is a transcriptional target of HIF1 α . It is indeed possible that STAT3 and HIF1 α form a loop mechanism influencing the expression of each other, though the overall effects seen on the cell would be complex and unpredictable and a long term and time point assay based inflammation model would be needed to analyze the effects of each transcription factor separately.

Thus data from this project clearly points to an essential role of DC expressed HIF1 α in progression of atherosclerosis. Using mice with HIF1 α deficient DCs, the effects of HIF1 α on DCs as well as in the entire

inflammatory process of atherosclerosis could be delineated. The HIF1 α deficient DCs showed decreased expression of transcription factor STAT3 and enhanced expression and release of pro-inflammatory cytokine IL-12. Apart from these changes, the HIF1 α deficient DCs did not show variations in MHCII, co-stimulatory molecules CD80 and CD86, NF κ B subunits p105 and p65, CCR7 or any other cytokines, namely IL-4, IL-6, IL-10, TGF β or TNF α .

Mice with such DCs lacking HIF1 α do not show a varied phenotype at the baseline when no inflammatory stimulus is present. But on crossing them with *Ldlr*^{-/-} mice and feeding them a high fat diet for 8 weeks, the CKO *Ldlr*^{-/-} mice develop enhanced atherosclerotic lesions in the aorta and aortic root as compared to controls. They show an advanced plaque phenotype with lower percentage of DCs and macrophages in the lesions but significantly increased necrotic core and SMCs. Also, the plaques show increased infiltration of T cells pointing to higher activation of T cells in these mice. By FACS it was clear that these mice had increased levels of CD44^{hi} activated T cells and reduced levels of CD62L naive T cells. These activated cells were also found to be of the T_h1 type, thus releasing increased amounts of IFN γ . No changes in IL-17a⁺ or FoxP3⁺ CD4⁺ cells were observed, clearly stating that the HIF1 α deficient DCs in these mice activated T cells and polarized them to the T_h1 phenotype by enhanced secretion of IL-12. Similarly, these DCs were capable of polarizing naive CD4⁺ T cells *in vitro* to the T_h1 type better than their WT counterparts, a process that was inhibited by blocking IL-12, signifying the crucial role of IL-12 in T-cell polarization.

In DCs, the IL-12 was mediated by STAT3 as seen by *in vitro* STAT3 overexpression and inhibition experiments. Overexpression of STAT3 led to decreased IL-12 whereas inhibition of STAT3 led to IL-12 up-regulation. STAT3 overexpression *in vivo* also led to reduced atherosclerotic lesion size in both the CKO and WT DCs. This states that STAT3 modulates IL-12 independent of HIF1 α and possibly downstream of it, thus further influencing atherosclerotic lesion formation. A direct control of STAT3 by HIF1 α was also confirmed by a transcription factor binding site analysis and ChIP assay. A figure explaining the circuitry in HIF1 α deficient DCs and their overall effects in inflammation can be outlined as in **Figure 5.1**.

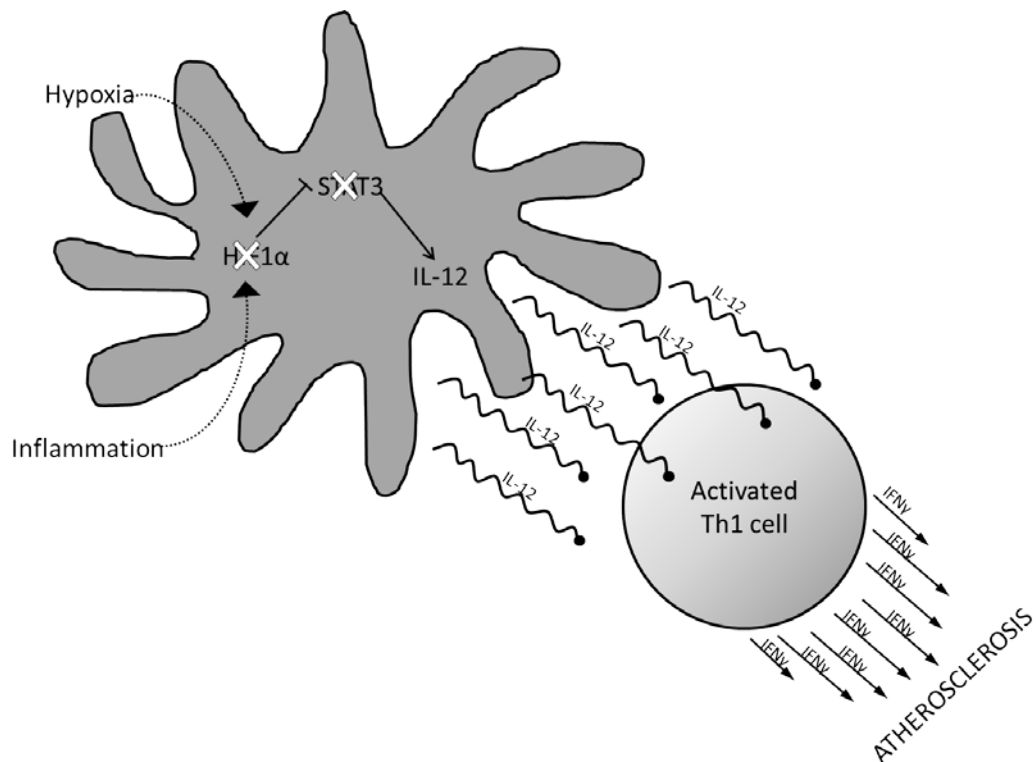


Figure 5.1 A model explaining molecular pathways in the HIF1 α deficient DCs that affect T-cell polarization and hence atherosclerosis

These findings for the first time demonstrate that HIF1 α , though dispensable under homeostatic conditions, serves to antagonize aberrant or exuberant DC activation and T_h1 polarization during atherogenesis in *Ldlr*^{-/-} mice and suppresses disease progression by directly binding to the STAT3 promoter and increasing its cellular reserves and further inhibiting IL-12 secretion of DCs (**Figure 5.2**). These conclusions offer unique insight into the function of HIF1 α in DCs, and provide the first evidence that this transcription factor is of paramount importance in restraining DC-driven T-cell activation and atherosclerosis, substantiating the critical role of DCs in controlling immune mechanisms that drive disease development.

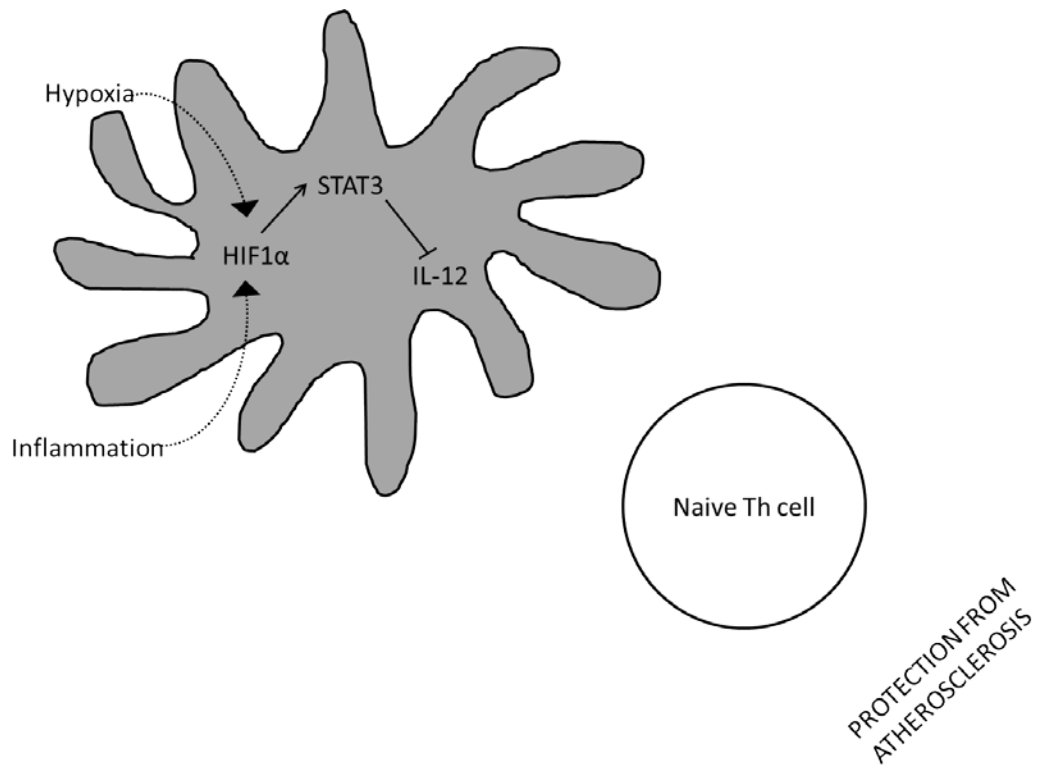


Figure 5.2 HIF1 α restrains inflammation and atherosclerosis by stimulating expression of STAT3 which inhibits IL-12 expression and therefore prevents aberrant polarization of T cells to the T_h1 phenotype, thus protecting from atherosclerosis.

6. REFERENCES

- 1 Steinman, R. M. & Cohn, Z. A. Identification of a novel cell type in peripheral lymphoid organs of mice. I. Morphology, quantitation, tissue distribution. *The Journal of experimental medicine* 137, 1142-1162 (1973).
- 2 Steinman, R. M. & Nussenzweig, M. C. Dendritic cells: features and functions. *Immunological reviews* 53, 127-147 (1980).
- 3 Wu, L. & Liu, Y. J. Development of dendritic-cell lineages. *Immunity* 26, 741-750, doi:10.1016/j.immuni.2007.06.006 (2007).
- 4 Inaba, K. *et al.* Granulocytes, macrophages, and dendritic cells arise from a common major histocompatibility complex class II-negative progenitor in mouse bone marrow. *Proceedings of the National Academy of Sciences of the United States of America* 90, 3038-3042 (1993).
- 5 Manz, M. G. *et al.* Dendritic cell development from common myeloid progenitors. *Annals of the New York Academy of Sciences* 938, 167-173; discussion 173-164 (2001).
- 6 Inaba, K. *et al.* Generation of large numbers of dendritic cells from mouse bone marrow cultures supplemented with granulocyte/macrophage colony-stimulating factor. *The Journal of experimental medicine* 176, 1693-1702 (1992).
- 7 Lutz, M. B. *et al.* An advanced culture method for generating large quantities of highly pure dendritic cells from mouse bone marrow. *Journal of immunological methods* 223, 77-92 (1999).
- 8 Randolph, G. J., Inaba, K., Robbiani, D. F., Steinman, R. M. & Muller, W. A. Differentiation of phagocytic monocytes into lymph node dendritic cells in vivo. *Immunity* 11, 753-761 (1999).
- 9 Chapuis, F. *et al.* Differentiation of human dendritic cells from monocytes in vitro. *European journal of immunology* 27, 431-441, doi:10.1002/eji.1830270213 (1997).
- 10 Kiertcher, S. M. & Roth, M. D. Human CD14⁺ leukocytes acquire the phenotype and function of antigen-presenting dendritic cells when cultured in GM-CSF and IL-4. *Journal of leukocyte biology* 59, 208-218 (1996).
- 11 Leon, B. *et al.* Dendritic cell differentiation potential of mouse monocytes: monocytes represent immediate precursors of CD8⁻ and CD8⁺ splenic dendritic cells. *Blood* 103, 2668-2676, doi:10.1182/blood-2003-01-0286 (2004).
- 12 Wu, L. *et al.* Development of thymic and splenic dendritic cell populations from different hemopoietic precursors. *Blood* 98, 3376-3382 (2001).

- 13 Manz, M. G., Traver, D., Miyamoto, T., Weissman, I. L. & Akashi, K. Dendritic cell potentials of early lymphoid and myeloid progenitors. *Blood* 97, 3333-3341 (2001).
- 14 Dakic, A. & Wu, L. Hemopoietic precursors and development of dendritic cell populations. *Leukemia & lymphoma* 44, 1469-1475, doi:10.3109/10428190309178766 (2003).
- 15 Steinman, R. M., Pack, M. & Inaba, K. Dendritic cells in the T-cell areas of lymphoid organs. *Immunological reviews* 156, 25-37 (1997).
- 16 Shortman, K. & Liu, Y. J. Mouse and human dendritic cell subtypes. *Nature reviews. Immunology* 2, 151-161, doi:10.1038/nri746 (2002).
- 17 Ziegler-Heitbrock, L. *et al.* Nomenclature of monocytes and dendritic cells in blood. *Blood* 116, e74-80, doi:10.1182/blood-2010-02-258558 (2010).
- 18 Naik, S. H. Demystifying the development of dendritic cell subtypes, a little. *Immunology and cell biology* 86, 439-452, doi:10.1038/icb.2008.28 (2008).
- 19 Idoyaga, J. *et al.* Specialized role of migratory dendritic cells in peripheral tolerance induction. *The Journal of clinical investigation* 123, 844-854, doi:10.1172/JCI65260 (2013).
- 20 Colonna, M., Trinchieri, G. & Liu, Y. J. Plasmacytoid dendritic cells in immunity. *Nature immunology* 5, 1219-1226, doi:10.1038/ni1141 (2004).
- 21 Kushwah, R. & Hu, J. Complexity of dendritic cell subsets and their function in the host immune system. *Immunology* 133, 409-419, doi:10.1111/j.1365-2567.2011.03457.x (2011).
- 22 Wu, L. & Dakic, A. Development of dendritic cell system. *Cellular & molecular immunology* 1, 112-118 (2004).
- 23 Drutman, S. B., Kendall, J. C. & Trombetta, E. S. Inflammatory spleen monocytes can upregulate CD11c expression without converting into dendritic cells. *Journal of immunology* 188, 3603-3610, doi:10.4049/jimmunol.1102741 (2012).
- 24 Wu, H. *et al.* Functional role of CD11c⁺ monocytes in atherogenesis associated with hypercholesterolemia. *Circulation* 119, 2708-2717, doi:10.1161/CIRCULATIONAHA.108.823740 (2009).
- 25 Geissmann, F., Gordon, S., Hume, D. A., Mowat, A. M. & Randolph, G. J. Unravelling mononuclear phagocyte heterogeneity. *Nature reviews. Immunology* 10, 453-460, doi:10.1038/nri2784 (2010).
- 26 Caton, M. L., Smith-Raska, M. R. & Reizis, B. Notch-RBP-J signaling controls the homeostasis of CD8⁻ dendritic cells in the spleen. *The Journal of experimental medicine* 204, 1653-1664, doi:10.1084/jem.20062648 (2007).

- 27 Birnberg, T. *et al.* Lack of conventional dendritic cells is compatible with normal development and T cell homeostasis, but causes myeloid proliferative syndrome. *Immunity* 29, 986-997, doi:10.1016/j.immuni.2008.10.012 (2008).
- 28 Hou, B., Reizis, B. & DeFranco, A. L. Toll-like receptors activate innate and adaptive immunity by using dendritic cell-intrinsic and -extrinsic mechanisms. *Immunity* 29, 272-282, doi:10.1016/j.immuni.2008.05.016 (2008).
- 29 Ohnmacht, C. *et al.* Constitutive ablation of dendritic cells breaks self-tolerance of CD4 T cells and results in spontaneous fatal autoimmunity. *The Journal of experimental medicine* 206, 549-559, doi:10.1084/jem.20082394 (2009).
- 30 Inaba, K. *et al.* Efficient presentation of phagocytosed cellular fragments on the major histocompatibility complex class II products of dendritic cells. *The Journal of experimental medicine* 188, 2163-2173 (1998).
- 31 Ardavin, C., Wu, L., Ferrero, I. & Shortman, K. Mouse thymic dendritic cell subpopulations. *Immunology letters* 38, 19-25 (1993).
- 32 Ardavin, C., Wu, L., Li, C. L. & Shortman, K. Thymic dendritic cells and T cells develop simultaneously in the thymus from a common precursor population. *Nature* 362, 761-763, doi:10.1038/362761a0 (1993).
- 33 Suss, G. & Shortman, K. A subclass of dendritic cells kills CD4 T cells via Fas/Fas-ligand-induced apoptosis. *The Journal of experimental medicine* 183, 1789-1796 (1996).
- 34 Shortman, K. & Heath, W. R. Immunity or tolerance? That is the question for dendritic cells. *Nature immunology* 2, 988-989, doi:10.1038/ni1101-988 (2001).
- 35 Steinman, R. M., Turley, S., Mellman, I. & Inaba, K. The induction of tolerance by dendritic cells that have captured apoptotic cells. *The Journal of experimental medicine* 191, 411-416 (2000).
- 36 Albert, M. L., Jegathesan, M. & Darnell, R. B. Dendritic cell maturation is required for the cross-tolerization of CD8+ T cells. *Nature immunology* 2, 1010-1017, doi:10.1038/ni722 (2001).
- 37 Villadangos, J. A. Presentation of antigens by MHC class II molecules: getting the most out of them. *Molecular immunology* 38, 329-346 (2001).
- 38 Mellman, I. & Steinman, R. M. Dendritic cells: specialized and regulated antigen processing machines. *Cell* 106, 255-258 (2001).
- 39 Steinman, R. M. The dendritic cell system and its role in immunogenicity. *Annual review of immunology* 9, 271-296, doi:10.1146/annurev.iy.09.040191.001415 (1991).

- 40 Steinman, R. M. & Hemmi, H. Dendritic cells: translating innate to adaptive immunity. *Current topics in microbiology and immunology* 311, 17-58 (2006).
- 41 Merad, M., Sathe, P., Helft, J., Miller, J. & Mortha, A. The dendritic cell lineage: ontogeny and function of dendritic cells and their subsets in the steady state and the inflamed setting. *Annual review of immunology* 31, 563-604, doi:10.1146/annurev-immunol-020711-074950 (2013).
- 42 Clark, G. J. *et al.* The role of dendritic cells in the innate immune system. *Microbes and infection / Institut Pasteur* 2, 257-272 (2000).
- 43 O'Shea, J. J. & Paul, W. E. Mechanisms underlying lineage commitment and plasticity of helper CD4+ T cells. *Science* 327, 1098-1102, doi:10.1126/science.1178334 (2010).
- 44 Moser, M. & Murphy, K. M. Dendritic cell regulation of TH1-TH2 development. *Nature immunology* 1, 199-205, doi:10.1038/79734 (2000).
- 45 Maldonado-Lopez, R. & Moser, M. Dendritic cell subsets and the regulation of Th1/Th2 responses. *Seminars in immunology* 13, 275-282, doi:10.1006/smim.2001.0323 (2001).
- 46 Macatonia, S. E. *et al.* Dendritic cells produce IL-12 and direct the development of Th1 cells from naive CD4+ T cells. *Journal of immunology* 154, 5071-5079 (1995).
- 47 Romagnani, S., Manetti, R., Annunziato, F. & Maggi, E. Role of IL12 in the development of human Th1 type cells. *Research in immunology* 146, 452-460 (1995).
- 48 Afkarian, M. *et al.* T-bet is a STAT1-induced regulator of IL-12R expression in naive CD4+ T cells. *Nature immunology* 3, 549-557, doi:10.1038/ni794 (2002).
- 49 Murphy, K. M. *et al.* Signaling and transcription in T helper development. *Annual review of immunology* 18, 451-494, doi:10.1146/annurev.immunol.18.1.451 (2000).
- 50 Schroder, K., Hertzog, P. J., Ravasi, T. & Hume, D. A. Interferon-gamma: an overview of signals, mechanisms and functions. *Journal of leukocyte biology* 75, 163-189, doi:10.1189/jlb.0603252 (2004).
- 51 Rosenzweig, S. D. & Holland, S. M. Defects in the interferon-gamma and interleukin-12 pathways. *Immunological reviews* 203, 38-47, doi:10.1111/j.0105-2896.2005.00227.x (2005).
- 52 Iwasaki, A. & Kelsall, B. L. Unique functions of CD11b+, CD8 alpha+, and double-negative Peyer's patch dendritic cells. *Journal of immunology* 166, 4884-4890 (2001).

- 53 Rincon, M., Anguita, J., Nakamura, T., Fikrig, E. & Flavell, R. A. Interleukin (IL)-6 directs the differentiation of IL-4-producing CD4+ T cells. *The Journal of experimental medicine* 185, 461-469 (1997).
- 54 Schmitz, J. *et al.* Induction of interleukin 4 (IL-4) expression in T helper (Th) cells is not dependent on IL-4 from non-Th cells. *The Journal of experimental medicine* 179, 1349-1353 (1994).
- 55 De Becker, G. *et al.* Regulation of T helper cell differentiation in vivo by soluble and membrane proteins provided by antigen-presenting cells. *European journal of immunology* 28, 3161-3171, doi:10.1002/(SICI)1521-4141(199810)28:10<3161::AID-IMMU3161>3.0.CO;2-Q (1998).
- 56 Ranger, A. M., Das, M. P., Kuchroo, V. K. & Glimcher, L. H. B7-2 (CD86) is essential for the development of IL-4-producing T cells. *International immunology* 8, 1549-1560 (1996).
- 57 Kidd, P. Th1/Th2 balance: the hypothesis, its limitations, and implications for health and disease. *Alternative medicine review : a journal of clinical therapeutic* 8, 223-246 (2003).
- 58 Kimura, A. & Kishimoto, T. IL-6: regulator of Treg/Th17 balance. *European journal of immunology* 40, 1830-1835, doi:10.1002/eji.201040391 (2010).
- 59 Bettelli, E. *et al.* Reciprocal developmental pathways for the generation of pathogenic effector TH17 and regulatory T cells. *Nature* 441, 235-238, doi:10.1038/nature04753 (2006).
- 60 Korn, T., Bettelli, E., Oukka, M. & Kuchroo, V. K. IL-17 and Th17 Cells. *Annual review of immunology* 27, 485-517, doi:10.1146/annurev.immunol.021908.132710 (2009).
- 61 Peters, A., Lee, Y. & Kuchroo, V. K. The many faces of Th17 cells. *Current opinion in immunology* 23, 702-706, doi:10.1016/j.coi.2011.08.007 (2011).
- 62 Korn, T., Oukka, M., Kuchroo, V. & Bettelli, E. Th17 cells: effector T cells with inflammatory properties. *Seminars in immunology* 19, 362-371, doi:10.1016/j.smim.2007.10.007 (2007).
- 63 Wilke, C. M., Bishop, K., Fox, D. & Zou, W. Deciphering the role of Th17 cells in human disease. *Trends in immunology* 32, 603-611, doi:10.1016/j.it.2011.08.003 (2011).
- 64 Cretney, E., Kallies, A. & Nutt, S. L. Differentiation and function of Foxp3(+) effector regulatory T cells. *Trends in immunology* 34, 74-80, doi:10.1016/j.it.2012.11.002 (2013).
- 65 Vignali, D. A., Collison, L. W. & Workman, C. J. How regulatory T cells work. *Nature reviews. Immunology* 8, 523-532, doi:10.1038/nri2343 (2008).

- 66 Cederbom, L., Hall, H. & Ivars, F. CD4+CD25+ regulatory T cells down-regulate co-stimulatory molecules on antigen-presenting cells. *European journal of immunology* 30, 1538-1543, doi:10.1002/1521-4141(200006)30:6<1538::AID-IMMU1538>3.0.CO;2-X (2000).
- 67 Shevach, E. M. Biological functions of regulatory T cells. *Advances in immunology* 112, 137-176, doi:10.1016/B978-0-12-387827-4.00004-8 (2011).
- 68 Randolph, G. J., Ochando, J. & Partida-Sanchez, S. Migration of dendritic cell subsets and their precursors. *Annual review of immunology* 26, 293-316, doi:10.1146/annurev.immunol.26.021607.090254 (2008).
- 69 Sozzani, S., Allavena, P., Vecchi, A. & Mantovani, A. Chemokines and dendritic cell traffic. *Journal of clinical immunology* 20, 151-160 (2000).
- 70 Randolph, G. J., Sanchez-Schmitz, G. & Angeli, V. Factors and signals that govern the migration of dendritic cells via lymphatics: recent advances. *Springer seminars in immunopathology* 26, 273-287, doi:10.1007/s00281-004-0168-0 (2005).
- 71 Forster, R. *et al.* CCR7 coordinates the primary immune response by establishing functional microenvironments in secondary lymphoid organs. *Cell* 99, 23-33 (1999).
- 72 Hansson, G. K., Robertson, A. K. & Soderberg-Naucler, C. Inflammation and atherosclerosis. *Annual review of pathology* 1, 297-329, doi:10.1146/annurev.pathol.1.110304.100100 (2006).
- 73 Hansson, G. K. & Libby, P. The immune response in atherosclerosis: a double-edged sword. *Nature reviews. Immunology* 6, 508-519, doi:10.1038/nri1882 (2006).
- 74 Dahlof, B. Cardiovascular disease risk factors: epidemiology and risk assessment. *The American journal of cardiology* 105, 3A-9A, doi:10.1016/j.amjcard.2009.10.007 (2010).
- 75 Ross, R. Atherosclerosis--an inflammatory disease. *The New England journal of medicine* 340, 115-126, doi:10.1056/NEJM199901143400207 (1999).
- 76 Hansson, G. K. & Hermansson, A. The immune system in atherosclerosis. *Nature immunology* 12, 204-212, doi:10.1038/ni.2001 (2011).
- 77 Weber, C. & Noels, H. Atherosclerosis: current pathogenesis and therapeutic options. *Nature medicine* 17, 1410-1422, doi:10.1038/nm.2538 (2011).
- 78 Ley, K., Miller, Y. I. & Hedrick, C. C. Monocyte and macrophage dynamics during atherogenesis. *Arteriosclerosis, thrombosis, and vascular biology* 31, 1506-1516, doi:10.1161/ATVBAHA.110.221127 (2011).

- 79 Rajavashisth, T. B. *et al.* Induction of endothelial cell expression of granulocyte and macrophage colony-stimulating factors by modified low-density lipoproteins. *Nature* 344, 254-257, doi:10.1038/344254a0 (1990).
- 80 Moore, K. J. & Tabas, I. Macrophages in the pathogenesis of atherosclerosis. *Cell* 145, 341-355, doi:10.1016/j.cell.2011.04.005 (2011).
- 81 Gerrity, R. G. The role of the monocyte in atherogenesis: I. Transition of blood-borne monocytes into foam cells in fatty lesions. *The American journal of pathology* 103, 181-190 (1981).
- 82 Weber, C., Schober, A. & Zernecke, A. Chemokines: key regulators of mononuclear cell recruitment in atherosclerotic vascular disease. *Arteriosclerosis, thrombosis, and vascular biology* 24, 1997-2008, doi:10.1161/01.ATV.0000142812.03840.6f (2004).
- 83 Gerrity, R. G. The role of the monocyte in atherogenesis: II. Migration of foam cells from atherosclerotic lesions. *The American journal of pathology* 103, 191-200 (1981).
- 84 de Villiers, W. J. *et al.* Macrophage phenotype in mice deficient in both macrophage-colony-stimulating factor (op) and apolipoprotein E. *Arteriosclerosis, thrombosis, and vascular biology* 18, 631-640 (1998).
- 85 Qiao, J. H. *et al.* Role of macrophage colony-stimulating factor in atherosclerosis: studies of osteopetrotic mice. *The American journal of pathology* 150, 1687-1699 (1997).
- 86 Bobryshev, Y. V. & Lord, R. S. Ultrastructural recognition of cells with dendritic cell morphology in human aortic intima. Contacting interactions of Vascular Dendritic Cells in athero-resistant and athero-prone areas of the normal aorta. *Archives of histology and cytology* 58, 307-322 (1995).
- 87 Jongstra-Bilen, J. *et al.* Low-grade chronic inflammation in regions of the normal mouse arterial intima predisposed to atherosclerosis. *The Journal of experimental medicine* 203, 2073-2083, doi:10.1084/jem.20060245 (2006).
- 88 Choi, J. H. *et al.* Identification of antigen-presenting dendritic cells in mouse aorta and cardiac valves. *The Journal of experimental medicine* 206, 497-505, doi:10.1084/jem.20082129 (2009).
- 89 Paulson, K. E. *et al.* Resident intimal dendritic cells accumulate lipid and contribute to the initiation of atherosclerosis. *Circulation research* 106, 383-390, doi:10.1161/CIRCRESAHA.109.210781 (2010).
- 90 Packard, R. R. *et al.* CD11c(+) dendritic cells maintain antigen processing, presentation capabilities, and CD4(+) T-cell priming efficacy under

hypercholesterolemic conditions associated with atherosclerosis. *Circulation research* 103, 965-973, doi:10.1161/CIRCRESAHA.108.185793 (2008).

91 Bobryshev, Y. V. Dendritic cells and their involvement in atherosclerosis. *Current opinion in lipidology* 11, 511-517 (2000).

92 Koltsova, E. K. & Ley, K. How dendritic cells shape atherosclerosis. *Trends in immunology* 32, 540-547, doi:10.1016/j.it.2011.07.001 (2011).

93 Randolph, G. J., Beaulieu, S., Lebecque, S., Steinman, R. M. & Muller, W. A. Differentiation of monocytes into dendritic cells in a model of transendothelial trafficking. *Science* 282, 480-483 (1998).

94 Liu, P. *et al.* CX3CR1 deficiency impairs dendritic cell accumulation in arterial intima and reduces atherosclerotic burden. *Arteriosclerosis, thrombosis, and vascular biology* 28, 243-250, doi:10.1161/ATVBAHA.107.158675 (2008).

95 Combadiere, C. *et al.* Combined inhibition of CCL2, CX3CR1, and CCR5 abrogates Ly6C(hi) and Ly6C(lo) monocytois and almost abolishes atherosclerosis in hypercholesterolemic mice. *Circulation* 117, 1649-1657, doi:10.1161/CIRCULATIONAHA.107.745091 (2008).

96 Sun, J. *et al.* Deficiency of antigen-presenting cell invariant chain reduces atherosclerosis in mice. *Circulation* 122, 808-820, doi:10.1161/CIRCULATIONAHA.109.891887 (2010).

97 Alderman, C. J. *et al.* Effects of oxidised low density lipoprotein on dendritic cells: a possible immunoregulatory component of the atherogenic micro-environment? *Cardiovascular research* 55, 806-819 (2002).

98 Nickel, T. *et al.* oxLDL uptake by dendritic cells induces upregulation of scavenger-receptors, maturation and differentiation. *Atherosclerosis* 205, 442-450, doi:10.1016/j.atherosclerosis.2009.01.002 (2009).

99 Han, J. W. *et al.* Vessel wall-embedded dendritic cells induce T-cell autoreactivity and initiate vascular inflammation. *Circulation research* 102, 546-553, doi:10.1161/CIRCRESAHA.107.161653 (2008).

100 Weber, C. *et al.* CCL17-expressing dendritic cells drive atherosclerosis by restraining regulatory T cell homeostasis in mice. *The Journal of clinical investigation* 121, 2898-2910, doi:10.1172/JCI44925 (2011).

101 Choi, J. H. *et al.* Flt3 signaling-dependent dendritic cells protect against atherosclerosis. *Immunity* 35, 819-831, doi:10.1016/j.immuni.2011.09.014 (2011).

102 Habets, K. L. *et al.* Vaccination using oxidized low-density lipoprotein-pulsed dendritic cells reduces atherosclerosis in LDL receptor-deficient mice. *Cardiovascular research* 85, 622-630, doi:10.1093/cvr/cvp338 (2010).

- 103 Stemme, S. *et al.* T lymphocytes from human atherosclerotic plaques recognize oxidized low density lipoprotein. *Proceedings of the National Academy of Sciences of the United States of America* 92, 3893-3897 (1995).
- 104 Uyemura, K. *et al.* Cross-regulatory roles of interleukin (IL)-12 and IL-10 in atherosclerosis. *The Journal of clinical investigation* 97, 2130-2138, doi:10.1172/JCI118650 (1996).
- 105 Frostegard, J. *et al.* Cytokine expression in advanced human atherosclerotic plaques: dominance of pro-inflammatory (Th1) and macrophage-stimulating cytokines. *Atherosclerosis* 145, 33-43 (1999).
- 106 Gupta, S. *et al.* IFN-gamma potentiates atherosclerosis in ApoE knock-out mice. *The Journal of clinical investigation* 99, 2752-2761, doi:10.1172/JCI119465 (1997).
- 107 Buono, C. *et al.* Influence of interferon-gamma on the extent and phenotype of diet-induced atherosclerosis in the LDLR-deficient mouse. *Arteriosclerosis, thrombosis, and vascular biology* 23, 454-460, doi:10.1161/01.ATV.0000059419.11002.6E (2003).
- 108 Whitman, S. C., Ravisankar, P., Elam, H. & Daugherty, A. Exogenous interferon-gamma enhances atherosclerosis in apolipoprotein E^{-/-} mice. *The American journal of pathology* 157, 1819-1824 (2000).
- 109 Davenport, P. & Tipping, P. G. The role of interleukin-4 and interleukin-12 in the progression of atherosclerosis in apolipoprotein E-deficient mice. *The American journal of pathology* 163, 1117-1125, doi:10.1016/S0002-9440(10)63471-2 (2003).
- 110 Hauer, A. D. *et al.* Blockade of interleukin-12 function by protein vaccination attenuates atherosclerosis. *Circulation* 112, 1054-1062, doi:10.1161/CIRCULATIONAHA.104.533463 (2005).
- 111 Lee, T. S., Yen, H. C., Pan, C. C. & Chau, L. Y. The role of interleukin 12 in the development of atherosclerosis in ApoE-deficient mice. *Arteriosclerosis, thrombosis, and vascular biology* 19, 734-742 (1999).
- 112 Buono, C. *et al.* T-bet deficiency reduces atherosclerosis and alters plaque antigen-specific immune responses. *Proceedings of the National Academy of Sciences of the United States of America* 102, 1596-1601, doi:10.1073/pnas.0409015102 (2005).
- 113 Elhage, R. *et al.* Reduced atherosclerosis in interleukin-18 deficient apolipoprotein E-knockout mice. *Cardiovascular research* 59, 234-240 (2003).
- 114 Branen, L. *et al.* Inhibition of tumor necrosis factor-alpha reduces atherosclerosis in apolipoprotein E knockout mice. *Arteriosclerosis, thrombosis, and vascular biology* 24, 2137-2142, doi:10.1161/01.ATV.0000143933.20616.1b (2004).

- 115 King, V. L., Cassis, L. A. & Daugherty, A. Interleukin-4 does not influence development of hypercholesterolemia or angiotensin II-induced atherosclerotic lesions in mice. *The American journal of pathology* 171, 2040-2047, doi:10.2353/ajpath.2007.060857 (2007).
- 116 King, V. L., Szilvassy, S. J. & Daugherty, A. Interleukin-4 deficiency decreases atherosclerotic lesion formation in a site-specific manner in female LDL receptor^{-/-} mice. *Arteriosclerosis, thrombosis, and vascular biology* 22, 456-461 (2002).
- 117 Taleb, S., Tedgui, A. & Mallat, Z. Interleukin-17: friend or foe in atherosclerosis? *Current opinion in lipidology* 21, 404-408, doi:10.1097/MOL.0b013e32833dc7f9 (2010).
- 118 de Boer, O. J. *et al.* Differential expression of interleukin-17 family cytokines in intact and complicated human atherosclerotic plaques. *The Journal of pathology* 220, 499-508, doi:10.1002/path.2667 (2010).
- 119 Eid, R. E. *et al.* Interleukin-17 and interferon-gamma are produced concomitantly by human coronary artery-infiltrating T cells and act synergistically on vascular smooth muscle cells. *Circulation* 119, 1424-1432, doi:10.1161/CIRCULATIONAHA.108.827618 (2009).
- 120 Erbel, C. *et al.* Inhibition of IL-17A attenuates atherosclerotic lesion development in apoE-deficient mice. *Journal of immunology* 183, 8167-8175, doi:10.4049/jimmunol.0901126 (2009).
- 121 van Es, T. *et al.* Attenuated atherosclerosis upon IL-17R signaling disruption in LDLr deficient mice. *Biochemical and biophysical research communications* 388, 261-265, doi:10.1016/j.bbrc.2009.07.152 (2009).
- 122 Smith, E. *et al.* Blockade of interleukin-17A results in reduced atherosclerosis in apolipoprotein E-deficient mice. *Circulation* 121, 1746-1755, doi:10.1161/CIRCULATIONAHA.109.924886 (2010).
- 123 Gao, Q. *et al.* A critical function of Th17 proinflammatory cells in the development of atherosclerotic plaque in mice. *Journal of immunology* 185, 5820-5827, doi:10.4049/jimmunol.1000116 (2010).
- 124 Taleb, S. *et al.* Loss of SOCS3 expression in T cells reveals a regulatory role for interleukin-17 in atherosclerosis. *The Journal of experimental medicine* 206, 2067-2077, doi:10.1084/jem.20090545 (2009).
- 125 Cheng, X. *et al.* Inhibition of IL-17A in atherosclerosis. *Atherosclerosis* 215, 471-474, doi:10.1016/j.atherosclerosis.2010.12.034 (2011).
- 126 Madhur, M. S. *et al.* Role of interleukin 17 in inflammation, atherosclerosis, and vascular function in apolipoprotein e-deficient mice. *Arteriosclerosis, thrombosis, and vascular biology* 31, 1565-1572, doi:10.1161/ATVBAHA.111.227629 (2011).

- 127 de Boer, O. J., van der Meer, J. J., Teeling, P., van der Loos, C. M. & van der Wal, A. C. Low numbers of FOXP3 positive regulatory T cells are present in all developmental stages of human atherosclerotic lesions. *PloS one* 2, e779, doi:10.1371/journal.pone.0000779 (2007).
- 128 Ait-Oufella, H. *et al.* Natural regulatory T cells control the development of atherosclerosis in mice. *Nature medicine* 12, 178-180, doi:10.1038/nm1343 (2006).
- 129 Mor, A. *et al.* Role of naturally occurring CD4⁺ CD25⁺ regulatory T cells in experimental atherosclerosis. *Arteriosclerosis, thrombosis, and vascular biology* 27, 893-900, doi:10.1161/01.ATV.0000259365.31469.89 (2007).
- 130 Getz, G. S. & Reardon, C. A. Animal models of atherosclerosis. *Arteriosclerosis, thrombosis, and vascular biology* 32, 1104-1115, doi:10.1161/ATVBAHA.111.237693 (2012).
- 131 Piedrahita, J. A., Zhang, S. H., Hagan, J. R., Oliver, P. M. & Maeda, N. Generation of mice carrying a mutant apolipoprotein E gene inactivated by gene targeting in embryonic stem cells. *Proceedings of the National Academy of Sciences of the United States of America* 89, 4471-4475 (1992).
- 132 Plump, A. S. *et al.* Severe hypercholesterolemia and atherosclerosis in apolipoprotein E-deficient mice created by homologous recombination in ES cells. *Cell* 71, 343-353 (1992).
- 133 Jawien, J., Nastalek, P. & Korbut, R. Mouse models of experimental atherosclerosis. *Journal of physiology and pharmacology : an official journal of the Polish Physiological Society* 55, 503-517 (2004).
- 134 Ishibashi, S., Goldstein, J. L., Brown, M. S., Herz, J. & Burns, D. K. Massive xanthomatosis and atherosclerosis in cholesterol-fed low density lipoprotein receptor-negative mice. *The Journal of clinical investigation* 93, 1885-1893, doi:10.1172/JCI117179 (1994).
- 135 Daugherty, A. Mouse models of atherosclerosis. *The American journal of the medical sciences* 323, 3-10 (2002).
- 136 Veniant, M. M., Withycombe, S. & Young, S. G. Lipoprotein size and atherosclerosis susceptibility in Apoe(-/-) and Ldlr(-/-) mice. *Arteriosclerosis, thrombosis, and vascular biology* 21, 1567-1570 (2001).
- 137 Semenza, G. L. Life with oxygen. *Science* 318, 62-64, doi:10.1126/science.1147949 (2007).
- 138 Semenza, G. L. Vascular responses to hypoxia and ischemia. *Arteriosclerosis, thrombosis, and vascular biology* 30, 648-652, doi:10.1161/ATVBAHA.108.181644 (2010).

- 139 Nizet, V. & Johnson, R. S. Interdependence of hypoxic and innate immune responses. *Nature reviews. Immunology* 9, 609-617, doi:10.1038/nri2607 (2009).
- 140 Semenza, G. L. Hypoxia-inducible factor 1: oxygen homeostasis and disease pathophysiology. *Trends in molecular medicine* 7, 345-350 (2001).
- 141 Cummins, E. P. & Taylor, C. T. Hypoxia-responsive transcription factors. *Pflugers Archiv : European journal of physiology* 450, 363-371, doi:10.1007/s00424-005-1413-7 (2005).
- 142 Semenza, G. L. & Wang, G. L. A nuclear factor induced by hypoxia via de novo protein synthesis binds to the human erythropoietin gene enhancer at a site required for transcriptional activation. *Molecular and cellular biology* 12, 5447-5454 (1992).
- 143 Wang, G. L., Jiang, B. H., Rue, E. A. & Semenza, G. L. Hypoxia-inducible factor 1 is a basic-helix-loop-helix-PAS heterodimer regulated by cellular O₂ tension. *Proceedings of the National Academy of Sciences of the United States of America* 92, 5510-5514 (1995).
- 144 Mimura, J., Ema, M., Sogawa, K. & Fujii-Kuriyama, Y. Identification of a novel mechanism of regulation of Ah (dioxin) receptor function. *Genes & development* 13, 20-25 (1999).
- 145 Bruick, R. K. & McKnight, S. L. A conserved family of prolyl-4-hydroxylases that modify HIF. *Science* 294, 1337-1340, doi:10.1126/science.1066373 (2001).
- 146 Jaakkola, P. *et al.* Targeting of HIF- α to the von Hippel-Lindau ubiquitylation complex by O₂-regulated prolyl hydroxylation. *Science* 292, 468-472, doi:10.1126/science.1059796 (2001).
- 147 Maxwell, P. & Salnikow, K. HIF-1: an oxygen and metal responsive transcription factor. *Cancer biology & therapy* 3, 29-35 (2004).
- 148 Ke, Q. & Costa, M. Hypoxia-inducible factor-1 (HIF-1). *Molecular pharmacology* 70, 1469-1480, doi:10.1124/mol.106.027029 (2006).
- 149 Iyer, N. V. *et al.* Cellular and developmental control of O₂ homeostasis by hypoxia-inducible factor 1 α . *Genes & development* 12, 149-162 (1998).
- 150 Kotch, L. E., Iyer, N. V., Laughner, E. & Semenza, G. L. Defective vascularization of HIF-1 α -null embryos is not associated with VEGF deficiency but with mesenchymal cell death. *Developmental biology* 209, 254-267, doi:10.1006/dbio.1999.9253 (1999).
- 151 Ryan, H. E., Lo, J. & Johnson, R. S. HIF-1 α is required for solid tumor formation and embryonic vascularization. *The EMBO journal* 17, 3005-3015, doi:10.1093/emboj/17.11.3005 (1998).

- 152 Tian, H., McKnight, S. L. & Russell, D. W. Endothelial PAS domain protein 1 (EPAS1), a transcription factor selectively expressed in endothelial cells. *Genes & development* 11, 72-82 (1997).
- 153 Ema, M. *et al.* A novel bHLH-PAS factor with close sequence similarity to hypoxia-inducible factor 1alpha regulates the VEGF expression and is potentially involved in lung and vascular development. *Proceedings of the National Academy of Sciences of the United States of America* 94, 4273-4278 (1997).
- 154 Gu, Y. Z., Moran, S. M., Hogenesch, J. B., Wartman, L. & Bradfield, C. A. Molecular characterization and chromosomal localization of a third alpha-class hypoxia inducible factor subunit, HIF3alpha. *Gene expression* 7, 205-213 (1998).
- 155 Florczyk, U. *et al.* Opposite effects of HIF-1alpha and HIF-2alpha on the regulation of IL-8 expression in endothelial cells. *Free radical biology & medicine* 51, 1882-1892, doi:10.1016/j.freeradbiomed.2011.08.023 (2011).
- 156 Loboda, A., Jozkowicz, A. & Dulak, J. HIF-1 versus HIF-2--is one more important than the other? *Vascular pharmacology* 56, 245-251, doi:10.1016/j.vph.2012.02.006 (2012).
- 157 Patten, D. A. *et al.* Hypoxia-inducible factor-1 activation in nonhypoxic conditions: the essential role of mitochondrial-derived reactive oxygen species. *Molecular biology of the cell* 21, 3247-3257, doi:10.1091/mbc.E10-01-0025 (2010).
- 158 Richard, D. E., Berra, E. & Pouyssegur, J. Nonhypoxic pathway mediates the induction of hypoxia-inducible factor 1alpha in vascular smooth muscle cells. *The Journal of biological chemistry* 275, 26765-26771, doi:10.1074/jbc.M003325200 (2000).
- 159 Liu, X. H. *et al.* Prostaglandin E2 induces hypoxia-inducible factor-1alpha stabilization and nuclear localization in a human prostate cancer cell line. *The Journal of biological chemistry* 277, 50081-50086, doi:10.1074/jbc.M201095200 (2002).
- 160 Treins, C., Giorgetti-Peraldi, S., Murdaca, J., Semenza, G. L. & Van Obberghen, E. Insulin stimulates hypoxia-inducible factor 1 through a phosphatidylinositol 3-kinase/target of rapamycin-dependent signaling pathway. *The Journal of biological chemistry* 277, 27975-27981, doi:10.1074/jbc.M204152200 (2002).
- 161 Feldser, D. *et al.* Reciprocal positive regulation of hypoxia-inducible factor 1alpha and insulin-like growth factor 2. *Cancer research* 59, 3915-3918 (1999).
- 162 Albina, J. E. *et al.* HIF-1 expression in healing wounds: HIF-1alpha induction in primary inflammatory cells by TNF-alpha. *American journal of physiology. Cell physiology* 281, C1971-1977 (2001).

- 163 Hellwig-Burgel, T., Rutkowski, K., Metzen, E., Fandrey, J. & Jelkmann, W. Interleukin-1beta and tumor necrosis factor-alpha stimulate DNA binding of hypoxia-inducible factor-1. *Blood* 94, 1561-1567 (1999).
- 164 Jung, Y. *et al.* Hypoxia-inducible factor induction by tumour necrosis factor in normoxic cells requires receptor-interacting protein-dependent nuclear factor kappa B activation. *The Biochemical journal* 370, 1011-1017, doi:10.1042/BJ20021279 (2003).
- 165 Sandau, K. B., Zhou, J., Kietzmann, T. & Brune, B. Regulation of the hypoxia-inducible factor 1alpha by the inflammatory mediators nitric oxide and tumor necrosis factor-alpha in contrast to desferroxamine and phenylarsine oxide. *The Journal of biological chemistry* 276, 39805-39811, doi:10.1074/jbc.M107689200 (2001).
- 166 Scharte, M., Han, X., Bertges, D. J., Fink, M. P. & Delude, R. L. Cytokines induce HIF-1 DNA binding and the expression of HIF-1-dependent genes in cultured rat enterocytes. *American journal of physiology. Gastrointestinal and liver physiology* 284, G373-384, doi:10.1152/ajpgi.00076.2002 (2003).
- 167 Haddad, J. J. & Land, S. C. A non-hypoxic, ROS-sensitive pathway mediates TNF-alpha-dependent regulation of HIF-1alpha. *FEBS letters* 505, 269-274 (2001).
- 168 Thornton, R. D. *et al.* Interleukin 1 induces hypoxia-inducible factor 1 in human gingival and synovial fibroblasts. *The Biochemical journal* 350 Pt 1, 307-312 (2000).
- 169 Li, J. P. *et al.* Lipopolysaccharide and hypoxia-induced HIF-1 activation in human gingival fibroblasts. *Journal of periodontology* 83, 816-824, doi:10.1902/jop.2011.110458 (2012).
- 170 Blouin, C. C., Page, E. L., Soucy, G. M. & Richard, D. E. Hypoxic gene activation by lipopolysaccharide in macrophages: implication of hypoxia-inducible factor 1alpha. *Blood* 103, 1124-1130, doi:10.1182/blood-2003-07-2427 (2004).
- 171 Frede, S., Stockmann, C., Freitag, P. & Fandrey, J. Bacterial lipopolysaccharide induces HIF-1 activation in human monocytes via p44/42 MAPK and NF-kappaB. *The Biochemical journal* 396, 517-527, doi:10.1042/BJ20051839 (2006).
- 172 van Uden, P., Kenneth, N. S. & Rocha, S. Regulation of hypoxia-inducible factor-1alpha by NF-kappaB. *The Biochemical journal* 412, 477-484, doi:10.1042/BJ20080476 (2008).
- 173 Kojima, H. *et al.* Abnormal B lymphocyte development and autoimmunity in hypoxia-inducible factor 1alpha -deficient chimeric mice. *Proceedings of the National Academy of Sciences of the United States of America* 99, 2170-2174, doi:10.1073/pnas.052706699 (2002).

- 174 Kojima, H., Sitkovsky, M. V. & Cascalho, M. HIF-1 alpha deficiency perturbs T and B cell functions. *Current pharmaceutical design* 9, 1827-1832 (2003).
- 175 Thiel, M. *et al.* Targeted deletion of HIF-1alpha gene in T cells prevents their inhibition in hypoxic inflamed tissues and improves septic mice survival. *PLoS one* 2, e853, doi:10.1371/journal.pone.0000853 (2007).
- 176 Lukashev, D. *et al.* Cutting edge: hypoxia-inducible factor 1alpha and its activation-inducible short isoform I.1 negatively regulate functions of CD4+ and CD8+ T lymphocytes. *Journal of immunology* 177, 4962-4965 (2006).
- 177 Higashiyama, M. *et al.* HIF-1 in T cells ameliorated dextran sodium sulfate-induced murine colitis. *Journal of leukocyte biology* 91, 901-909, doi:10.1189/jlb.1011518 (2012).
- 178 Nutsch, K. & Hsieh, C. When T cells run out of breath: the HIF-1alpha story. *Cell* 146, 673-674, doi:10.1016/j.cell.2011.08.018 (2011).
- 179 Dang, E. V. *et al.* Control of T(H)17/T(reg) balance by hypoxia-inducible factor 1. *Cell* 146, 772-784, doi:10.1016/j.cell.2011.07.033 (2011).
- 180 Shi, L. Z. *et al.* HIF1alpha-dependent glycolytic pathway orchestrates a metabolic checkpoint for the differentiation of TH17 and Treg cells. *The Journal of experimental medicine* 208, 1367-1376, doi:10.1084/jem.20110278 (2011).
- 181 Ben-Shoshan, J., Maysel-Auslender, S., Mor, A., Keren, G. & George, J. Hypoxia controls CD4+CD25+ regulatory T-cell homeostasis via hypoxia-inducible factor-1alpha. *European journal of immunology* 38, 2412-2418, doi:10.1002/eji.200838318 (2008).
- 182 Clambey, E. T. *et al.* Hypoxia-inducible factor-1 alpha-dependent induction of FoxP3 drives regulatory T-cell abundance and function during inflammatory hypoxia of the mucosa. *Proceedings of the National Academy of Sciences of the United States of America* 109, E2784-2793, doi:10.1073/pnas.1202366109 (2012).
- 183 Imtiyaz, H. Z. & Simon, M. C. Hypoxia-inducible factors as essential regulators of inflammation. *Current topics in microbiology and immunology* 345, 105-120, doi:10.1007/82_2010_74 (2010).
- 184 Cramer, T. *et al.* HIF-1alpha is essential for myeloid cell-mediated inflammation. *Cell* 112, 645-657 (2003).
- 185 Peyssonnaud, C. *et al.* Cutting edge: Essential role of hypoxia inducible factor-1alpha in development of lipopolysaccharide-induced sepsis. *Journal of immunology* 178, 7516-7519 (2007).
- 186 Peyssonnaud, C. *et al.* HIF-1alpha expression regulates the bactericidal capacity of phagocytes. *The Journal of clinical investigation* 115, 1806-1815, doi:10.1172/JCI23865 (2005).

- 187 Kuhlicke, J., Frick, J. S., Morote-Garcia, J. C., Rosenberger, P. & Eltzschig, H. K. Hypoxia inducible factor (HIF)-1 coordinates induction of Toll-like receptors TLR2 and TLR6 during hypoxia. *PLoS one* 2, e1364, doi:10.1371/journal.pone.0001364 (2007).
- 188 Anand, R. J. *et al.* Hypoxia causes an increase in phagocytosis by macrophages in a HIF-1alpha-dependent manner. *Journal of leukocyte biology* 82, 1257-1265, doi:10.1189/jlb.0307195 (2007).
- 189 Kong, T., Eltzschig, H. K., Karhausen, J., Colgan, S. P. & Shelley, C. S. Leukocyte adhesion during hypoxia is mediated by HIF-1-dependent induction of beta2 integrin gene expression. *Proceedings of the National Academy of Sciences of the United States of America* 101, 10440-10445, doi:10.1073/pnas.0401339101 (2004).
- 190 Walmsley, S. R., Cadwallader, K. A. & Chilvers, E. R. The role of HIF-1alpha in myeloid cell inflammation. *Trends in immunology* 26, 434-439, doi:10.1016/j.it.2005.06.007 (2005).
- 191 Walmsley, S. R. *et al.* Neutrophils from patients with heterozygous germline mutations in the von Hippel Lindau protein (pVHL) display delayed apoptosis and enhanced bacterial phagocytosis. *Blood* 108, 3176-3178, doi:10.1182/blood-2006-04-018796 (2006).
- 192 Walmsley, S. R. *et al.* Hypoxia-induced neutrophil survival is mediated by HIF-1alpha-dependent NF-kappaB activity. *The Journal of experimental medicine* 201, 105-115, doi:10.1084/jem.20040624 (2005).
- 193 Toussaint, M. *et al.* Myeloid hypoxia-inducible factor 1alpha prevents airway allergy in mice through macrophage-mediated immunoregulation. *Mucosal immunology* 6, 485-497, doi:10.1038/mi.2012.88 (2013).
- 194 Kobayashi, H. *et al.* Myeloid cell-derived hypoxia-inducible factor attenuates inflammation in unilateral ureteral obstruction-induced kidney injury. *Journal of immunology* 188, 5106-5115, doi:10.4049/jimmunol.1103377 (2012).
- 195 Jantsch, J. *et al.* Hypoxia and hypoxia-inducible factor-1 alpha modulate lipopolysaccharide-induced dendritic cell activation and function. *Journal of immunology* 180, 4697-4705 (2008).
- 196 Spirig, R. *et al.* Effects of TLR agonists on the hypoxia-regulated transcription factor HIF-1alpha and dendritic cell maturation under normoxic conditions. *PLoS one* 5, e0010983, doi:10.1371/journal.pone.0010983 (2010).
- 197 Jantsch, J. *et al.* Toll-like receptor activation and hypoxia use distinct signaling pathways to stabilize hypoxia-inducible factor 1alpha (HIF1A) and result in differential HIF1A-dependent gene expression. *Journal of leukocyte biology* 90, 551-562, doi:10.1189/jlb.1210683 (2011).

- 198 Ogino, T. *et al.* Inclusive estimation of complex antigen presentation functions of monocyte-derived dendritic cells differentiated under normoxia and hypoxia conditions. *Cancer immunology, immunotherapy : CII* 61, 409-424, doi:10.1007/s00262-011-1112-5 (2012).
- 199 Mancino, A. *et al.* Divergent effects of hypoxia on dendritic cell functions. *Blood* 112, 3723-3734, doi:10.1182/blood-2008-02-142091 (2008).
- 200 Elia, A. R. *et al.* Human dendritic cells differentiated in hypoxia down-modulate antigen uptake and change their chemokine expression profile. *Journal of leukocyte biology* 84, 1472-1482, doi:10.1189/jlb.0208082 (2008).
- 201 Kohler, T., Reizis, B., Johnson, R. S., Weighardt, H. & Forster, I. Influence of hypoxia-inducible factor 1alpha on dendritic cell differentiation and migration. *European journal of immunology* 42, 1226-1236, doi:10.1002/eji.201142053 (2012).
- 202 Rama, I. *et al.* Hypoxia stimulus: An adaptive immune response during dendritic cell maturation. *Kidney international* 73, 816-825, doi:10.1038/sj.ki.5002792 (2008).
- 203 Ricciardi, A. *et al.* Transcriptome of hypoxic immature dendritic cells: modulation of chemokine/receptor expression. *Molecular cancer research : MCR* 6, 175-185, doi:10.1158/1541-7786.MCR-07-0391 (2008).
- 204 Blengio, F. *et al.* The hypoxic environment reprograms the cytokine/chemokine expression profile of human mature dendritic cells. *Immunobiology* 218, 76-89, doi:10.1016/j.imbio.2012.02.002 (2013).
- 205 Bosco, M. C. & Varesio, L. Dendritic cell reprogramming by the hypoxic environment. *Immunobiology* 217, 1241-1249, doi:10.1016/j.imbio.2012.07.023 (2012).
- 206 Wang, Q. *et al.* Reoxygenation of hypoxia-differentiated dendritic cells induces Th1 and Th17 cell differentiation. *Molecular immunology* 47, 922-931, doi:10.1016/j.molimm.2009.09.038 (2010).
- 207 Yang, M. *et al.* Hypoxia skews dendritic cells to a T helper type 2-stimulating phenotype and promotes tumour cell migration by dendritic cell-derived osteopontin. *Immunology* 128, e237-249, doi:10.1111/j.1365-2567.2008.02954.x (2009).
- 208 Naldini, A. *et al.* Hypoxia affects dendritic cell survival: role of the hypoxia-inducible factor-1alpha and lipopolysaccharide. *Journal of cellular physiology* 227, 587-595, doi:10.1002/jcp.22761 (2012).
- 209 Forsythe, J. A. *et al.* Activation of vascular endothelial growth factor gene transcription by hypoxia-inducible factor 1. *Molecular and cellular biology* 16, 4604-4613 (1996).

- 210 Ferrara, N. Vascular endothelial growth factor: basic science and clinical progress. *Endocrine reviews* 25, 581-611, doi:10.1210/er.2003-0027 (2004).
- 211 Ferrara, N. Vascular endothelial growth factor. *Arteriosclerosis, thrombosis, and vascular biology* 29, 789-791, doi:10.1161/ATVBAHA.108.179663 (2009).
- 212 Ferrara, N., Gerber, H. P. & LeCouter, J. The biology of VEGF and its receptors. *Nature medicine* 9, 669-676, doi:10.1038/nm0603-669 (2003).
- 213 Belaiba, R. S. *et al.* Hypoxia up-regulates hypoxia-inducible factor-1alpha transcription by involving phosphatidylinositol 3-kinase and nuclear factor kappaB in pulmonary artery smooth muscle cells. *Molecular biology of the cell* 18, 4691-4697, doi:10.1091/mbc.E07-04-0391 (2007).
- 214 Rius, J. *et al.* NF-kappaB links innate immunity to the hypoxic response through transcriptional regulation of HIF-1alpha. *Nature* 453, 807-811, doi:10.1038/nature06905 (2008).
- 215 Cummins, E. P. *et al.* Prolyl hydroxylase-1 negatively regulates IkappaB kinase-beta, giving insight into hypoxia-induced NFkappaB activity. *Proceedings of the National Academy of Sciences of the United States of America* 103, 18154-18159, doi:10.1073/pnas.0602235103 (2006).
- 216 Jeong, H. J. *et al.* Expression of proinflammatory cytokines via HIF-1alpha and NF-kappaB activation on desferrioxamine-stimulated HMC-1 cells. *Biochemical and biophysical research communications* 306, 805-811 (2003).
- 217 Jeong, H. J. *et al.* Activation of hypoxia-inducible factor-1 regulates human histidine decarboxylase expression. *Cellular and molecular life sciences : CMLS* 66, 1309-1319, doi:10.1007/s00018-009-9001-1 (2009).
- 218 Lee, K. S. *et al.* Mast cells can mediate vascular permeability through regulation of the PI3K-HIF-1alpha-VEGF axis. *American journal of respiratory and critical care medicine* 178, 787-797, doi:10.1164/rccm.200801-008OC (2008).
- 219 Zhong, H. *et al.* Overexpression of hypoxia-inducible factor 1alpha in common human cancers and their metastases. *Cancer research* 59, 5830-5835 (1999).
- 220 Talks, K. L. *et al.* The expression and distribution of the hypoxia-inducible factors HIF-1alpha and HIF-2alpha in normal human tissues, cancers, and tumor-associated macrophages. *The American journal of pathology* 157, 411-421 (2000).
- 221 Liao, D. & Johnson, R. S. Hypoxia: a key regulator of angiogenesis in cancer. *Cancer metastasis reviews* 26, 281-290, doi:10.1007/s10555-007-9066-y (2007).
- 222 Semenza, G. L. Targeting HIF-1 for cancer therapy. *Nature reviews. Cancer* 3, 721-732, doi:10.1038/nrc1187 (2003).

- 223 Maxwell, P. H. *et al.* Hypoxia-inducible factor-1 modulates gene expression in solid tumors and influences both angiogenesis and tumor growth. *Proceedings of the National Academy of Sciences of the United States of America* 94, 8104-8109 (1997).
- 224 Semenza, G. L. Hypoxia-inducible factors in physiology and medicine. *Cell* 148, 399-408, doi:10.1016/j.cell.2012.01.021 (2012).
- 225 Smith, T. G. *et al.* Mutation of von Hippel-Lindau tumour suppressor and human cardiopulmonary physiology. *PLoS medicine* 3, e290, doi:10.1371/journal.pmed.0030290 (2006).
- 226 Kilani, M. M., Mohammed, K. A., Nasreen, N., Tepper, R. S. & Antony, V. B. RSV causes HIF-1 α stabilization via NO release in primary bronchial epithelial cells. *Inflammation* 28, 245-251, doi:10.1007/s10753-004-6047-y (2004).
- 227 Hwang, H., Watson, I. R., Der, S. D. & Ohh, M. Loss of VHL confers hypoxia-inducible factor (HIF)-dependent resistance to vesicular stomatitis virus: role of HIF in antiviral response. *Journal of virology* 80, 10712-10723, doi:10.1128/JVI.01014-06 (2006).
- 228 Yoo, Y. G. *et al.* Hepatitis B virus X protein enhances transcriptional activity of hypoxia-inducible factor-1 α through activation of mitogen-activated protein kinase pathway. *The Journal of biological chemistry* 278, 39076-39084, doi:10.1074/jbc.M305101200 (2003).
- 229 Nasimuzzaman, M., Waris, G., Mikolon, D., Stupack, D. G. & Siddiqui, A. Hepatitis C virus stabilizes hypoxia-inducible factor 1 α and stimulates the synthesis of vascular endothelial growth factor. *Journal of virology* 81, 10249-10257, doi:10.1128/JVI.00763-07 (2007).
- 230 Lu, Z. H., Wright, J. D., Belt, B., Cardiff, R. D. & Arbeit, J. M. Hypoxia-inducible factor-1 facilitates cervical cancer progression in human papillomavirus type 16 transgenic mice. *The American journal of pathology* 171, 667-681, doi:10.2353/ajpath.2007.061138 (2007).
- 231 Cai, Q. *et al.* Kaposi's sarcoma-associated herpesvirus latent protein LANA interacts with HIF-1 α to upregulate RTA expression during hypoxia: Latency control under low oxygen conditions. *Journal of virology* 80, 7965-7975, doi:10.1128/JVI.00689-06 (2006).
- 232 Kempf, V. A. *et al.* Activation of hypoxia-inducible factor-1 in bacillary angiomatosis: evidence for a role of hypoxia-inducible factor-1 in bacterial infections. *Circulation* 111, 1054-1062, doi:10.1161/01.CIR.0000155608.07691.B7 (2005).
- 233 Rupp, J. *et al.* Chlamydia pneumoniae directly interferes with HIF-1 α stabilization in human host cells. *Cellular microbiology* 9, 2181-2191, doi:10.1111/j.1462-5822.2007.00948.x (2007).

- 234 Spear, W. *et al.* The host cell transcription factor hypoxia-inducible factor 1 is required for *Toxoplasma gondii* growth and survival at physiological oxygen levels. *Cellular microbiology* 8, 339-352, doi:10.1111/j.1462-5822.2005.00628.x (2006).
- 235 Gao, L., Chen, Q., Zhou, X. & Fan, L. The role of hypoxia-inducible factor 1 in atherosclerosis. *Journal of clinical pathology* 65, 872-876, doi:10.1136/jclinpath-2012-200828 (2012).
- 236 Sluimer, J. C. *et al.* Hypoxia, hypoxia-inducible transcription factor, and macrophages in human atherosclerotic plaques are correlated with intraplaque angiogenesis. *Journal of the American College of Cardiology* 51, 1258-1265, doi:10.1016/j.jacc.2007.12.025 (2008).
- 237 Murdoch, C., Muthana, M. & Lewis, C. E. Hypoxia regulates macrophage functions in inflammation. *Journal of immunology* 175, 6257-6263 (2005).
- 238 Bjornheden, T. & Bondjers, G. Oxygen consumption in aortic tissue from rabbits with diet-induced atherosclerosis. *Arteriosclerosis* 7, 238-247 (1987).
- 239 Jurrus, E. R. & Weiss, H. S. In vitro tissue oxygen tensions in the rabbit aortic arch. *Atherosclerosis* 28, 223-232 (1977).
- 240 Niinikoski, J., Heughan, C. & Hunt, T. K. Oxygen tensions in the aortic wall of normal rabbits. *Atherosclerosis* 17, 353-359 (1973).
- 241 Crawford, D. W. & Krams, D. M. The oxygen environment of the arterial media in early rabbit hypertension. *Experimental and molecular pathology* 49, 215-233 (1988).
- 242 Zempenyi, T., Crawford, D. W. & Cole, M. A. Adaptation to arterial wall hypoxia demonstrated in vivo with oxygen microcathodes. *Atherosclerosis* 76, 173-179 (1989).
- 243 Parathath, S. *et al.* Hypoxia is present in murine atherosclerotic plaques and has multiple adverse effects on macrophage lipid metabolism. *Circulation research* 109, 1141-1152, doi:10.1161/CIRCRESAHA.111.246363 (2011).
- 244 Kurobe, H. *et al.* Role of hypoxia-inducible factor 1alpha in T cells as a negative regulator in development of vascular remodeling. *Arteriosclerosis, thrombosis, and vascular biology* 30, 210-217, doi:10.1161/ATVBAHA.109.192666 (2010).
- 245 Parathath, S., Yang, Y., Mick, S. & Fisher, E. A. Hypoxia in murine atherosclerotic plaques and its adverse effects on macrophages. *Trends in cardiovascular medicine* 23, 80-84, doi:10.1016/j.tcm.2012.09.004 (2013).
- 246 Bjornheden, T., Levin, M., Evaldsson, M. & Wiklund, O. Evidence of hypoxic areas within the arterial wall in vivo. *Arteriosclerosis, thrombosis, and vascular biology* 19, 870-876 (1999).

- 247 Durand, R. E. & Raleigh, J. A. Identification of nonproliferating but viable hypoxic tumor cells in vivo. *Cancer research* 58, 3547-3550 (1998).
- 248 Hulten, L. M. & Levin, M. The role of hypoxia in atherosclerosis. *Current opinion in lipidology* 20, 409-414, doi:10.1097/MOL.0b013e3283307be8 (2009).
- 249 Bostrom, P. *et al.* Hypoxia converts human macrophages into triglyceride-loaded foam cells. *Arteriosclerosis, thrombosis, and vascular biology* 26, 1871-1876, doi:10.1161/01.ATV.0000229665.78997.0b (2006).
- 250 Libby, P. & Folco, E. Tension in the plaque: hypoxia modulates metabolism in atheroma. *Circulation research* 109, 1100-1102, doi:10.1161/RES.0b013e31823bdb84 (2011).
- 251 Vink, A. *et al.* HIF-1 alpha expression is associated with an atheromatous inflammatory plaque phenotype and upregulated in activated macrophages. *Atherosclerosis* 195, e69-75, doi:10.1016/j.atherosclerosis.2007.05.026 (2007).
- 252 Luque, A. *et al.* Overexpression of hypoxia/inflammatory markers in atherosclerotic carotid plaques. *Frontiers in bioscience : a journal and virtual library* 13, 6483-6490 (2008).
- 253 Higashida, T., Kanno, H., Nakano, M., Funakoshi, K. & Yamamoto, I. Expression of hypoxia-inducible angiogenic proteins (hypoxia-inducible factor-1alpha, vascular endothelial growth factor, and E26 transformation-specific-1) and plaque hemorrhage in human carotid atherosclerosis. *Journal of neurosurgery* 109, 83-91, doi:10.3171/JNS/2008/109/7/0083 (2008).
- 254 Karshovska, E. *et al.* Expression of HIF-1alpha in injured arteries controls SDF-1alpha mediated neointima formation in apolipoprotein E deficient mice. *Arteriosclerosis, thrombosis, and vascular biology* 27, 2540-2547, doi:10.1161/ATVBAHA.107.151050 (2007).
- 255 Na, T. Y. *et al.* Positive cross-talk between hypoxia inducible factor-1alpha and liver X receptor alpha induces formation of triglyceride-loaded foam cells. *Arteriosclerosis, thrombosis, and vascular biology* 31, 2949-2956, doi:10.1161/ATVBAHA.111.235788 (2011).
- 256 Jiang, G. *et al.* RNA interference for HIF-1alpha inhibits foam cells formation in vitro. *European journal of pharmacology* 562, 183-190, doi:10.1016/j.ejphar.2007.01.066 (2007).
- 257 Gessi, S. *et al.* Adenosine modulates HIF-1{alpha}, VEGF, IL-8, and foam cell formation in a human model of hypoxic foam cells. *Arteriosclerosis, thrombosis, and vascular biology* 30, 90-97, doi:10.1161/ATVBAHA.109.194902 (2010).

- 258 Ben-Shoshan, J. *et al.* HIF-1alpha overexpression and experimental murine atherosclerosis. *Arteriosclerosis, thrombosis, and vascular biology* 29, 665-670, doi:10.1161/ATVBAHA.108.183319 (2009).
- 259 Sluimer, J. C. & Daemen, M. J. Novel concepts in atherogenesis: angiogenesis and hypoxia in atherosclerosis. *The Journal of pathology* 218, 7-29, doi:10.1002/path.2518 (2009).
- 260 Shatrov, V. A., Sumbayev, V. V., Zhou, J. & Brune, B. Oxidized low-density lipoprotein (oxLDL) triggers hypoxia-inducible factor-1alpha (HIF-1alpha) accumulation via redox-dependent mechanisms. *Blood* 101, 4847-4849, doi:10.1182/blood-2002-09-2711 (2003).
- 261 Poitz, D. M. *et al.* OxLDL and macrophage survival: essential and oxygen-independent involvement of the Hif-pathway. *Basic research in cardiology* 106, 761-772, doi:10.1007/s00395-011-0186-8 (2011).
- 262 Hutter, R. *et al.* Macrophages Transmit Potent Proangiogenic Effects of oxLDL In Vitro and In Vivo Involving HIF-1alpha Activation: a Novel Aspect of Angiogenesis in Atherosclerosis. *Journal of cardiovascular translational research*, doi:10.1007/s12265-013-9469-9 (2013).
- 263 Cartharius, K. *et al.* MatInspector and beyond: promoter analysis based on transcription factor binding sites. *Bioinformatics* 21, 2933-2942, doi:10.1093/bioinformatics/bti473 (2005).
- 264 Watford, W. T., Moriguchi, M., Morinobu, A. & O'Shea, J. J. The biology of IL-12: coordinating innate and adaptive immune responses. *Cytokine & growth factor reviews* 14, 361-368 (2003).
- 265 Yoo, J. K., Cho, J. H., Lee, S. W. & Sung, Y. C. IL-12 provides proliferation and survival signals to murine CD4+ T cells through phosphatidylinositol 3-kinase/Akt signaling pathway. *Journal of immunology* 169, 3637-3643 (2002).
- 266 Ivashkiv, L. B. & Hu, X. Signaling by STATs. *Arthritis research & therapy* 6, 159-168, doi:10.1186/ar1197 (2004).
- 267 Melillo, J. A. *et al.* Dendritic cell (DC)-specific targeting reveals Stat3 as a negative regulator of DC function. *Journal of immunology* 184, 2638-2645, doi:10.4049/jimmunol.0902960 (2010).
- 268 Nefedova, Y. *et al.* Activation of dendritic cells via inhibition of Jak2/STAT3 signaling. *Journal of immunology* 175, 4338-4346 (2005).
- 269 Nakajima, K. *et al.* A central role for Stat3 in IL-6-induced regulation of growth and differentiation in M1 leukemia cells. *The EMBO journal* 15, 3651-3658 (1996).

- 270 Kissler, S. *et al.* In vivo RNA interference demonstrates a role for Nramp1 in modifying susceptibility to type 1 diabetes. *Nature genetics* 38, 479-483, doi:10.1038/ng1766 (2006).
- 271 Stern, P. *et al.* A system for Cre-regulated RNA interference in vivo. *Proceedings of the National Academy of Sciences of the United States of America* 105, 13895-13900, doi:10.1073/pnas.0806907105 (2008).
- 272 Folco, E. J. *et al.* Hypoxia but not inflammation augments glucose uptake in human macrophages: Implications for imaging atherosclerosis with 18fluorine-labeled 2-deoxy-D-glucose positron emission tomography. *Journal of the American College of Cardiology* 58, 603-614, doi:10.1016/j.jacc.2011.03.044 (2011).
- 273 Weber, C., Zernecke, A. & Libby, P. The multifaceted contributions of leukocyte subsets to atherosclerosis: lessons from mouse models. *Nature reviews. Immunology* 8, 802-815, doi:10.1038/nri2415 (2008).
- 274 Wigren, M., Nilsson, J. & Kolbus, D. Lymphocytes in atherosclerosis. *Clinica chimica acta; international journal of clinical chemistry* 413, 1562-1568, doi:10.1016/j.cca.2012.04.031 (2012).
- 275 Tellides, G. *et al.* Interferon-gamma elicits arteriosclerosis in the absence of leukocytes. *Nature* 403, 207-211, doi:10.1038/35003221 (2000).
- 276 Zhou, X., Paulsson, G., Stemme, S. & Hansson, G. K. Hypercholesterolemia is associated with a T helper (Th) 1/Th2 switch of the autoimmune response in atherosclerotic apo E-knockout mice. *The Journal of clinical investigation* 101, 1717-1725, doi:10.1172/JCI1216 (1998).
- 277 Leon, M. L. & Zuckerman, S. H. Gamma interferon: a central mediator in atherosclerosis. *Inflammation research : official journal of the European Histamine Research Society ... [et al.]* 54, 395-411, doi:10.1007/s00011-005-1377-2 (2005).
- 278 McLaren, J. E. & Ramji, D. P. Interferon gamma: a master regulator of atherosclerosis. *Cytokine & growth factor reviews* 20, 125-135, doi:10.1016/j.cytogfr.2008.11.003 (2009).
- 279 Klingenberg, R. *et al.* Depletion of FOXP3+ regulatory T cells promotes hypercholesterolemia and atherosclerosis. *The Journal of clinical investigation* 123, 1323-1334, doi:10.1172/JCI63891 (2013).
- 280 Mallat, Z., Ait-Oufella, H. & Tedgui, A. Regulatory T-cell immunity in atherosclerosis. *Trends in cardiovascular medicine* 17, 113-118, doi:10.1016/j.tcm.2007.03.001 (2007).
- 281 Taleb, S., Tedgui, A. & Mallat, Z. Regulatory T-cell immunity and its relevance to atherosclerosis. *Journal of internal medicine* 263, 489-499, doi:10.1111/j.1365-2796.2008.01944.x (2008).

- 282 Chen, S., Crother, T. R. & Ardit, M. Emerging role of IL-17 in atherosclerosis. *Journal of innate immunity* 2, 325-333, doi:10.1159/000314626 (2010).
- 283 Zhao, W. *et al.* Hypoxia suppresses the production of matrix metalloproteinases and the migration of human monocyte-derived dendritic cells. *European journal of immunology* 35, 3468-3477, doi:10.1002/eji.200526262 (2005).
- 284 Qu, X. *et al.* Hypoxia inhibits the migratory capacity of human monocyte-derived dendritic cells. *Immunology and cell biology* 83, 668-673, doi:10.1111/j.1440-1711.2005.01383.x (2005).
- 285 de Jong, E. C., Smits, H. H. & Kapsenberg, M. L. Dendritic cell-mediated T cell polarization. *Springer seminars in immunopathology* 26, 289-307, doi:10.1007/s00281-004-0167-1 (2005).
- 286 Ni, K. & O'Neill, H. C. The role of dendritic cells in T cell activation. *Immunology and cell biology* 75, 223-230, doi:10.1038/icb.1997.35 (1997).
- 287 O'Garra, A., Hosken, N., Macatonia, S., Wenner, C. A. & Murphy, K. The role of macrophage- and dendritic cell-derived IL12 in Th1 phenotype development. *Research in immunology* 146, 466-472 (1995).
- 288 Elia, A. R. *et al.* Human dendritic cells differentiated in hypoxia down-modulate antigen uptake and change their chemokine expression profile. *J Leukoc Biol* 84, 1472-1482, doi:10.1189/jlb.0208082 (2008).
- 289 Jantsch, J. *et al.* Hypoxia and hypoxia-inducible factor-1 alpha modulate lipopolysaccharide-induced dendritic cell activation and function. *J Immunol* 180, 4697-4705 (2008).
- 290 Yoshimura, A., Naka, T. & Kubo, M. SOCS proteins, cytokine signalling and immune regulation. *Nature reviews. Immunology* 7, 454-465, doi:10.1038/nri2093 (2007).
- 291 Kubo, M., Hanada, T. & Yoshimura, A. Suppressors of cytokine signaling and immunity. *Nature immunology* 4, 1169-1176, doi:10.1038/ni1012 (2003).
- 292 Hanada, T. *et al.* Induction of hyper Th1 cell-type immune responses by dendritic cells lacking the suppressor of cytokine signaling-1 gene. *Journal of immunology* 174, 4325-4332 (2005).
- 293 Shen, L., Evel-Kabler, K., Strube, R. & Chen, S. Y. Silencing of SOCS1 enhances antigen presentation by dendritic cells and antigen-specific anti-tumor immunity. *Nature biotechnology* 22, 1546-1553, doi:10.1038/nbt1035 (2004).
- 294 Kimura, H. *et al.* Identification of hypoxia-inducible factor 1 ancillary sequence and its function in vascular endothelial growth factor gene induction by hypoxia and nitric oxide. *The Journal of biological chemistry* 276, 2292-2298, doi:10.1074/jbc.M008398200 (2001).

- 295 Takeda, K. *et al.* Targeted disruption of the mouse Stat3 gene leads to early embryonic lethality. *Proceedings of the National Academy of Sciences of the United States of America* 94, 3801-3804 (1997).
- 296 Akira, S. Functional roles of STAT family proteins: lessons from knockout mice. *Stem cells* 17, 138-146, doi:10.1002/stem.170138 (1999).
- 297 Akira, S. Roles of STAT3 defined by tissue-specific gene targeting. *Oncogene* 19, 2607-2611, doi:10.1038/sj.onc.1203478 (2000).
- 298 Park, S. J. *et al.* IL-6 regulates in vivo dendritic cell differentiation through STAT3 activation. *Journal of immunology* 173, 3844-3854 (2004).
- 299 Kortylewski, M. *et al.* Inhibiting Stat3 signaling in the hematopoietic system elicits multicomponent antitumor immunity. *Nature medicine* 11, 1314-1321, doi:10.1038/nm1325 (2005).
- 300 Kortylewski, M. *et al.* Interleukin-6 and oncostatin M-induced growth inhibition of human A375 melanoma cells is STAT-dependent and involves upregulation of the cyclin-dependent kinase inhibitor p27/Kip1. *Oncogene* 18, 3742-3753, doi:10.1038/sj.onc.1202708 (1999).
- 301 Kano, M., Igarashi, H., Saito, I. & Masuda, M. Cre-loxP-mediated DNA flip-flop in mammalian cells leading to alternate expression of retrovirally transduced genes. *Biochemical and biophysical research communications* 248, 806-811, doi:10.1006/bbrc.1998.9011 (1998).
- 302 Jung, J. E. *et al.* STAT3 is a potential modulator of HIF-1-mediated VEGF expression in human renal carcinoma cells. *FASEB journal : official publication of the Federation of American Societies for Experimental Biology* 19, 1296-1298, doi:10.1096/fj.04-3099fje (2005).

ACKNOWLEDGEMENTS

A lot of work has gone into this project and the resultant thesis and it would not have been possible without the efforts and contribution of certain people. Firstly I would like to thank my supervisor Prof. Dr. Alma Zernecke for giving me the opportunity to work on this project, the freedom to experiment, make mistakes and learn in the process. I appreciate her patience and enthusiasm during these years and the discussions and advice will help me always.

I would sincerely like to thank Prof. Dr. Thomas Hünig and Prof. Dr. Christian Weber for spending precious time and effort in supervising over my work and reading my thesis. Many heartfelt thanks go to Dr. Heike Hermanns and Dr. Stephan Kissler who have contributed a lot towards this project in terms of experimental help, useful discussions and valuable advice. I would also like to thank Dr. Judith Sluimer for contributing towards some experiments in this project.

This project would not have been what it is without my lab mates Miriam Koch, Martin Busch, Helga Manthey, Clément Cochain, Melanie Schott, Theresa Henninger, Louisa Molinari, Yvonne Kerstan and Sabine Wilhelm. They have not only been the most amazing colleagues but also wonderful friends. Their help with all the different techniques, planning and actual experimentation is what has made this thesis complete and more importantly the wonderful work environment they provided could not have been better. I would specially like to thank Miriam, Martin and Helga for the fun in and outside the lab. I am grateful to them for always being there when I needed them and making my stay in Germany a wonderful memory for life.

I also would like to acknowledge the help provided by Peilin Zheng and Celia Caballero-Franco for the virus experiments and all the members of the Hermanns, Nieswandt and Kissler labs for experimental help and support. The mice work in this project would have been impossible without the assistance of the animal care takers at the ZEMM and RVZ. Special thanks to Marie Blum, Petra Klausnitzer and Sandra Umbenhauer for taking care of our mice and bearing with our whims. I also appreciate the help and support of the non-scientific staff at the RVZ, without whom, work would not have sailed so smoothly.

I am grateful to Nilesh Joshi, Martin Busch, Miriam Koch and Pearl Bakhru for undertaking the painful task of reading the thesis draft, editing it and giving useful suggestions and advice, without which this thesis would not have ended so beautifully.

I would like to specially acknowledge my friends Shuchi Gupta, Aruna Srinivasan, Priya Panjwani, Neha Gottlieb and Saba Rehman for making my stay here as comfortable and enjoyable as possible. I will miss the wonderful get-togethers, movie nights, outings and food parties we have had. I would also like to extend my thanks to the entire Indian community in Würzburg who have made it possible to have the great feeling of being at home so many miles away. Special heartfelt thanks to Somdatta Karak who has been the most wonderful friend, for all the help, advice and fun during these years.

I would like to thank my cousin Prachiti Raut, a special person who has stood by me through thick and thin - my sister, friend and a wonderful role model to look up to, admire and follow. I am also indebted to the rest of my family who has always been a great motivation and inspiration for me and without whom I would not have reached the stage I am at now.

Lastly I would like to thank the most important and beautiful people in my life – my parents. I am truly honored to be blessed with such amazing parents who are my best friends, advisors and confidants. Thanks for making me what I am today and for always standing by me, believing in me and giving me the best of everything. I dedicate not just this thesis but my whole life to you.

CURRICULUM VITAE

Name: Sweena M. Chaudhari

Date of birth: 8th October 1985

Place of Birth: Mumbai, India

Nationality: Indian

Education:

June 2009 – present

Doctor of Philosophy (Ph.D.)

Group of Prof. Dr. Alma Zerneck
Julius-Maximilians Universität Würzburg
Rudolf Virchow Zentrum,
DFG research center for experimental
biomedicine,
Würzburg, Germany

July 2006 – May 2008

Master of Science (MSc, Virology)

University of Pune,
National Institute of Virology,
Pune, India

June 2003 – May 2006

Bachelor of Science (BSc, Biotechnology)

University of Mumbai,
V. G. Vaze College of arts, science and
commerce,
Mumbai, India

Projects / Work experience:

June 2008 – April 2009

Trainee scientist

Research and development department,
Actis Biologics Pvt. Ltd.,
Mumbai, India

January 2008 – May 2008

Master's thesis project

Group of Dr. Devendra T. Mourya
National Institute of Virology,
Pune, India

LIST OF PUBLICATIONS

1. Sweena M. Chaudhari*, Judith C. Sluimer*, Miriam Koch, Helga D. Manthey, Martin Busch, Mat J. Daemen, Celia Caballero-Franco, Stephan Kissler, Heike M. Hermanns, Alma Zerneck: HIF1alpha in dendritic cells restrains inflammation and atherosclerosis in mice (submitted)
2. Clément Cochain*, Sweena M. Chaudhari*, Miriam Koch, Heinz Wiendl, Hans-Henning Eckstein, Alma Zerneck: PD-1 deficiency exacerbates T cell activation and atherogenesis despite expansion of regulatory T cells in atherosclerosis-prone mice (submitted)
3. Döring Y, Soehnlein O, Drechsler M, Shagdarsuren E, Chaudhari SM, Meiler S, Hartwig H, Hristov M, Koenen RR, Hieronymus T, Zenke M, Weber C, Zerneck A.: Hematopoietic interferon regulatory factor 8-deficiency accelerates atherosclerosis in mice. *Arterioscler Thromb Vasc Biol.* 2012 Jul; 32(7):1613-23 (published)
4. Helga D. Manthey*, Clément Cochain*, Stefanie Barnsteiner*, Ela Karshovska, Jaroslav Pelisek, Miriam Koch, Sweena M. Chaudhari, Martin Busch, Hans-Henning Eckstein, Christian Weber, Rory R. Koenen, Alma Zerneck: "Role of the chemokine receptor Ccr6 in monocyte recruitment and atherosclerosis in mice." (accepted)
5. Miriam Koch, Helga D. Manthey, Martin Busch, Sweena M. Chaudhari, Ina Thielmann, David Stegner, Bernhard Nieswandt*, Alma Zerneck*: Coagulation factor XII promotes atherosclerosis and pro-inflammatory T cell responses in mice (submitted)
6. Pragya D Yadav, Barde PV, Jyoti Bhat, Sweena M. Chaudhari, Prasanna Yergolkar, Devendra T Mourya: Confirmation of presence of Simbu group of viruses (Ingwavuma and Oya virus) in pigs and humans in India (submitted)

* equal contribution

LIST OF ORAL AND POSTER PRESENTATIONS

1. Poster presentation titled "Role of HIF1 α in immuneregulation of atherosclerosis" at the 6th European meeting for Vascular biology and medicine in Krakow, Poland (September 2011)
2. Poster presentation titled "Role of HIF1 α in immuneregulation of atherosclerosis" at the 6th Cardiovascular healing symposium of the Comprehensive heart failure center and Collaborative research center SFB688 in Wuerzburg, Germany (June 2012)
3. Poster presentation titled "Role of HIF1 α in immuneregulation of atherosclerosis" at the 7th International symposium of the Graduate school of life sciences, University of Wuerzburg in Wuerzburg, Germany (October 2012)
4. Oral presentation titled "Role of HIF1 α in dendritic cells in immunopathogenesis of atherosclerosis" at the 4th Neurowind meeting in Motzen, Germany (November 2012)
5. Poster presentation titled "Role of HIF1 α in immuneregulation of atherosclerosis" at the 81st Congress of the European atherosclerosis society in Lyon, France (June 2013)

AFFIDAVIT

I hereby confirm that my thesis titled “Role of Hypoxia-Inducible Factor (HIF) 1 α in Dendritic Cells in Immune Regulation of Atherosclerosis” is the result of my own work. I did not receive any help or support from commercial consultants. All resources and/or materials applied are listed and specified in the thesis.

Furthermore I confirm that this thesis has not been submitted as part of another examination process neither in identical nor in a similar form. Furthermore, I confirm that this thesis has not yet been submitted as part of another examination process neither in identical nor in similar form.

Würzburg, 2013

EIDESSTATTLICHE ERKLÄRUNG

Hiermit erkläre ich an Eides statt, die Dissertation “Rolle von Hypoxie Induziertem Faktor (HIF) 1 α in dendritischen Zellen in der Immunregulation der Atherosklerose” eigenständig und ohne Hilfe eines kommerziellen Promotionsberaters angefertigt, und keine anderen als die angegebenen Quellen und Hilfsmittel verwendet zu haben.

Ich erkläre außerdem, dass die Dissertation weder in gleicher noch in ähnlicher Form bereits in einem anderen Prüfungsverfahren vorgelegen hat.

Würzburg, 2013

